

# **Inactivation of cyclin E1 inhibits chemically induced hepatocarcinogenesis in mice**

Von der Fakultät für Mathematik, Informatik und Naturwissenschaften der RWTH Aachen University zur Erlangung des akademischen Grades einer Doktorin der Naturwissenschaften genehmigte Dissertation

vorgelegt von

Diplom-Ingenieurin

Nives Moro

aus Zagreb, Kroatien

Berichter: Universitätsprofessor Dr. rer. nat. Michael Huber

Privatdozent Dr. rer. nat. Christian Liedtke

Tag der mündlichen Prüfung: 05.12.2011

Diese Dissertation ist auf den Internetseiten der Hochschulbibliothek online verfügbar.

Teile dieser Arbeit wurden bereits vorab veröffentlicht:

1. Freimuth J, Gassler N, **Moro N**, Günther RW, Trautwein C, Liedtke C, Krombach GA (2010). *Application of magnetic resonance imaging in transgenic and chemical mouse models of hepatocellular carcinoma*. Mol Cancer 9:94
2. **Moro N**, Gassler N, Nevzorova YA, Sicinski P, Trautwein C, Liedtke C (2010). *Deletion of cyclin E1 inhibits DEN induced hepatocarcinogenesis in mice*. Poster, 26. Jahrestagung der GASL (German Association for the Study of the Liver), Bonn
3. **Moro N**, Gassler N, Nevzorova YA, Sicinski P, Trautwein C, Liedtke C (2009): *Inactivation of cyclin E1 inhibits chemical hepatocarcinogenesis in mice*. Journal of Hepatology 50, S46. Vortrag, 44. Jahrestagung der EASL (European Association for the Study of the Liver), Kopenhagen, Dänemark
4. **Moro N**, Gassler N, Nevzorova YA, Sicinski P, Trautwein C, Liedtke C (2009): *Inactivation of cyclin E1 but not of cyclin E2 inhibits chemically induced hepatocarcinogenesis in mice*. Hepatology 50. Poster, 60. Jahrestagung der AASLD (American Association for the Study of Liver Diseases), Boston, MA, USA

# Table of contents

1	Introduction.....	1
1.1	Regulation of the mammalian cell cycle .....	1
1.2	To regulate and be regulated: Cyclin - Cdk.....	3
1.2.1	Regulation and structural properties of Cdk2 and E-type cyclins.....	4
1.3	Supervising the supervisor - CKIs .....	7
1.4	Tumor suppressor p53: a role in cell cycle regulation .....	9
1.5	Consequences of CcnE-Cdk2 ablation <i>in vivo</i> .....	10
1.6	The biology of hepatocellular carcinoma.....	10
1.7	CcnE and cancer.....	11
1.8	Experimental mouse models of HCC .....	12
1.9	Aim of the present study .....	15
2	Materials and Methods .....	16
2.1	Materials .....	16
2.1.1	Chemicals.....	16
2.1.2	Standard buffer and media .....	21
2.1.3	Standard kits and enzymes .....	21
2.1.4	Diverse .....	22
2.1.5	Antibodies used for immunostaining and/or western blot.....	23
2.1.6	Primer sequences used for Q-RT-PCR .....	24
2.1.7	Primer sequences used for genotyping PCR .....	25
2.1.8	Instruments and other equipment .....	25
2.2	Methods .....	28
2.2.1	Animal maintenance and treatments .....	28
2.2.2	Genotyping .....	29
2.2.3	Blood sampling and serology.....	30

2.2.4	Extraction and sectioning of livers .....	31
2.2.5	Assessment of HCC .....	31
2.2.6	Liver perfusion and isolation of primary hepatocytes .....	32
2.2.7	Mouse primary hepatocyte culture .....	33
2.2.8	Flow cytometry.....	33
2.2.9	RNA extraction, cDNA preparation, Real-Time PCR .....	34
2.2.10	DNA isolation from frozen livers.....	35
2.2.11	DNA labelling and measuring of AP sites .....	36
2.2.12	Whole cell protein extracts.....	36
2.2.13	Isolation of nuclear and cytoplasmic cell fractions .....	37
2.2.14	Protein concentration measurement .....	37
2.2.15	Western Blot .....	38
2.2.16	Immunoprecipitation Assay.....	39
2.2.17	Gel silver staining .....	40
2.2.18	Caspase-3 Assay.....	40
2.2.19	Immunofluorescence staining .....	41
2.2.20	$\beta$ -galactosidase activity staining .....	42
2.2.21	Immunohistochemistry .....	42
3	Results .....	44
3.1	Cyclin E1 deletion inhibits DEN-induced hepatocarcinogenesis .....	44
3.2	Analysis of the immediate response after DEN-induced acute liver injury .....	52
3.2.1	Ablation of CcnE1 or CcnE2 does not result in alterations of DEN- induced liver necrosis and apoptosis .....	52
3.2.2	DEN induces differential immune response in CcnE1 <sup>-/-</sup> and CcnE2 <sup>-/-</sup> livers..	56
3.2.3	CcnE1 deficiency results in prolonged cell cycle arrest after DEN induced toxic liver injury .....	58
3.2.4	Ablation of CcnE1 triggers prolonged p53-checkpoint activation after DEN-induced DNA damage.....	65

3.2.5 Ablation of CcnE1 does not induce cellular senescence in acute DEN-mediated liver injury.....	69
3.3 Implementations for the acute DEN-model in juvenile mice .....	70
3.4 Analysis of DEN-dependent effects on cell cycle activation and apoptosis in primary hepatocytes .....	72
3.5 The cell cycle inhibitor p27 is negatively regulated by CcnE1 during early HCC progression.....	74
3.6 The oncogenic potential of CcnE1 in the liver depends on functional Cdk2 in hepatocytes .....	77
4 Discussion .....	82
4.1 Distinct roles of CcnE1 and CcnE2 in hepatocarcinogenesis.....	82
4.2 New signaling pathways involved during CcnE1-driven carcinogenesis .....	84
4.3 Oncogene CcnE1 function is Cdk2 dependent.....	88
4.4 Future impacts and directions .....	89
5 Summary.....	90
6 Zusammenfassung.....	91
7 References .....	92
8 Appendix.....	107
8.1 Abbreviations.....	107
9 Eidesstattliche Erklärung.....	111
10 Acknowledgements.....	113
11 Lebenslauf.....	115



# 1. Introduction

## 1.1. Regulation of the mammalian cell cycle

Cell growth and cell division are fundamental events of cell behavior in all organisms. There are two main events or states during the cell cycle that consist of interphase and mitosis including cytokinesis. Proper division of the eukaryotic cell depends on two main processes, first, the high fidelity and faithful copying of its genome and second, equal distribution of the duplicated genome and cell material into the daughter cells.

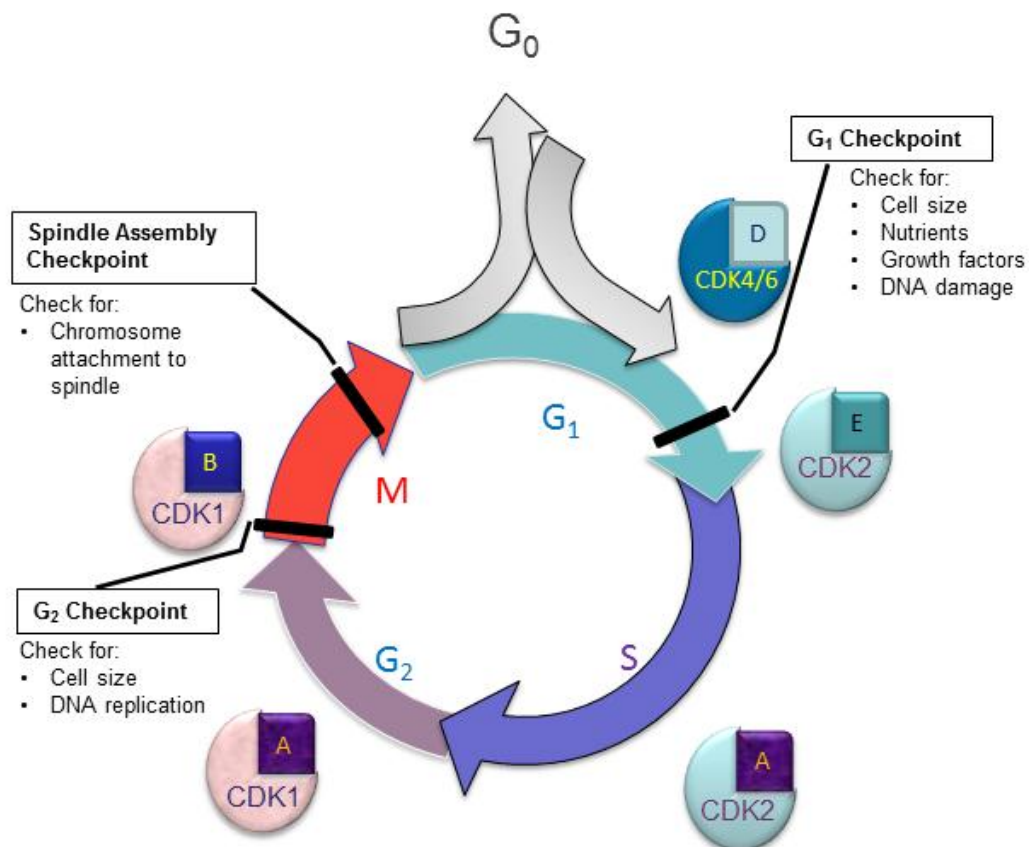


**Figure 1.1 Mammalian cell cycle and its control.** The cell cycle is divided into four phases; G<sub>1</sub> (GAP1), S (DNA synthesis), G<sub>2</sub> (GAP2) and M (Mitosis) phase. The progression through the cell cycle is regulated by complexes containing a cyclin and a cyclin-dependent kinase. CcnD interacts with Cdk4 and Cdk6 and the cell enters the cell cycle. CcnE-Cdk2 complex is important for G<sub>1</sub>-S transition, CcnA-Cdk2 directs the progression through S-phase and CcnA-Cdk1 leads the cell through G<sub>2</sub> restriction point. Finally, CcnB-Cdk1 trigger mitosis (Malumbres and Barbacid, 2005).

Within interphase there are two control points called G<sub>1</sub> (GAP1) and G<sub>2</sub> (GAP2) phase which control the transition from one phase to the next. G<sub>1</sub> controls

entry into synthesis phase (S-phase) and entry into Mitosis (M-phase) is safeguarded by  $G_2$  (Figure 1.1). The cell cycle starts with cell growth and preparation of the chromosomes for replication, followed by synthesis of DNA and duplication of the centrosome, then providing that replication was correct finally undergoes mitosis (Norbury and Nurse, 1992). The time required for completion of one eukaryotic cell cycle is highly variable and cell type specific. The most crucial decision of the cell is whether to continue another round of cell division or to exit the cell cycle and enter a quiescent state known as  $G_0$  (G zero). Most cells in an adult organism including hepatocytes are quiescent in order to carry out their main functions such as secretion, storage or metabolism of compounds. Only specialized cells maintain active proliferation, such as those found in the hematopoietic system and the gut epithelium.

The cell cycle machinery is usually activated by the presence of mitogen factors leading to induction of the initiators of the cell cycle, the family of D-type cyclins. The D-type cyclins preferentially bind to and activate Cdk4/Cdk6. These complexes then phosphorylate and partially inactivate members of retinoblastoma pocket proteins (Rb, p107, p130) (Bartek et al., 1996; Harbour et al., 1999; Sherr, 1996). Phosphorylation of Rb, a transcriptional repressor, leads to the release of the transcription factor family E2Fs resulting in the induction of E-type cyclins which then bind and activate Cdk2. CcnE-Cdk2 complexes phosphorylate additional proteins such as NPM and CP110 involved in centrosome duplication, Cdt1 involved in DNA synthesis, and perpetuates the cell cycle. This positive feedback loop generates a rapid rise in E2F-dependent transcription and leads to the onset of S-phase. This restriction point is a stage where cells no longer require mitogen signals. CcnE-Cdk2 activity is thought to be essential for the initiation of DNA replication (Dannenberg et al., 2000; Ezhevsky et al., 2001; Hwang and Clurman, 2005; Lauper et al., 1998; Lundberg and Weinberg, 1998; Sage et al., 2000). A-type cyclins accumulate throughout S-phase. Cdk2 kinase also binds CcnA and the formation of this complex plays a role in progression through DNA synthesis and passing through the  $G_2$  phase. At the end of interphase, CcnA activates Cdk1 to facilitate the onset of mitosis. After nuclear envelope breakdown, A-type cyclins are degraded, enabling the formation of CcnB-Cdk1 complexes. B-type cyclins in association with Cdk1 are



essential for triggering mitosis (Figure 1.1) (Edgar et al., 1994a; Edgar et al., 1994b; Malumbres and Barbacid, 2005; Nigg, 1995).

The Anaphase-Promoting Complex (APC), also known as cyclosome, is a large multi-subunit complex that acts as an E3 enzyme to catalyse the transfer of ubiquitin to various mitotic substrates, including cyclins and controls the exit from mitosis. APC activity is high in G<sub>1</sub> and then declines upon the appearance of G<sub>1</sub> cyclins (Peters et al., 1996).

## 1.2. To regulate and be regulated: Cyclin - Cdk

The phases of the cell cycle are precisely coordinated and follow in a well-orchestrated and systematic order to assure proper DNA duplication and cell division. The supervisors of the cell cycle are the cyclin-dependent kinases (Cdks), a group of serine/threonine kinases that form active heterodimer complexes upon binding to cyclins. Cyclins are regulatory subunits that are expressed in a cyclical manner throughout the cell cycle; as such they are produced and degraded as needed (Morgan, 1997; Sherr, 2000).

Cdks are defined as protein kinase catalytic subunits that are closely related to the prototypical Cdc2 in *Saccharomyces cerevisiae* and Cdc28 in *Schizosaccharomyces pombe* (Nasmyth, 1996; Stern and Nurse, 1996). However, complete activation of Cdk requires more than just cyclin binding. The Cdk subunit must be phosphorylated by kinases referred to as Cdk-activating kinase (CAK) (Fisher and Morgan, 1994). Human Cdk1-CcnB, Cdk2-CcnA or Cdk2-CcnE complexes interact with high affinity in the absence of other components or modifications (Desai et al., 1995). Some complexes, such as Cdk1-CcnA and Cdk7-CcnH do not bind tightly unless the Cdk subunit is phosphorylated at the activating threonine residue (Desai et al., 1995; Ducommun et al., 1991; Fisher et al., 1995).

Cyclins are defined as proteins with structural homology to prototypical cyclins described in yeast and possess the ability to activate a Cdk catalytic subunit. Cyclins share a sequence motif known as the cyclin box, a 100 amino acid section with a high sequence homology amongst all known cyclins, which is necessary for Cdk binding and activation (Kobayashi et al., 1992; Lees and Harlow, 1993). There are

several types of cyclins that are active during different parts of the cell cycle, which leads the phosphorylation of various substrates by Cdk. In addition, there are also several "orphan" cyclins for which no Cdk partner has been identified yet (Malumbres and Barbacid, 2005; Morgan, 1997).

Some cyclins and Cdks are not only regulating the cell cycle, but are also involved in the regulation of transcription and mRNA processing. In higher eukaryotes CAK is a Cdk complex containing Cdk7-CcnH (Nigg, 1996). Some of the Cdk7-CcnH complexes found in humans are associated with transcription factor TFIIH, where it may act as a kinase that phosphorylates the C-terminal domain (CTD) of RNA polymerase II during transcription (Svejstrup et al., 1996; Tassan et al., 1995). Cdk8-CcnC also associates with RNA polymerase II and phosphorylates CTD (Leclerc and Leopold, 1996; Leclerc et al., 1996; Rickert et al., 1996; Tassan et al., 1995). Cdk9 was found to be a component of the complex TAK/P-TEFb, an elongation factor for RNA polymerase II-directed transcription, and phosphorylates CTD of the largest subunit of RNA polymerase II. The Cdk9 kinase forms a complex with CcnT or CcnK (Cabart et al., 2004; Fu et al., 1999; Peng et al., 1998). CcnD1 binds RAD51 and BRCA2 proteins and promotes homologous recombination mediated DNA repair independently of Cdk4/6 activity (Jirawatnotai et al., 2011; Li et al., 2010).

### 1.2.1. Regulation and structural properties of Cdk2 and E-type cyclins

Cyclin-dependent kinase 2 (Cdk2) is a Ser/Thr protein kinase with a molecular weight of 34 kDa. It is an important component of the cell cycle machinery; its kinase activity is regulated by association with a cyclin subunit and is found mainly in the nucleus (Elledge and Spottswood, 1991; Koff et al., 1991; Satyanarayana et al., 2008). Main activating cyclins are E-type and A-type cyclins (Koff et al., 1992; Tsai et al., 1991), which possess a nuclear localization signal (NLS), so Cdk2 depends on cyclin for its nuclear translocation (Diehl and Sherr, 1997). Typical substrates of Cdk2-CcnE kinase are involved in histone modification, DNA replication, DNA repair and centrosome duplication. Cdk2-CcnA substrates include proteins important for exit of S-phase, but also proteins involved in DNA replication, DNA repair, histone modification and cell cycle checkpoints (Chi et al., 2008; Higashi et al., 1995).

Interestingly, it has been shown in mammals that inhibition or deletion of Cdk2 is dispensable for cell proliferation and this is likely due to compensation of other kinases (Kaldis and Aleem, 2005). For example, Cdk1, which was found to be essential for cell cycle, can take over the functions for all interphase Cdks (Cdk2, Cdk4 and Cdk6) in mouse embryos until midgestation in the case of their genetic inactivation (Santamaria et al., 2007).

CcnE1, historically referred to as CcnE, was first identified by its ability to compensate for the proliferative defects found in cyclin-deficient yeast cells (Koff et al., 1991; Lew et al., 1991). A second member of the family, termed CcnE2, was discovered recently, shares a 47% overall amino-acid homology with CcnE1, and is 70% homologous with the cyclin box (Gudas et al., 1999; Lauper et al., 1998; Zariwala et al., 1998). Although specific studies on CcnE2 are limited, the two CcnE family members were thought to exhibit similar activities based on high homology. Nevertheless, there is increasing evidence for differential and nonredundant functions of both E-cyclins (Caldon and Musgrove, 2010).

The mammalian CcnE gene encodes for several polypeptides with molecular weights ranging from 39 to 52 kDa. The main CcnE protein contains a cyclin box domain for recognition of substrates or inhibitors, a substrate recognition motif (VxCxE) that binds Rb protein (Kelly et al., 1998) and a PEST domain that is responsible for targeting CcnE for degradation (Rechsteiner and Rogers, 1996; Rogers and Rechsteiner, 1986).

CcnE1 is required for entry into S-phase and has a cyclical expression, peaking at the G<sub>1</sub>-S transition and then decaying as S-phase progresses. CcnE1-Cdk2 activity is highest in G<sub>1</sub>-S cells and lowest in quiescent cells (Dulic et al., 1992; Ekholm et al., 2001; Koff et al., 1992). The amount of CcnE1 available was thought to be the limiting factor for the progression through G<sub>1</sub> phase (Dulic et al., 1992; Jackson et al., 1995; Koff et al., 1991; Koff et al., 1992; Lew et al., 1991; Morgan, 1996; Ohtsubo et al., 1995; Planas-Silva and Weinberg, 1997; Rempel et al., 1995; Resnitzky and Reed, 1995; Resnitzky et al., 1994).

Transcriptional control of the E-type cyclins is mediated by E2F transcription factors, which are activated via release from Rb following hyperphosphorylation during late G<sub>1</sub> (Bartek et al., 1997; Sherr and McCormick, 2002). E2F is a

transcription factor that regulates the expression of many different genes involved in S-phase (DeGregori et al., 1995; Ohtani et al., 1995; Weinberg, 1996). CcnE1 itself is an E2F target gene and the CcnE1 promoter has been shown to contain defined E2F binding sites (Figure 1.2) (Geng et al., 1996; Le Cam et al., 1999; Ohtani et al., 1995).

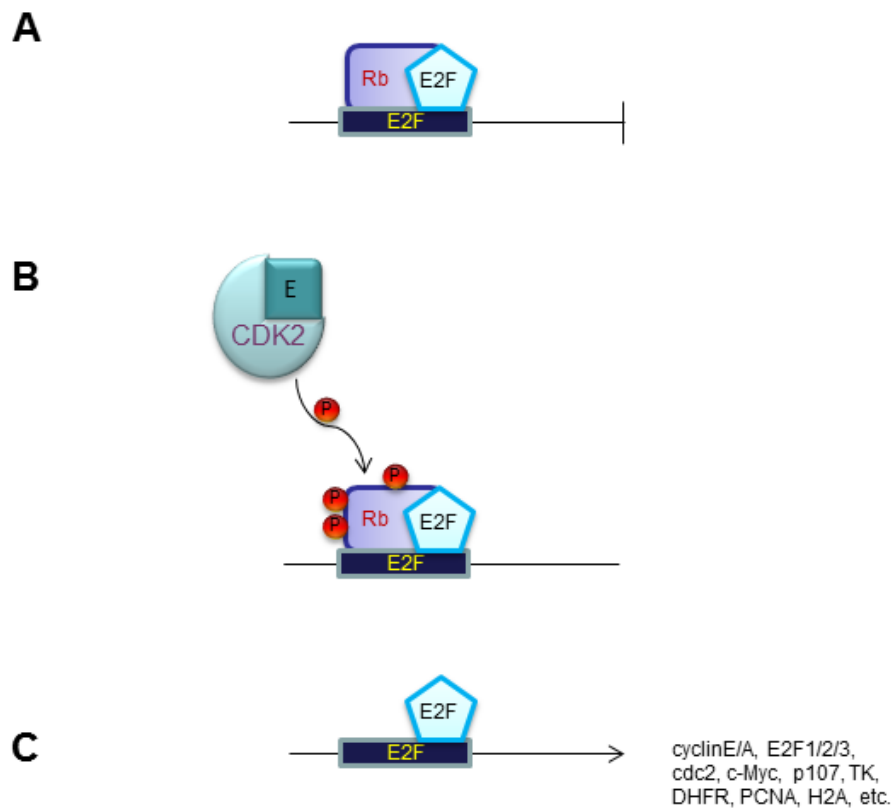


**Figure 1.2 The basic regulatory mechanism of the CcnE-Cdk2 complex.** In order to pass through the G<sub>1</sub> restriction point, phosphorylation of the transcriptional repressor Rb by the CcnE-Cdk2 complex must occur. (A) The repressor Rb binds to transcriptional start sites and inhibits E2F and gene transcription of other target genes; (B) CcnE-Cdk2 hyperphosphorylates and thus inactivates Rb and (C) transcription of S-phase genes starts.

CcnE is an unstable protein that is degraded by two distinct pathways both involving the ubiquitin-proteasome system. The accessibility of CcnE to these proteolytic pathways depends upon whether CcnE is monomeric or bound to Cdk2. Monomeric CcnE is exceptionally labile and degraded by cullin-3 (Cul-3), a scaffolding protein for ubiquitin ligases (E3). When CcnE is in complex with Cdk2 a second pathway of CcnE degradation involving the SCF-Fbw7 ubiquitin ligase is utilized. This interaction between Fbw7 and CcnE requires CcnE-Cdk kinase activity

and autophosphorylations (Clurman et al., 1996; Koepp et al., 2001; Singer et al., 1999; Won and Reed, 1996).

E-type cyclins primarily activate Cdk2, but they can also interact with Cdk1 in some cell types once Cdk2 is genetically inactivated (Dulic et al., 1992; Koff et al., 1992). In a Cdk2-independent manner, CcnE associates with DNA near replication origins, and facilitates loading of MCM (*minichromosome maintenance*) through direct interaction with MCM2-7 complex and Cdt1, a component of the origin recognition complex (ORC) in order to initiate G<sub>0</sub> to S-phase progression (Geng et al., 2007).

### 1.3. Supervising the supervisor - CKIs

The activity of many Cdk-Ccn complexes is controlled by Cdk-inhibitors (CKIs) that are assigned to one of two families based on their structures and Cdk targets (Table 1.1). The Cip/Kip (*CDK interacting protein/Kinase inhibitory protein*) and Ink4 (*Inhibitor of Kinase 4*) gene families provide a tissue-specific mechanism by which cell cycle progression can be restrained in response to extracellular and intracellular signals (Harper et al., 1995).

**Table 1.1 CKI families and their members**

Family	Members:	Encoded by:
<b>Cip/Kip family</b>	p21 <sup>Cip1 Waf1</sup>	Cdkn1a
	p27 <sup>Kip1</sup>	Cdkn1b
	p57 <sup>Kip2</sup>	Cdkn1c
<b>Ink4 family</b>	p15 <sup>Ink4b</sup>	Cdkn2b
	p16 <sup>Ink4a</sup>	Cdkn2a
	p18 <sup>Ink4c</sup>	Cdkn2c
	p19 <sup>Ink4d</sup>	Cdkn2d

The Cip/Kip family includes p21<sup>Cip1</sup>, p27<sup>Kip1</sup>, and p57<sup>Kip2</sup>, all of which contain characteristic motifs within their amino-terminal moieties that enable them to bind to G<sub>1</sub> specific cyclin and Cdk subunits, rendering them inactive and thereby preventing further progression of the cell cycle (Besson et al., 2008; Nakayama, 1998). This is accomplished via domains at the N-terminus of p21 and p27 which are required for cyclin and Cdk binding (Ball and Lane, 1996; Chen et al., 1996; Fotedar et al., 1996).

Sequences similar to the cyclin-binding motifs found in p21 and p27 are also present in the transcription factor E2F and the pRb-related protein p107 (Adams et al., 1996; Shiyanov et al., 1996; Zhu et al., 1995). The Ink4 (inhibitors of CDK4) family contains four members p15<sup>Ink4b</sup>, p16<sup>Ink4a</sup>, p18<sup>Ink4c</sup>, and p19<sup>Ink4d</sup>, all of which have the ability to specifically inhibit Cdk4/6 (Ortega et al., 2002; Roussel, 1999). CKIs of the Cip/Kip family were all initially thought to predominantly inhibit the activities of CcnD-, CcnE-, and CcnA-dependent kinases. However, recent studies revealed that they also might promote activation of CcnD–Cdk4/6 complexes by directing it to the cell nucleus and by increasing the stability of the D-type cyclins (Cheng et al., 1999; Harper et al., 1995; LaBaer et al., 1997; Soos et al., 1996; Zhang et al., 1994).

p21 is a well-known tumor suppressor and its loss is a hallmark of many cancers, including hepatocellular carcinoma (Hui et al., 2008). Mammalian p21 appears to be controlled primarily at the transcriptional level by p53, a transcriptional regulator mediating the cell cycle arrest that occurs after DNA damage (Harper and Elledge, 1996). Under various conditions, p21 accumulation leads to growth arrest, differentiation or cellular senescence. Phosphorylation of the p21 protein affects its stabilization and localisation. Phosphorylation by CcnE-Cdk2 promotes its binding to SKP2 (S-phase kinase associated protein 2) leading to its ubiquitination and subsequent proteolysis; while other phosphorylations can lead to nuclear exclusion thereby promoting antiapoptotic functions and/or its degradation (Abbas and Dutta, 2009).

p27 is a potential tumor suppressor and a prognostic indicator since its decreased or absent expression is observed in various types of human cancers with poor prognosis including HCCs (Lee and Kim, 2009; Matsuda, 2008). However, some controversial data also indicate additional roles for promoting tumor growth

depending on the cellular localization (Abukhdeir and Park, 2008). It is constitutively expressed in quiescent cells, for example liver cells, but downregulated during liver regeneration (Kossatz et al., 2004). p27 is regulated primarily at the posttranslational level by several mechanisms. Part of its regulation is mediated via CcnE-Cdk2 dependent phosphorylation at the Thr187 which directs p27 to cytoplasm and subsequent proteasomal degradation mediated by SCF<sup>SKP2</sup> (Skp-Cullin-F-box) E3 ubiquitin ligase complex (Vervoorts and Luscher, 2008).

#### 1.4. Tumor suppressor p53: a role in cell cycle regulation

p53 is a transcription factor encoded by the *TP53* gene that regulates the cell cycle and modulates cellular responses against potentially tumorigenic events, and is therefore described as a tumor suppressor. p53 is involved in a broad repertoire of cellular functions like cell metabolism, stem cell renewal, autophagy, oxidative status, etc. (Brady and Attardi, 2010). In response to stimuli that activate p53, cells can undergo either apoptosis or cell cycle arrest. Apoptosis induced by the transcriptional activity of p53 occurs by activating target genes such as *Bax*, *Noxa*, *PUMA* and *PTEN* or by interaction with Bcl-2 family of proteins via translocation of p53 to the mitochondria (Pietsch et al., 2008). The p53 protein can interfere with cell cycle progression by direct or indirect repression of cell cycle regulators (Bohlig and Rother, 2011).

In cell homeostasis, p53 is rapidly bound by MDM2, a RING finger E3 ligase that promotes the polyubiquitination and proteasomal degradation of p53. The tumor suppressor p53 becomes activated in response to various stress signals, such as those from kinases ATM and ATR which lead to the phosphorylation of p53. The main posttranslational modifications that stabilize p53 are numerous phosphorylations and acetylations which inhibit the binding of MDM2 and its subsequent degradation. The p53 pathway is of critical importance in mediating innate tumor suppression in cells that have sustained genetic deviations that drive tumor initiation and progression (Meek, 2009; Meek and Anderson, 2009).

## 1.5. Consequences of CcnE-Cdk2 ablation *in vivo*

Before CcnE1, CcnE2 or Cdk2 knockout mice were generated, the general opinion was that CcnE-Cdk2 complex was the master regulator of the G<sub>1</sub>-S transition and that CcnE1 executes its cell cycle functions via Cdk2-dependent phosphorylation of its substrates. Surprisingly, single knockouts of CcnE1, CcnE2 or Cdk2 develop mainly normally, although defects in meiosis were evident in the CcnE2 and Cdk2 knockout mice (Berthet et al., 2003; Geng et al., 2003; Ortega et al., 2003; Parisi et al., 2003). However, CcnE1 and CcnE2 double knockout mice are embryonic lethal, although this was not cell cycle dependent but rather due to impaired endoreplication of trophoblast giant cells and megakaryocytes. CcnE1<sup>-/-</sup>CcnE2<sup>-/-</sup> mouse embryonic fibroblasts (MEFs) proliferate, but have a defect in exit from G<sub>0</sub>. Double CcnE-deficient MEFs also show resistance to transformation with oncogene pairs H-Ras/c-Myc, H-Ras/p53<sup>DN</sup> or H-Ras/ E1A. These results revealed that E-type cyclins are dispensable for continuously cycling cells but suggest a requirement for cell cycle reentry from quiescence and oncogenic transformation (Geng et al., 2003). A recent regeneration study using a model of partial hepatectomy (PH) revealed that single deletion of CcnE1 or CcnE2 does not prevent quiescent hepatocytes from entering the cell cycle; however, CcnE1 seems to be important for endoreplication and polyploidy in hepatocytes (Nevzorova et al., 2009).

The results from these studies initiated some speculations about the function of E-cyclins. First of all, neither CcnE nor Cdk2 are essential for cell division; secondly, CcnE1 is required for endoreplication; thirdly, CcnE1 is required for oncogenic transformation; and finally, CcnE2 and Cdk2 are required for meiosis.

## 1.6. The biology of hepatocellular carcinoma

Hepatocellular carcinoma (HCC) is a primary cancer of the liver and it is among the five most frequent cancers in the world (WHO-World Health Organization 2011). Mortality from liver cancer is very high and increasing during last two decades in comparison to other malignancies and therapy options are limited due to late diagnosis. The major risk factor for the development of HCC is chronic liver injury resulting from hepatitis infection, alcohol abuse or exposure to aflatoxin B1 (Jemal et



al., 2009; Lee et al., 2004; Llovet et al., 2003). More recently, obesity is a worldwide rising problem and a risk for a range of human diseases; growing evidence suggests that fatty liver (NAFLD – *nonalcoholic fatty liver disease*, NASH - *nonalcoholic steatohepatitis*) increases the risk for HCC (Starley et al., 2010). Besides chronic liver damage, additional risk factors are dietary exposure to carcinogens, environmental pollutants and cigarette smoke shown to induce liver cancer in experimental animals (Bosch and Munoz, 1988; Bosch et al., 2004). Due to the climbing mortality rates associated with HCC new and more effective therapies are required and are the focus of much attention in research. Recently, progress has been made in clinical trials with Sorafenib, a multikinase inhibitor (inhibits BRAF, VEGFR, PDGFR). This therapeutic approach is now standard care for patients with advanced stages of HCC. However, the need for new specific therapies still exists. Therefore, more than 50 chemicals are currently being tested for use in the treatment of HCC (Villanueva and Llovet).

## 1.7. CcnE and cancer

CcnE1 expression has been extensively studied in human cancers. Many cancers overexpress CcnE1 protein or mRNA, including carcinomas (breast, lung, cervix, endometrium, gastrointestinal tract), lymphoma, leukemia, sarcomas and adrenocortical tumors. CcnE1 overexpression has been shown to predict poor survival of patients with breast cancer, non-small-cell lung carcinoma (NSLC), squamous cell carcinoma of the larynx and adrenocortical tumors (Hwang and Clurman, 2005). Several mechanisms have been shown to deregulate CcnE1 expression in tumors, such as mutations in regulatory elements of the Rb pathway and *CcnE1* gene amplifications and disrupted proteolysis. Furthermore, overexpression of CcnE low molecular weight (LMW) isoforms increases with the loss of p53 control and promotes tumor development (Delk et al., 2009; Wingate et al., 2009).

These data suggest that CcnE1 might be a potential oncogene and its overexpression, especially in a hyperstable form, is associated with increased incidence of mouse neoplasia and increased susceptibility to the effects of other oncogenes (Bortner and Rosenberg, 1997; Loeb et al., 2005; Ma et al., 2007).

## 1.8. Experimental mouse models of HCC

Several animal models of hepatocarcinogenesis have been described; one well established model comprises the single application of diethylnitrosamine (DEN) into mice or rats (Heindryckx et al., 2009). DEN has been demonstrated to be a DNA-reactive carcinogen requiring tissue specific biotransformation for metabolic activation. Ethyl-DNA adducts are formed after *in vivo* exposure to DEN and their persistence is related to tumor induction.

The putative mechanism of DEN induced DNA adduct formation was examined by several groups. The first bioactivation step is P450-mediated  $\alpha$ -hydroxylation, which produces  $\alpha$ -hydroxynitrosamine. DEN is hydroxylated principally by the ethanol-inducible CYP2E1 in liver, as well as by other P450 isozymes (Michejda and Koepke, 1982; Singer and Andrews, 1983; Swenberg et al., 1991). After DEN is bioactivated to an electrophilic ethyldiazonium ion, it attacks nucleophiles, including DNA bases, and forms DNA adducts (Figure 1.3). Vulnerability to adduct formation is dependent on individual negative charge at each atom on the DNA base, and it is impeded by double stranded hydrogen bonding. A single dose of DEN administered i.p. to 10 day old rats induced formation of 58% ethyl adducts at the hydrogen linked phosphotriester oxygen, where they should not directly cause base mispairing, but might cause strand breaks (Singer, 1985; Singer and Andrews, 1983). Consequently, the O<sup>6</sup>-ethyldeoxyguanosine (O<sup>6</sup>-EtdG) and the O<sup>4</sup>-ethyldeoxythymidine (O<sup>4</sup>-EtdT) adducts are most likely the effective mutagenic compounds as they are potentially miscoding and are formed in the greatest amounts (Boucheron et al., 1987; Saffhill, 1985; Saffhill and Hall, 1985; Singer, 1985).

All tested species have been found to be susceptible to the carcinogenic effects of DEN. In 1967 Hartwell and Shubik (Hartwell, 1967) compiled a comprehensive review of DEN carcinogenicity testing that was performed between 1961 and 1967. These authors reported that mice had liver, gastrointestinal, skin, respiratory and hematopoietic tumors. In mouse liver, there was evidence of DEN-related hepatocellular and Kupffer cell tumors. In a study examining DEN and other carcinogens in a monkey model, DEN was judged by the authors to be the most predictable and potent hepatocarcinogen as compared to 2-acetyl-aminofluorene and aflatoxin B<sub>1</sub> (Thorgeirsson et al., 1994). Phenotypic changes identified in the

neoplastic foci were cytoplasmic basophilia, decreased glucose-6-phosphatase and increased glycogen storage (Scherer et al., 1972). Single liver cells that are positive for the placental form of glutathione S-transferase have been found following DEN administration and other carcinogens (Moore et al., 1987).

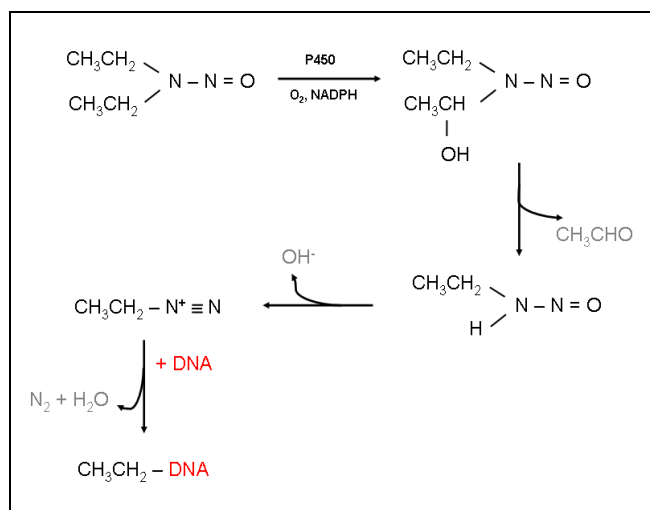


**Figure 1.3 Biotransformation of DEN and DNA adduct formation.** DEN is bioactivated in presence of oxygen and NADPH and mediated by P450 enzymes into α-hydroxynitrosamine. Reactive ethyldiazonium ion is formed after cleavage of acetaldehyde and reacts with DNA resulting in DNA adducts (Verna et al., 1996).

Importantly, it was further shown that three week old rats were more susceptible to liver tumors than 20-week-old rats, which was attributed to greater cell proliferation in the weanlings (Gray et al., 1991; Peto et al., 1984).

As stated above, there are many animal studies describing the potent carcinogenic effects of DEN exposure and there is also evidence which suggests a possible linkage to human cancers as direct dietary sources of DEN have been clearly established (Grasso, 1973). The authors report finding levels of DEN associated with many human consumables, for example, salted, pickled or smoked fish have been found with up to 147 ppb DEN, cooked bacon 17 ppb, whiskey 1,6 ppb (Sen et al., 1980), and cigarette smoke yielded a range from 0,1 to 8,3 ng DEN/cigarette (Hoffmann et al., 1980).

The purpose of mouse DEN carcinogenicity bioassay is to identify potential human liver cancer markers. Single injection of DEN to neonatal mice results in

moderate liver damage and formation of DNA adducts which lead to liver tumors owing to active hepatocyte proliferation in weanlings. This approach does not reflect the features of chronic liver injury that is the leading cause of HCC in humans, progressing from fibrosis to cirrhosis and finally to cancer. Therefore it has been discussed if DEN is an appropriate model to study human HCC development. However, genetic analysis revealed that DEN-induced tumors reflect a gene expression profile similar to highly malignant human HCCs with poor prognosis (Lee et al., 2004). In addition, besides mouse advantages in breeding capacity and gene targeting, DEN allows tumor induction and investigation in an acceptable time.

## 1.9. Aim of the present study

In the past years a variety of studies have indicated an involvement of E-type cyclins in cancerogenesis. However, due to the anticipated redundancy of CcnE1 and CcnE2 the role of each individual E-type cyclin in cancer is poorly investigated. The focus of the present study was to analyse in detail the role of CcnE1 and CcnE2 in hepatocarcinogenesis as many cancers, including hepatocellular carcinoma (HCC), overexpress CcnE1, which is associated with reduced patient survival. To address this question, the diethylnitrosamine (DEN) model of chemically induced HCC will be employed in genetically modified CcnE1<sup>-/-</sup> and CcnE2<sup>-/-</sup> mice with the ultimate aim to further elucidate the function of both E-type cyclins in liver cancer. Specific aims are:

1. *To study how the loss of CcnE1 or CcnE2 affect tumour initiation and progression in a model of DEN-induced hepatocarcinogenesis.* In this model, wildtype mice develop HCC approximately 30-40 weeks after single application of DEN. Using both CcnE<sup>-/-</sup> mice it will be investigated if tumor formation is enhanced, or inhibited by the constitutive deletion of a single E-type cyclin.

2. *To characterise tumors derived from constitutive CcnE1 and CcnE2 knockout and wildtype mice.* The consequence of CcnE ablation with respect to histological changes and proliferative response of developed tumors following DEN-treatment will be addressed in detail.

3. *To decipher the early and immediate events in liver tumor initiation.* To address this question, the immediate response after acute DEN liver injury will be investigated in order to dissect the impact of CcnE1 or CcnE2 for early oncogenic signalling pathways. This model will provide an insight into immediate early events of cell transformation.

4. *To prove if the predicted function of E-type cyclins for malignant hepatocyte proliferation depends on a functional Cdk2 kinase.* The canonical function of CcnE involves complex formation with Cdk2 and phosphorylation of downstream targets. However, recent data hints at additional non-canonical, Cdk2-independent functions for CcnE. Using mice deficient for Cdk2 alone or Cdk2 and CcnE2 the present study will address the question if CcnE1 may contribute to hepatocarcinogenesis in a Cdk2-independent manner.

## 2. Materials and Methods

### 2.1. Materials

#### 2.1.1. Chemicals

Reagent	Manufacturer
$\beta$ -Mercaptoethanol	AppliChem, Darmstadt
Ac-DEVD-AFC Fluorogenic Substrate	Biomol, Hamburg
Acetic acid (glacial) 100% ( $\text{CH}_3\text{COOH}$ )	Merck, Darmstadt
Acetone ( $\text{C}_3\text{H}_6\text{O}$ )	VWR, Darmstadt
Acrylamide 30%	Bio-Rad, Munich
Agar-Agar	Becton Dickinson, Heidelberg
Agarose Electrophoresis Grade	Serva, Heidelberg
Albumin bovine	Sigma, Steinheim
Ammoniumperoxodisulfat ( $\text{H}_8\text{N}_2\text{O}_8\text{S}_2$ )	Roth, Karlsruhe
Ampicilin	Sigma, Steinheim
Aprotinin	Sigma, Steinheim
ATP (Adenosine triphosphate)	Invitrogen, Karlsruhe
Boric acid ( $\text{H}_3\text{BO}_3$ )	AppliChem, Darmstadt
Bromphenol blue	Bio-Rad, Munich
CHAPS ( $\text{C}_{32}\text{H}_{58}\text{N}_2\text{O}_7\text{S}$ )	Sigma, Steinheim
Chloroform ( $\text{CHCl}_3$ )	AppliChem, Darmstadt
Collagen from rat tail	Sigma, Steinheim

Reagent	Manufacturer
Complete Mini (protease inhibitors)	Roche, Mannheim
Coomassie Brilliant Blue	Bio-Rad, Munich
DAKO REAL Peroxidase Blocking Solution	Dako, Hamburg
3,3 Diaminobenzidine tablets (Sigma fast)	Sigma, Steinheim
DMF (N,N-Dimethylformamid) ((CH <sub>3</sub> ) <sub>2</sub> NC(O)H)	Sigma, Steinheim
DMSO (Dimethyl sulfoxide)	Sigma, Steinheim
DNA standard	Invitrogen, Karlsruhe
DTT (Dithiothreitol) (C <sub>4</sub> H <sub>10</sub> O <sub>2</sub> S <sub>2</sub> )	Sigma, Steinheim
EDTA (Ethylene Diamine Tetraacetate)	AppliChem, Darmstadt
EGTA (Ethylene glycol tetraacetic acid)	AppliChem, Darmstadt
Eosin	Sigma, Steinheim
Ethanol (C <sub>2</sub> H <sub>5</sub> OH)	AppliChem, Darmstadt
Ethidium bromide (C <sub>21</sub> H <sub>20</sub> BrN <sub>3</sub> )	Invitrogen, Karlsruhe
Fast Red Tablets	Roche, Mannheim
Fetal bovine serum	Invitrogen, Karlsruhe
Formaldehyde 37% (CH <sub>2</sub> O)	Roth, Karlsruhe
Gelatin from porcine skin Type A	Sigma, Steinheim
Glutaraldehyde (C <sub>5</sub> H <sub>8</sub> O <sub>2</sub> )	Roth, Karlsruhe
Glutathione-Agarose	Sigma, Steinheim
Glycerin (C <sub>3</sub> H <sub>5</sub> (OH) <sub>3</sub> )	Roth, Karlsruhe
Glycerol gelatin	Sigma, Steinheim
Glycine (C <sub>2</sub> H <sub>5</sub> NO <sub>2</sub> )	AppliChem, Darmstadt

Reagent	Manufacturer
Goat serum	Promocell, Heidelberg
Haematoxylin	Sigma, Steinheim
HEPES (C <sub>8</sub> H <sub>18</sub> N <sub>2</sub> O <sub>4</sub> S)	Roth, Karlsruhe
Hydrogen peroxide 30% (H <sub>2</sub> O <sub>2</sub> )	AppliChem, Darmstadt
Hydrochloric acid (HCl)	Merck, Darmstadt
Isopropyl alcohol (C <sub>3</sub> H <sub>8</sub> O)	AppliChem, Darmstadt
IPTG	Sigma, Steinheim
L-Glutathione reduced	Sigma, Steinheim
Lymphocyte LSM 1077	PAA, Cölbe
Magnesium chloride (MgCl <sub>2</sub> )	Merck, Darmstadt
Methanol (CH <sub>4</sub> O)	VWR, Darmstadt
Nonfat dried milk powder	AppliChem, Darmstadt
Nonidet P-40	AppliChem, Darmstadt
Novex Sharp protein standard	Invitrogen, Karlsruhe
Nuclear Fast Red Solution	Sigma, Steinheim
Phenilenediamine dihydrochloride	Sigma, Steinheim
<sup>32</sup> P gamma-ATP	Hartmann, Braunschweig
Paraformaldehyd ((CH <sub>2</sub> O) <sub>n</sub> )	Roth, Karlsruhe
Pefabloc SC Protease Inhibitor	Roth, Karlsruhe
Penicillin-Streptomycin	Invitrogen, Karlsruhe
peqGOLD RNA Pure™	Peqlab, Erlangen
PhosSTOP	Roche, Mannheim



Reagent	Manufacturer
PIPES ( $C_8H_{18}N_2O_6S_2$ )	Sigma, Steinheim
PMSF (Phenylmethylsulphonyl fluoride)	Roth, Karlsruhe
Poly dl:dC	GE Healthcare, Munich
Ponceau S	Sigma, Steinheim
Potassium chloride (KCl)	Merck, Darmstadt
Potassium Ferricyanide ( $C_6N_6FeK_3$ )	Sigma, Steinheim
Potassium Ferrocyanide ( $C_6N_6FeK_4$ )	Sigma, Steinheim
Roti-Histokit	Roth, Karlsruhe
SDS (Sodium Dodecylsulfate) ( $NaC_{12}H_{25}SO_4$ )	Roth, Karlsruhe
Serum, human	Sigma, Steinheim
Serum, mouse	Sigma, Steinheim
Serum, rabbit	Sigma, Steinheim
SIGMA FAST 3,3'-Diaminobenzidine tablets	Sigma, Steinheim
Silver nitrate ( $AgNO_3$ )	Merck, Darmstadt
Sodium acetate anhydrous ( $C_2H_3NaO_2$ )	AppliChem, Darmstadt
Sodium azide ( $NaN_3$ )	AppliChem, Darmstadt
Sodium tetraborate anhydrous ( $Na_2B_4O_7$ )	Sigma, Steinheim
Sodium carbonate ( $Na_2CO_3$ )	Merck, Darmstadt
Sodium chloride (NaCl)	AppliChem, Darmstadt
Sodium fluoride (NaF)	Sigma, Steinheim
Sodium hydroxide (NaOH) 1 mol/l	AppliChem, Darmstadt
Sodium hydroxide pellets	Merck, Darmstadt

Reagent	Manufacturer
Sodium orthovanadate ( $\text{Na}_3\text{VO}_4$ )	AppliChem, Darmstadt
Sodium thiosulfate ( $\text{Na}_2\text{S}_2\text{O}_3$ )	Sigma, Steinheim
SuperSignal West Pico Substrate	Thermo Scientific, Bonn
TEMED (Tetramethylethylenediamine)	Bio-Rad, Munich
Tissue Tek	Dako, Hamburg
Trichloroacetic acid ( $\text{C}_2\text{HCl}_3\text{O}_2$ )	Merck, Darmstadt
Trypsin Inhibitor	Sigma, Steinheim
Tris ( $\text{C}_4\text{H}_{11}\text{NO}_3$ )	AppliChem, Darmstadt
Tri-sodium citrate dihydrate ( $\text{Na}_3\text{C}_6\text{H}_5\text{O}_7 \cdot 2\text{HCl}$ )	Roth, Karlsruhe
Triton X100	Roth, Karlsruhe
Trypton	Becton Dickinson, Heidelberg
Tween® 20	Sigma, Steinheim
Vectashield mounting medium with DAPI	Dako, Hamburg
Vectastain ABC Kit	Dako, Hamburg
X-gal (5-bromo-4-chloro-3-indolyl $\beta$ -D-galactopyranoside)	Sigma, Steinheim
Xylene	VWR, Darmstadt
Xylene cyanole FF ( $\text{C}_{25}\text{H}_{27}\text{N}_2\text{NaO}_6\text{S}_2$ )	Sigma, Steinheim
Yeast extract	Becton Dickinson, Heidelberg

## 2.1.2. Standard buffer and media

<b>Buffers</b>	<b>Manufacturer</b>
Phosphate buffered saline (PBS)	PAA, Cölbe
Restore Western Blot Stripping Buffer	Thermo Scientific, Bonn
Roti Block 10x	Roth, Karlsruhe
Rothiphorese10x SDS PAGE	Roth, Karlsruhe
TAE 50x	AppliChem, Darmstadt

<b>Cell culture medium</b>	<b>Manufacturer</b>
DMEM (Dulbeco's Modified Eagle Medium)	PAA, Cölbe
EBSS (Earle's Balanced Salt Solution) w/o Ca <sup>2+</sup> & Mg <sup>2+</sup>	Invitrogen, Karsruhe
EBSS (Earle's Balanced Salt Solution) with Ca <sup>2+</sup> & Mg <sup>2+</sup>	Invitrogen, Karsruhe
HBSS (Hank's Balanced Salt Solution)	PAA, Cölbe
RPMI (Roswell Park Memorial Institute)	PAA, Cölbe

## 2.1.3. Standard kits and enzymes

<b>Kit / Assay</b>	<b>Manufacturer</b>
BIO-RAD Protein Assay	Bio-Rad, Munich
<i>In Situ</i> Cell Death Detection Kit, Fluorescein	Roche, Mannheim
Omniscript RT Kit	Qiagen, Hilden
OxiSelect Oxidative DNA Damage Quatitation Kit (AP sites)	Cell Biolabs / Biocat, Heidelberg
Pierce Crosslink Immunoprecipitation Kit	Thermo Scientific, Bonn

<b>Enzyme</b>	<b>Manufacturer</b>
Collagenase Type II	CellSystems, Troisdorf
HotStarTaq™ Master Mix	Qiagen, Hilden
Liberase	Roche, Mannheim
Proteinase K – Solution	AppliChem, Darmstadt
ReadyMix™ redtaq™ PCR reaction mix with MgCl <sub>2</sub>	Sigma, Steinheim
RNAse	Sigma, Steinheim
SYBR® GreenER™ qPCR Super Mix	Invitrogen, Karlsruhe

#### 2.1.4. Diverse

<b>Diverse products</b>	<b>Manufacturer</b>
Hyperfilm	GE Healthcare, München
Novex® Midi Gel System	Invitrogen, Karlsruhe
Oligo DT	Qiagen, Hilden
Protein A/G PLUS – Agarose Immunoprecipitation Reagent	Santa Cruz, Heidelberg
PROTRAN® Nitrocellulose Transfer Membrane	Whatman GmbH, Dassel
PureLink™ HiPure Precipitator Module	Invitrogen, Karlsruhe

## 2.1.5. Antibodies used for immunostaining and/or western blot

<b>Primary Antibody</b>	<b>Catalog Number</b>	<b>Company</b>
CD11b	550282	BD
Cleaved caspase-3	#9661	Cell Signaling
F4/80	MCA497GA	AbD serotec
Ki67	discontinued	Dianova
Ly6G	550291	BD
p21	sc-397	Santa Cruz
p27	#3698	Cell Signaling
p27	554069	BD
p-p27	sc-16324	Santa Cruz
PCNA	13-3900	Invitrogen
pH2A.X	#2577	Cell Signaling
p53	#9284	Cell Signaling
pJNK1/2	#9251	Cell Signaling

<b>Secondary Antibody</b>	<b>Catalog Number</b>	<b>Company</b>
Anti-rabbit HRP	#7074	Cell Signaling
Anti-mouse HRP	sc-2954	Santa Cruz
Anti-goat HRP	sc-2768	Santa Cruz
Anti-rat HRP	sc-2956	Santa Cruz
Alexa Fluor488 anti-mouse	A-11059	Invitrogen
Alexa Fluor 488 anti-rabbit	A-11008	Invitrogen
Alexa Fluor 546 anti-rabbit	A-11071	Invitrogen
Alexa Fluor 594 anti-rabbit	A-11072	Invitrogen

## 2.1.6. Primer sequences used for Q-RT-PCR

<b>Gene</b>	<b>Forward</b>	<b>Reverse</b>
Bax	CGAGCTGATCAGAACCATCA	GGTCCCGAAGTAGGAGAGGA
Bcl2	GCTGAGCAGGGTCTTCAGAG	AGTACCTGAACCGGCATCTG
Bcl-6	AGTTTCTAGGAAAGGCCGGA	GATACAGCTGTCAGCCGGG
Bcl-XL	GCTGCATTGTTCCCGTAGAG	GTTGGATGGCCACCTATCTG
Bim	GCCCCTACCTCCCTACAGAC	GCTCCTGTGCAATCCGTATC
bNIP3	TGTCGCAGTTGGGTTTCG	CCATTGCCATTGCTGAAGTG
Cat	AAAACGATAATCCGGGCTTC	TTGCTAAGCCCTAACCTTTCA
Ccna2	GTGGTGATTCAAACTGCCA	AGAGTGTGAAGATGCCCTGG
Ccne1	TCCACGCATGCTGAATTATC	TTGCAAGACCCAGATGAAGA
Ccne2	AAAAAGTCTTGGGCAAGGTAAG	GCATTCTGACCTGGAACCAC
Ccnd1	AAGCATGCACAGACCTTTGTGG	TTCAGGCCTTGCATCGCAGC
E2F1	AGAGTGAGCAGCAGCTGGAT	GGTCCTGGCAGGTCACATAG
E2F2	AGTTGCTCCCTGAGCTTCAA	GCTCCTTGAAGTTGCCTACG
Fas (CD95)	TCCAGAAGGACCTTGAAAA	CCTCTTTCATGGCTGGAAC
FasL	GTTTTCTGAGCCGACCTTTG	TCATTGCACTGGAGGTATGC
Fibronectin	ACCTCTGCAGACCTACCCAG	TTGGTGATGTGTGAAGGCTC
GADD45 $\alpha$	ACCCTCATCCGTGCGTTCT	TCCAGTAGCAGCAGCTCAGCTA
GAPDH	TGTTGAAGTCACAGGAGACAACCT	AACCTGCCAAGTATGATGACATCA
IL-6	CTTCCATCCAGTTGCCTTCTT	AATTAAGCCTCCGACTTGTGAAG
Mdm2	AGAAGGAGATCCATTAGTGAGACA	TCCCTCAGCTCACACAGACC
MnSOD	AGCATTTAGGGTTCCCTTGC	GACCCAATGAGCCAAAGAAA
Noxa	CTGAGATGCCCGGGAGAA	CCACGTGCAATACACTTTGTGTC
p16	CTTTGTGTACCGCTGGGAAC	CTGAGGCCGGATTTAGCTCT
p19	GCTCTGGCTTTTCGTGAACAT	TGAGCAGAAGAGCTGCTACG
p21	TTGCACTCTGGTGTCTGAGC	TCTGCGCTTGGAGTGATAGA
p27	GACAATCAGGCTGGGTTAGC	TCTGTTCTGTTGGCCCTTTT
p53	AAAGGATGCCCATGCTACAG	TATGGCGGGAAGTAGACTGG
Puma	ACCTCAACGCGCAGTACG	GGGAGGAGTCCCATGAAGAG
Smarca4	CCCACGTTTCTTCTGCTTCT	ACGTAAGCGTAAGCGAGACA
Smarcc1	TCCTGAGTACGGCTTCCAAC	TGGAAGGGAGTGGACAGAAC
TRAIL	TGGAGTCCCAGAAATCCTCA	TCACCAACGAGATGAAGCAG

## 2.1.7. Primer sequences used for genotyping PCR

Mouse strain	Primer name	sequence
CcnE1 <sup>-/-</sup>	E11-A	CGCCATGGTTATCCGGGAGATGG
	11-2	CGCATACTGAGACACAGACT
	3N3	GATCTCTCGTGGGATCATTG
CcnE2 <sup>-/-</sup>	E2G	GGTTCTCCCATTTAGAGCACAG
	E2L	GCTATAGCAGTTGTTTCTGTTTG
	3N3	GATCTCTCGTGGGATCATTG
Cdk2 <sup>Δhepa</sup>	Cdk2-3B8	CAAGTTGACGGGAGAAGTTGTG
	Cdk2-3B9	GAAGACCCTCCAGGTGAATGAA
Cdk2 <sup>Δhepa</sup>	Cdk2 exon1	GGAGAACTTCCAAAAGGTGGA
	Cdk2 exon4	ACAGGGACTCCAAAGGCTCT

## 2.1.8. Instruments and other equipment

Instruments	Manufacturer
Axiolmager Z1	Carl Zeiss, Jena
Blotting chamber Trans-Blot cell	Biorad, Munich
Bright Field Microscope DM1000	Leica, Wetzlar
Cell culture bench BSB6A	Gelaire Flow Laboratories, Meckenheim
Cell incubator Haereus BB 6220	Thermo Scientific, Dreieich
Centrifuge Eppendorf Tabletop 5417	Eppendorf, Hamburg
Centrifuge Heraeus-Kendro Megafuge 1.0R	Thermo Scientific, Dreieich
Centrifuge Heraeus Pico 17	Thermo Scientific, Dreieich
Cryostat HM 550	Microm Thermo Scientific, Dreieich
DISKUS Z16 APO	Leica, Wetzlar

FACS Canto II Flow Cytometer	BD, Erlangen
FUJI FILM LAS-4000	FUJI FILM Europe, Düsseldorf
Gel chamber Subcell GT	Biorad, München
Gel chamber	Peqlab, Erlangen
Homogenizer	Janke & Kunkel, Staufen
Microcentrifuge IR 220 VAC	Roth, Karlsruhe
Real-Time PCR System 7300	Applied Biosystems, Darmstadt
Thermocycler T3000	Biometra, Göttingen
Thermomixer	Eppendorf, Hamburg
Vortex Reax top	Heidolph, Nürnberg

<b>Plastic and Glassware</b>	<b>Manufacturer</b>
Beakers (10 – 1000 mL)	Schott-Duran, Mainz
Bottles (25- 2000 mL)	Schott-Duran, Mainz
SuperFrost slides	Roth, Karlsruhe
Pasteur pipettes	Brand, Giessen
96-well plates for RNA/DNA measurement	Greiner Bio-one, Frickenhausen
96-well plates for protein measurement	Greiner Bio-one, Frickenhausen
96-well plates for Real-Time PCR	StarLab, Ahrensburg
Pipettes tips with filter for liquid handling	VWR, Darmstadt; BioHit, Rosbach v.d. Höhe; Biozym, Hess. Oldendorf
Reaction tubes (0,5 – 2mL)	Eppendorf, Hamburg
8 vial strips for PCR (0,2mL)	Sarstedt, Nümbrecht
Reaction tubes 15mL	Sarstedt, Nümbrecht



Reaction tubes 50 mL	GreinerBio-one, Frickenhausen
Sterile pipettes (2-50mL)	Sarstedt, Nümbrecht
Cell Strainer (70 µm)	BD, Erlangen
Cryotubes 1,5 mL	Nunc, Langenselbold
6; 12; 24-well plates	BD-Falcon, Heidelberg

<b>Animal experiment consumables</b>	<b>Manufacturer</b>
General chow for rodents	Altromin, Lage
Hematocrit capillary	Hirschmann Laborgeräte, Eberstadt
Heparine (Liquemin <sup>(R)</sup> )	Roche, Mannheim
Injection needles Sterican <sup>(R)</sup>	Braun, Melsungen
Isoflurane	Abbott, Ludwigshafen
Ketamin 10%	CEVA TIERGESUNDHEIT GmbH, Düsseldorf
Micro tube (1,1 ml Z-Gel)	Sarstedt, Nümbrecht
Sodium chloride 0,9% (NaCl)	DeltaSelect, Dreieich
Sunflower seed oil	Sigma, Steinheim
Surgical instruments	FST, Heidelberg
Syringe Omnican <sup>(R)</sup>	Braun, Melsungen
Xylazin 2%	Bernburg Medistar, Holzwickede

## 2.2. Methods

### 2.2.1. Animal maintenance and treatments

All mice were bred and maintained under specific pathogen-free conditions at the animal facility of the University Hospital Aachen. Upon approval by the local government (AZ 8.87-50.10.35.08.284), all experiments were performed in accordance with the German legislation on protection of animals and the National Institutes of Health 'Guide for the Care and Use of Laboratory Animals' (Institute of Laboratory Animal Resources, National Research Council; NIH publication 86-23 revised 1985). Mice were housed in macrolon cages providing food and water *ad libitum* and were grouped up to 5-10 animals per cage. Tail biopsies for genotyping were taken after weaning and ear marking.

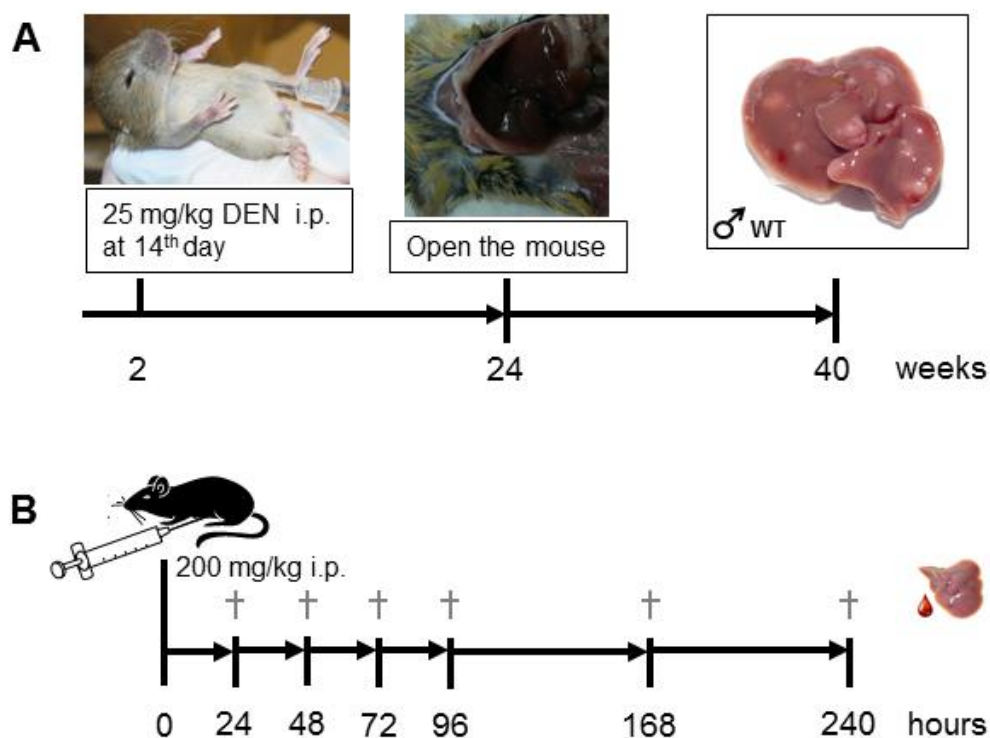


**Figure 2.1 Experimental designs.** (A) Induction of cancer with a single injection of diethylnitrosamine (DEN) at the day 14 and follow up at the age of 24 or 40 weeks. (B) Induction of acute liver injury with high dose of DEN and liver and/or blood sampling at 0, 24, 48, 72, 96, 168 and 240 hours after injection.

Wild type, CcnE1 and CcnE2 knockout mice were kept on a 129/ola background. Hepatocyte specific Cdk2 knockout was generated by crossing Cdk2<sup>ff</sup> mice (Ortega et al., 2003) with Alb-cre mice (Kellendonk et al., 2000). CcnE2 knockout mice were crossed with Cdk2<sup>ff</sup> Alb-cre mice to generate double deficient animals. These animals were intercrossed at least six times.

For hepatocarcinogenesis, a single dose of DEN (25 mg/kg body weight) was injected intraperitoneally at two weeks of age. After 4 or 8 months on normal chow, male mice were sacrificed, their livers were removed and analysed for the presence of HCCs. To induce acute liver damage, 6-8 week old male animals were injected intraperitoneally with 200mg/kg DEN, livers were removed 24 to 240 hours after injection and analysed (Figure 2.1).

### 2.2.2. Genotyping

The correct genotypes were verified by PCR analysis. DNA was prepared from fresh mouse tail biopsies using NID buffer. Mouse tails were digested with 200µl of NID buffer and 1µl of proteinase K at 56°C overnight. Enzyme activity was stopped by heating at 95°C for 5 minutes. The hairs were shortly spun down and 2µl of the supernatant was used for PCR reaction.

NID buffer content	End concentration
KCl	0.05 M
Tris	0.01 M
MgCl <sub>2</sub>	2 mM
Gelatine type 3	0.1 mg/ml
NP-40	0.45 %
Tween 20	0.45 %

PCR reaction and programs were as follows:

Reaction volume	25 $\mu$ l
Primer sense (0,1nmol)	1 $\mu$ l
Primer antisense (0,1nmol)	1 $\mu$ l
Polymerase mix *	12.5 $\mu$ l
dH <sub>2</sub> O	8.5 $\mu$ l
DNA template	2 $\mu$ l

\* ReadyMix™ redtaq™ or HotStarTaq™ Master Mix

Stage	Cyclins PCR		Cre PCR		CDK2 <sup>ff</sup> PCR		cycles
	temp	time	temp	time	temp	time	
Denaturation	95°C	2 min	98°C	2 min	95°C	15 min	1
Denaturation	98°C	15 sec	95°C	15 sec	98°C	20 sec	33-36
Annealing	52°C	30 sec	54°C	30 sec	56°C	30 sec	
Elongation	72°C	30 sec	72°C	30 sec	72°C	1 min	
Additional elongation	72°C	2 min	72°C	5 min	72°C	5 min	1

PCR products were separated by size on 2% (w/v) agarose gels. The agarose was boiled in TAE buffer, cooled at RT for 5-10 min, and 0.4  $\mu$ g/ml ethidium bromide (EtBr) was added. 5x loading dye were added to the samples before application to the gel slots. Gels were run in TAE at 60-120 V. DNA markers were used to determine the specific size of fragments. EtBr, which intercalates into the DNA, enabled the visualisation of the DNA on a UV-transilluminator.

### 2.2.3. Blood sampling and serology

Blood sampling was performed in mice under transient anaesthesia with Isoflurane by penetrating the retro-orbital sinus with a glass capillary. Blood samples were collected in a serum tube and centrifuged at 5000g for 10 minutes. Serum was transferred into a fresh tube and stored at -20°C. Serum transaminases are specific markers for liver damage. In this study, measurement of ALT and AST (alanine-aminotransferase and aspartate-aminotransferase, respectively) was performed in

the clinical routine laboratories of the Institute of Clinical Chemistry and Pathobiochemistry, UK Aachen.

#### 2.2.4. Extraction and sectioning of livers

Mice were sacrificed by cervical dislocation; the abdominal cavity was cut open along the *Linea alba*. Two relaxation cuts were placed along the costal arches at the lateral abdominal walls and liver was removed by dissecting the ligaments and placed in ice cold PBS.

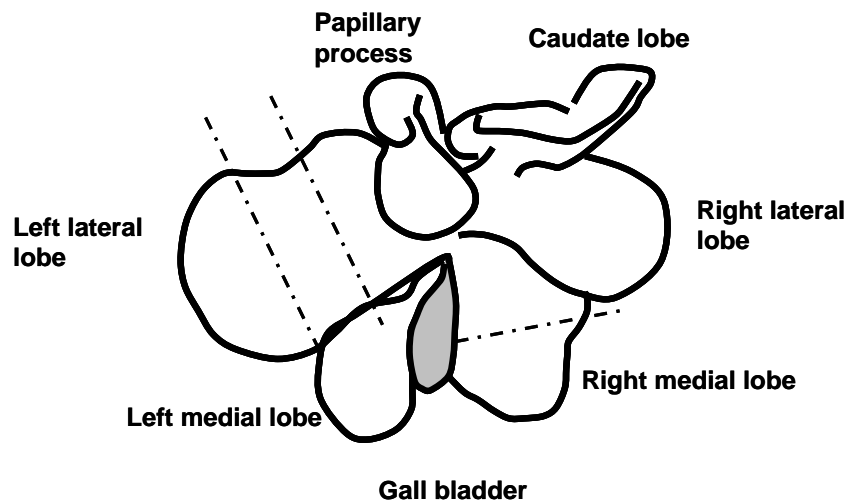


**Figure 2.2 Mouse liver.** Visceral aspect indicating cut levels for sampling (Ruehl-Fehlert et al., 2003).

The gall bladder was removed, third of left lateral lobe, right lateral and caudate lobe were embedded in Tissue-Tek and stored at  $-80^{\circ}\text{C}$ . Middle third of left lateral lobe and half of right medial lobe were placed in 4% PFA for paraffin embedding. Third of left lateral lobe, left medial lobe, half of right medial lobe and papillary process were snap frozen in liquid nitrogen and stored at  $-80^{\circ}\text{C}$ .

#### 2.2.5. Assessment of HCC

Immediately after sacrifice, visible tumors were counted and the size was measured using calliper and Diskus system (Leica).

### 2.2.6. Liver perfusion and isolation of primary hepatocytes

The mice were anaesthetized by intraperitoneal injection of ~300 µl of Ketamin-Xylazin solution. Anesthetized mice were immobilized with tape on all four limbs, the abdomen was opened and intestine was moved aside to expose the *vena portae*. The cannula was inserted in the portal vein and was fixed with a nylon monofilament wire to avoid that the blood pressure removes the needle at the beginning of the perfusion. Perfusion was started with 30 ml solution A, pH 7.4. As soon as the perfusion is started, the hepatic vein was immediately cut to allow perfusate to run out. Liver was perfused with a flow rate of 5 ml/min. Next, the liver was perfused with 30 ml of B solution pH 7.4. Finally, perfusing was switched to solution C with collagenase. At this stage the hepatic tissue was rapidly disaggregated. The tissue was collected and transferred into a plate, gallbladder was removed, and the liver tissue is swirled around to wash hepatocytes out.

<b>Perfusion solutions</b>	<b>Content</b>	<b>Amount</b>
Solution A	EBSS without Ca <sup>2+</sup> & Mg <sup>2+</sup> EGTA	50 ml 100 mM
Solution B	EBSS with Ca <sup>2+</sup> & Mg <sup>2+</sup> HEPES, pH 7.4	30 ml 10 mM
Solution C	EBSS with Ca <sup>2+</sup> & Mg <sup>2+</sup> HEPES, pH 7.4 Collagenase Soybean trypsin inhibitor	50 ml 10 mM 0.3 mg/ml 0.04 mg/ml
<b>Anesthesia</b>	<b>Volume (µl)</b>	
Ketamin	450	
Xylazin	50	
NaCl 0.9%	4500	

Hepatocytes and remaining tissue were collected in 5 ml DMEM and filtered cells through a 70 µm cell strainer. Cells were centrifuged at 500rpm for 1min at room temperature. Pellet was washed with PBS two times. Supernatant was removed and the pellet was resuspended in 20 ml high glucose DMEM supplemented with serum (10% FCS) and antibiotics (Penicillin, Streptomycin). The hepatocytes were counted and plated on precoated plates (Collagen from mouse tail). Mouse primary hepatocytes were cultured in DMEM/high glucose media supplemented with 10%

FCS in a humidified atmosphere containing 5% CO<sub>2</sub> at 37°C. The cells were grown in 100 mm dishes, 6-well or 96-well plates. The cells were allowed to settle down and adhere to culture dishes for 4-5h and then the medium was replaced with fresh one or immediately stimulated.

### 2.2.7. Mouse primary hepatocyte culture

Mouse primary hepatocytes were cultured in DMEM/high glucose media supplemented with 10% FCS in a humidified atmosphere containing 5% CO<sub>2</sub> at 37°C. 10<sup>6</sup> hepatocytes were grown in 100 mm dishes and stimulated with 5 mM DEN for 24 hours following 24, 48 or 72 hours stimulation with EGF (10 ng/ml) and Insulin (20 U/μl), cells were harvested and stored at -80°C. In a 6-well 1.5 x 10<sup>5</sup> hepatocytes were grown and stimulated as well with 5 mM DEN and EGF/Insulin.

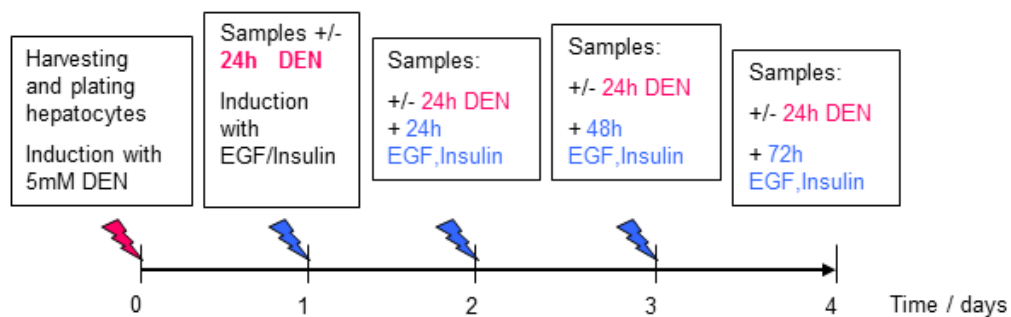


**Figure 2.3 Cell culture experimental design.** Primary hepatocytes were treated with 5 mM DEN for 24 hours and/or subsequently with EGF and Insulin for further 24, 48 or 72 hours.

### 2.2.8. Flow cytometry

Hepatic immune cells and cultured primary hepatocytes were passed through a fluorescence-activated cell sorter (FACS) in order to characterize immune cell populations in the liver and DNA content in cultured primary hepatocytes. Fluorescent markers that specifically stain relevant cellular molecules are detected by FACS and thus allow determination of the number of stained cells as well as the intensity of staining in each cell.

DNA content in primary hepatocytes after DEN and EGF/Insulin stimulation was determined with propidium iodide staining. Propidium iodide stains the DNA and RNA in cells, the intensity of the fluorescence of each cell can be correlated with the cell's DNA content, which in turn correlates with the cell cycle phase. Cells were detached from Petri dishes using 750  $\mu$ l acutase per 6-well for 15 minutes at 37°C and collected. After washing with PBS, cells were fixed in 4% PFA for 15 minutes at RT. Permeabilization was performed with 0.1% Na-Citrate, 0.1% Triton-100x in H<sub>2</sub>O, for 20 minutes at RT. Cells were washed with PBS and stained, 500 $\mu$ l of PI staining solution per stain was used and measured within 30 minutes.

### 2.2.9. RNA extraction, cDNA preparation, Real-Time PCR

RNA was extracted from mouse livers or primary hepatocytes using peqGOLD RNA Pure<sup>TM</sup> (Peqlab) following manufacturer's instructions. A piece of liver tissue was minced in peqGOLD RNA with an electric homogenizer. Lysates were incubated at room temperature for five minutes. After addition of 0.2 volumes of chloroform to the supernatants followed by centrifugation at 12000g, the upper phases were incubated 10 minutes with isopropanol and RNA was pelleted by centrifugation at 12000g at 4°C. The pellets were washed two times with 1 ml of 70% ethanol, air dried for 5 minutes and eluted in RNase-free water. RNAs were quantified by spectrophotometry at an optical density (OD) of 260 nm. A 260/280 ratio  $\geq$ 1.8 was considered high purity.

<b>Reverse transcription reaction mix</b>	<b>Volume per reaction</b>
10x Buffer RT	2 $\mu$ l
dNTP mix	2 $\mu$ l
Oligo DT	2 $\mu$ l
Omniscript Reverse transcriptase	1 $\mu$ l
Template RNA (1 $\mu$ g/ $\mu$ l)	2 $\mu$ l
<b>Total reaction volume</b>	<b>20 <math>\mu</math>l</b>

Reverse transcription was performed using an Omniscript kit (Qiagen) according to the manufacturer's protocol. Reactions were carried out in 20  $\mu$ l volumes. Reactions were incubated in a PCR thermocycler at 37°C for 60 min, and



95°C for 5 min and then cooled to 4°C. After reverse transcriptase, samples were diluted by adding purified water.

For real-time quantitative RT-PCR, the Real-Time PCR System (AB 7300) was used. RT-PCR was performed in duplicate in 25 µl reaction volumes. Three-step PCR cycling was carried out as follows: 50 °C for 2 min (1 cycle), 95°C for 10 min (1 cycle), 95°C for 15 s, and 60°C for 1 min (40 cycles). At the end of the PCR, baselines and threshold values were established using AB 7300 System SDS software, and the Ct values were exported to Microsoft Excel (Microsoft Corp., Redmond, WA) for analysis. Expression of mRNA was calculated using a relative quantification method (Pfaffl, 2001), which determines the relative quantification of a target gene in comparison to a reference gene. Analysis was carried out using the sequence detection software supplied with the AB 7300. This software calculates the Ct for each reaction and uses it to quantify the amount of starting template in the reaction. The relative expression ratio of a target gene is calculated based Ct deviation of an unknown sample versus a control and is expressed in comparison to the reference gene GAPDH.

<b>Real-time PCR reaction mix</b>	<b>Volume per reaction</b>
Primer sense	2 µl
Primer antisense	2 µl
SYBR green	12.5 µl
cDNA	5 µl
dH <sub>2</sub> O	3.5 µl
<b>Total reaction volume</b>	<b>25 µl</b>

#### 2.2.10. DNA isolation from frozen livers

A small piece of frozen liver was incubated in 700 µl of lysis buffer (50 mM Tris-HCl pH 8, 100 mM EDTA pH 8, 100 mM NaCl, 1% SDS) supplemented with 35 µl proteinase K and incubated at 37°C, 350 rpm on a thermomixer overnight. The solution was centrifuged at 5000g and 4°C for 5 minutes, supernatant containing DNA was transferred in a clean microcentrifuge tube and precipitated with 800 µl isopropanol. After centrifugation at 13000g, 4°C for 10 minutes, the supernatant was discarded and pellet was washed twice with 1 ml of cold 70 % ethanol. Pellet was

dissolved in 50  $\mu$ l TE buffer (10 mM Tris, pH 7.5 with 1 mM EDTA) and concentration was determined by measuring OD at 260. A 260/280 ratio  $\geq 1.8$  was considered high purity.

### 2.2.11. DNA labelling and measuring of AP sites

AP sites are apurinic/aprimidinic (abasic) sites in DNA, resembling one of the prevalent lesions of oxidative DNA damage. Unrepaired abasic site inhibit topoisomerase, replication and transcription, can be mutagenic because of bypass synthesis on nontemplated DNA. The measurement of AP sites was done by comparing samples to the standard curve using OxiSelect Oxidative DNA Damage Quantitation Kit (AP sites). Genomic DNA was labelled with ARP (Aldehyde Reactive Probe) using OxiSelect Oxidative DNA Damage Quantitation Kit (AP sites) following manufacturer's instructions.

### 2.2.12. Whole cell protein extracts

A piece of frozen liver was minced in NP-40 protein extraction buffer and centrifuged 10 min at 12000g, 4 °C. In case of cultured cells, hepatocytes were collected in PBS to microcentrifuge tube, spun down 1 min at 500 rpm, supernatant was removed. Pellet was resuspended in NP-40 protein extraction buffer, then snap frozen and warmed up few times to break the cell membrane and finally centrifuged 10 min at 12000g, 4 °C. Supernatant with whole cell proteins was aliquoted and frozen at -80 °C.

<b>NP-40 protein extraction buffer</b>	
Tris-HCl pH 7.5	50 mM
NaCl	150 mM
NP-40	0.50%
NaF	50 mM
Na <sub>3</sub> VO <sub>4</sub>	1 mM
DTT	1 mM
PMSF	1 mM
1 Complete mini tablet per 10 ml buffer	
1 PhosSTOP tablet per 10 ml buffer	

### 2.2.13. Isolation of nuclear and cytoplasmic cell fractions

A piece of frozen liver was minced in buffer A, incubated for 10 min at 4 °C. 10% of NP-40 added, mixed with tipping the tube, and incubated at 4°C for 1 min. Nuclei were pelleted for 1 min at 10000 rpm and 4 °C. Supernatant was saved and frozen at -80 °C as cytoplasm fraction. Nuclei pellet was washed with 1 ml of buffer A 2-3 times. Pellet was resuspended in buffer C, incubated 30 min on ice, mixed gently, and spun down 10 min at 10000 rpm, 4 °C. Nuclear proteins (supernatant) were saved and frozen at -80 °C. Buffers A and C are made as follows:

Buffer A		Buffer C	
HEPES pH 7.6	10 mM	HEPES pH 7.8	50 mM
MgCl <sub>2</sub>	2 mM	KCl	50 mM
KCl	10 mM	NaCl	300 mM
EDTA	0.1 mM	EDTA	0.1 mM
+ Protease inhibitors		Glycerol	10%
		+ Protease inhibitors	

### 2.2.14. Protein concentration measurement

The concentration of whole protein extracts was performed using BIO-RAD Protein Assay reagent. This technique was first described by Bradford *et al.* (Bradford, 1976) and based on the absorbance maximum for an acidic solution of Coomassie Brilliant Blue G-250 shifts from 465 nm to 595 nm when binding to protein occurs. According to manufacturer's protocol protein and standard were measured in a spectrophotometer at OD<sub>595</sub>. The OD<sub>595</sub> of each sample was compared to a standard curve prepared with BSA.

Nuclear extract concentrations were measured using Bio-Rad Dc Protein Assay because of higher sensitivity for low protein concentrations. According to manufacturer's protocol, protein and standard were measured in a spectrophotometer at OD<sub>750</sub>. The OD<sub>750</sub> of each sample was compared to a standard curve prepared with BSA.

### 2.2.15. Western Blot

Protein samples were separated electrophoretically on 10%, 12% or 15% denaturing SDS-polyacrylamide gel or on pre-cast 4-12% polyacrylamide gel (Invitrogen). Gel and buffer were prepared according to table (Laemmli, 1970):

5x Protein loading buffer		1x SDS Running buffer	
Tris-HCl pH 6.8	125 mM	Tris-Base	1.25 M
Glycerol	50%	Glycine	2 M
SDS	5%	SDS	1%
Bromphenol blue	0.025%		
β-Mercaptoethanol 50 µl per 1 ml loading buffer			

In short, 5x Protein loading buffer was added to each sample in appropriate volumes and samples were boiled at 96 °C for 5 min before loading to the gel slot. Separation was performed in 1x SDS running buffer at 50-80 V overnight or in MOPS running buffer at 120 V for approximately 2 h (pre-cast gel system). For immunological detection, the separated proteins in gel were transferred to a nitrocellulose membrane.

Reagent	Resolving Gel			Stacking Gel
	10%	12.5%	15%	5%
Percent	10%	12.5%	15%	5%
dH <sub>2</sub> O	20 ml	16.4 ml	12.3 ml	13 ml
1.5M Tris-HCl, pH 8.8	12.5 ml	12.5 ml	12.5 ml	-
0.5M Tris-HCl, pH 6.8	-	-	-	6,25 ml
30% Acrilamide	16.5 ml	20.3 ml	24.35 ml	5 ml
10 % SDS	500 µl	500 µl	500 µl	250 µl
10 % APS	500 µl	500 µl	500 µl	500 µl
100 % TEMED	37.5 µl	37.5 µl	37.5 µl	37.5 µl

A wet blotting chamber (PeqLab) was used to transfer the separated proteins from the polyacrilamide gel to a nitrocellulose membrane. Whatman paper, nitrocellulose membrane and polyacrilamide gel were soaked in transfer buffer. Transfer was performed according to standard proceedings.

<b>20x MOPS running buffer (500 ml)</b>		
<b>Reagent</b>	<b>Mass (gram)</b>	<b>Final concentration (1x)</b>
MOPS	104.6	50 mM
Tris base	60.6	50 mM
SDS	10.0	3.5 mM
EDTA	3.0	1 mM

Successful transfer and equal loading was confirmed by Ponceau Red staining. For immunological detections, the non-specific binding sites were blocked for 1.5 hours in 5% non-fat dry milk diluted in PBS-Tween (PBST) or in 1x Roti-block. The membrane was shortly washed and then incubated overnight at 4 °C in PBST with primary antibody at optimized dilutions. The membrane was washed 3x5 min in PBST and then incubated with secondary antibody diluted 1:5000 in PBST for 1h at RT. After incubation, the membrane was washed 3x5 min in PBST and then incubated in ECL Substrate (Pierce) for 5 min. The membrane was exposed to hyperfilm (Amersham) or a digital detection system (FUJIFILM).

#### 2.2.16. Immunoprecipitation Assay

Protein-protein interactions were identified by immunoprecipitation experiments using protein A/G agarose beads. Total protein extracts (1 mg in 500  $\mu$ l volume) were precleared with protein A/G agarose beads to remove all proteins that bind unspecific to the beads and murine immunoglobulin for 2 hours at 4°C on overhead shaker. The mixture was centrifuged at 2000g at 4°C, the pellet was discarded and the supernatant was transferred into fresh tube and incubated with 4  $\mu$ l of antibody at 4°C with overhead rotation overnight. Immunoprecipitated complexes were collected with 40  $\mu$ l of protein A/G agarose beads for 1 hour, then spun down and pellet was washed twice with 1 ml of cold NP40 buffer. Protein-protein-antibody complexes were dissolved from the beads by denaturation in 10  $\mu$ l 5x SDS loading buffer supplemented with  $\beta$ -mercaptoethanol and boiling at 95°C for 10 minutes. Agarose beads were spun down at 12000 rpm and the supernatant containing precipitated proteins was loaded on SDS PAGE gel or stored at -20°C

### 2.2.17. Gel silver staining

SDS-PAGE was fixed directly after running in a mixture of 40% ethanol and 10% acetic acid for 30 minutes. The fixed gel was then incubated in sensitizer (30% EtOH, 0.2% sodium thiosulphate, 7% sodium acetate) for 30 min and washed with dH<sub>2</sub>O three times 5 min before silver staining. Silver staining was performed with 0.5 % silver nitrate for approximately 10 min. After washing for 5 min with dH<sub>2</sub>O, gel was developed with 2.5% sodium carbonate and 0.02% formaldehyde mixture until bands are clearly seen (approx. 3-4 min). The developing reaction was stopped with 0.5% Glycine for 30 min. All reactions were performed at RT.

### 2.2.18. Caspase 3 Assay

For protein extractions from frozen livers, AFC lysis buffer was used. Samples were shock frozen in liquid nitrogen and stored at -80°C.

<b>AFC Lysis buffer</b>	<b>End concentration</b>
Hepes pH 7.4	10 mM
Chaps	0.1 %
EDTA pH 8	2 mM
DTT	5 mM
Pefa Block	1 mM
Complete mini	1 tablet

Caspases-3 is a key enzyme in apoptosis. The assay made use of a Caspase-3 specific substrate (DEVD) linked to a fluorochrome (AFC). Active Caspase-3 specifically cleaves the substrate DEVD between D and AFC, thus releasing free AFC which can be quantified by UV spectrofluorometry. These tetrapeptide substrates are used to identify and quantify Caspase-3 activity in apoptotic protein lysates. Per reaction tube 487.5 µl master mix and 12.5 µl proteins were mixed. Following 200 µl in duplicate were pipetted into a 96-well-cellstar plate and incubated at 37°C. Master mix with lysis buffer was set as blank. AFC-release was measured in 5 minute intervals and stopped after 2 h.

<b>Caspase-3 assay mix (Volume per reaction)</b>		<b>25x Reaction buffer (End concentration)</b>	
25x Reaction Buffer	20 $\mu$ l	Pipes	250 mM
dH <sub>2</sub> O	465 $\mu$ l	EDTA	50 mM
substrate	2.5 $\mu$ l	Chaps	2.5 %
Protein sample	12.5 $\mu$ l	DTT	125 mM

### 2.2.19. Immunofluorescence staining

Cryosections (5 $\mu$ m), from mouse livers, were fixed with 4% paraformaldehyde for 15 min and rehydrated with PBS for 15 min. All subsequent steps were carried out at room temperature unless otherwise indicated in a humid light tight box to prevent drying and fading. PBS containing 5% goat serum and 0.3% Triton was used for blocking for one hour followed by an overnight incubation with primary antibody in blocking solution at optimized dilutions at 4°C. Slides were washed with PBS for 15 min and incubated with secondary antibody diluted 1:200 in PBS for one hour at RT. Nuclei were counterstained with DAPI in mounting medium. Expression was visualized and documented by fluorescence microscopy (Zeiss).

For CD11b, F4/80 and Ly6G immune cells staining cryosections were fixed with 4% paraformaldehyde for 15 min and rehydrated with PBS (supplemented with 0.02% sodium azide) three times for 3 min. Tissue sections were blocked with PBS-azide containing 0.2% BSA for 5 minutes at RT. CD11b, F4/80 or Ly6G antibody were diluted in PBS-azide with 1% mouse serum at 1:200 dilutions. Incubation with primary antibody was for 45 minutes at RT in a humidified chamber. Slides were washed with PBS-azide and blocked once again with PBS-azide + 0.2% mouse serum. Secondary antibody was diluted 1:300 in PBS-azide with 1% mouse serum and sections were incubated for 45 minutes at same conditions as before. Stained sections were washed three times in PBS-azide, three times in deionized water and mounted with mounting medium containing DAPI.

TUNEL (TdT-mediated dUTP nick end labelling) is an established method for in situ labelling of DNA strand brakes that occur early during apoptosis. Terminal deoxynucleotidyl transferase (TdT) is used to introduce labelled nucleotides into partially degraded DNA. Liver cryosections were fixed with 4% paraformaldehyde for

20 min and rehydrated with PBS for 30 min. Sections were treated with 3% H<sub>2</sub>O<sub>2</sub> in methanol for 10 min, and then permeabilized with 0.1% Triton 100x, 0.1% Na-citrate for 2 min at 4°C. Slides were washed with PBS and stained with TUNEL mix (per section: 0.5µl enzyme, 4.5µl TUNEL dilution buffer, 45µl buffer) in humidified chamber overnight at 4°C. After washing with PBS stained sections were mounted with DAPI mounting medium or proceeded with staining for IHC.

#### 2.2.20. β-galactosidase activity staining

Cryosections (7µm) from mouse livers were fixed with 0.5% glutaraldehyde in PBS supplemented with 1mM MgCl<sub>2</sub> for 15 min at RT and then washed with PBS, 1mM MgCl<sub>2</sub> for approximately 15 minutes at RT. Staining was performed with staining solution (0.2 mg/ml x-gal, 5mM potassium ferricyanide, 5mM potassium ferrocyanide in PBS, 1mM MgCl<sub>2</sub>) overnight in the humid chamber at 37°C. Sections were washed in PBS, 1mM MgCl<sub>2</sub>, counterstained with nuclear fast red and mounted with glycerol gelatine.

#### 2.2.21. Immunohistochemistry

Paraffin embedded sections were deparaffinised and rehydrated with xylene and decreasing percentages of ethanol. Antigen retrieval was performed by cooking sections in sodium citrate buffer for 6 minutes in a microwave. After cooling for 15 minutes, sections were rinsed in running tap water and endogenous peroxidases were quenched for 15 minutes. Sections were washed under running water, washed 5 minutes in PBS. Following blocking with biotin blocking reagent for 15 minutes and with avidin D blocking reagent for 15 minutes, sections were blocked in PBT (PBS, 0.1% BSA, 0.2% TritonX-100) and then incubated overnight with primary antibody at 4°C in a humid atmosphere. Slides were washed twice with PBS and secondary antibody was applied for 1 hour at room temperature in humidifying box, parallel the HRP-ABC solution was made and incubated at least 30 minutes at room temperature before applying to slides. Sections were rinsed twice in PBS and HRP-ABC solution was applied for 1 hour at room temperature in a humidified box. After washing twice in PBS, signal was developed with DAB and counterstained with haematoxylin.



Dehydrating was performed increasing percentages of ethanol and xylene, mounted with Roti-histokit and visualized by bright field microscopy.

## 3. Results

### 3.1. Cyclin E1 deletion inhibits DEN-induced hepatocarcinogenesis

The role of E-type cyclins for cell proliferation and cancer development is incompletely understood due to contradictory findings. On the one hand, cyclin E1 (CcnE1) and cyclin E2 (CcnE2) are not absolutely essential for development or proliferation of continuously cycling cells (Geng et al., 2003) and ablation of CcnE1 or CcnE2 in the liver does not result in impaired hepatocyte proliferation or liver regeneration (Nevzorova et al., 2009). On the other hand, CcnE1 is overexpressed in various tumors including hepatocellular carcinoma (HCC) and correlates with poor prognosis of those patients (Jung et al., 2001).

To further evaluate the function of E-type cyclins for hepatocarcinogenesis, liver tumors were induced in CcnE1<sup>-/-</sup>, CcnE2<sup>-/-</sup> and wild type (WT) mice by a single injection of diethylnitrosamine (DEN) at two weeks of age (Vesselinovitch, 1980). In agreement with earlier studies (McClain et al., 2001), 95% of WT mice (21/22) developed macroscopically visible tumor nodules 38 weeks after DEN treatment (Figure 3.1A, upper panel and Figure 3.1B) with an average number of 36 tumors ( $\pm 6$ ) per liver. Similarly, 100% of DEN-treated CcnE2<sup>-/-</sup> mice (19/19) revealed HCC at the age of 40 weeks with an average of 40 tumors per liver and median tumor diameter of 7 mm ( $\pm 3$  mm, Figure 3.1A, medium panel and Figure 3.1B). In sharp contrast, CcnE1<sup>-/-</sup> mice were highly protected from DEN-mediated hepatocarcinogenesis. Tumor initiation and tumor progression were strongly inhibited by ablation of CcnE1. Only 50% (8/16) of CcnE1<sup>-/-</sup> animals developed liver tumors at all with low average frequency (3 tumors per liver, Figure 3.1A, lower panel and Figure 3.1B) and size (diameter of 2mm  $\pm 1$  mm), compared to WT or CcnE2<sup>-/-</sup> mice (Figure 3.1C). In agreement with strongly decreased tumor burden in DEN-treated CcnE1<sup>-/-</sup> mice, the liver mass index in these mice at the age of 40 weeks was normal (approximately 5%  $\pm 1$ %) (Figure 3.1D) compared to healthy WT mice (Nevzorova et al., 2009). In contrast, WT and CcnE2<sup>-/-</sup> mice showed strongly increased liver mass index (9%  $\pm 5$ %) which served as an additional proof for massive tumor load in these animals.

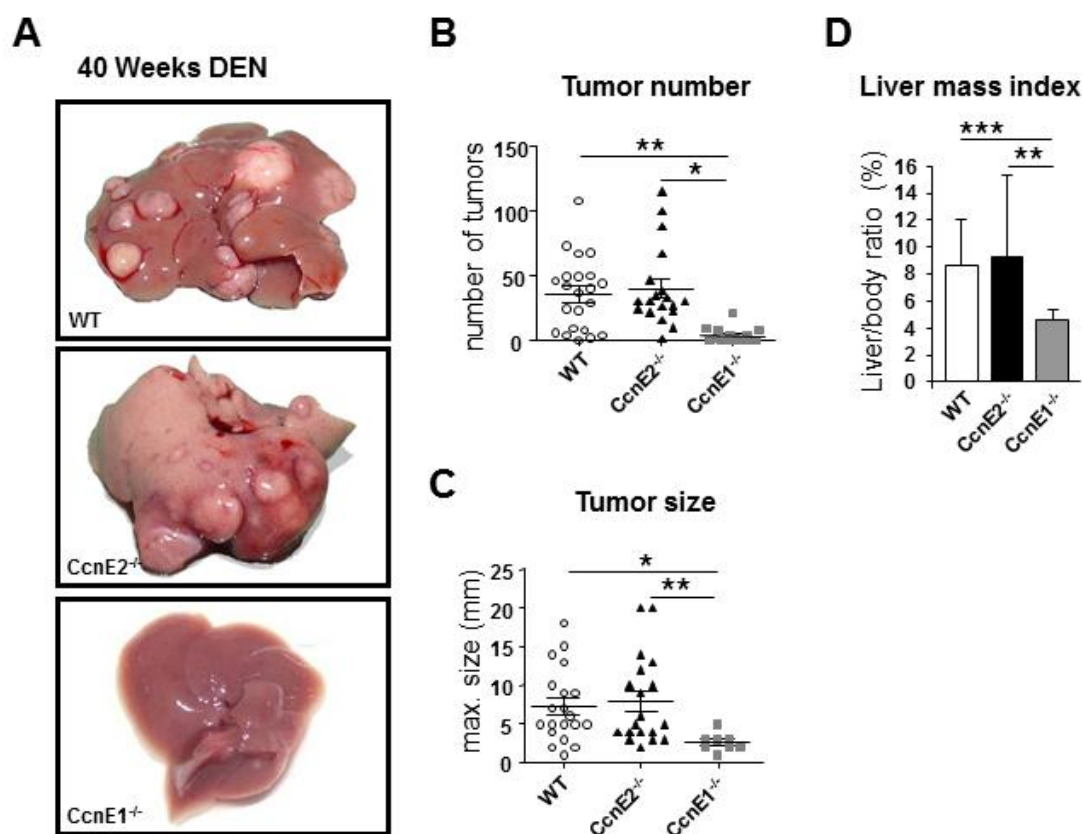


**Figure 3.1 Deletion of CcnE1 inhibits DEN-induced hepatocarcinogenesis.** WT (n=22), CcnE1<sup>-/-</sup> (n=16) and CcnE2<sup>-/-</sup> (n=19) male mice at the age of 14 days were treated once with DEN (25mg/kg i.p.). Animals were sacrificed at the age of 40 weeks and analysed for markers of hepatocellular carcinoma. (A) Macroscopic appearance of representative 40 week old livers and tumors derived from WT, CcnE2<sup>-/-</sup> and CcnE1<sup>-/-</sup> mice. Tumor burden for each individual mouse was characterized by analysing total number of visible tumors per mouse (B) and maximal tumor size per mouse (C). (D) Liver/body weight ratio in DEN-treated WT, CcnE2<sup>-/-</sup> and CcnE1<sup>-/-</sup> mice at the age of 40 weeks. \*: p<0.05; \*\*: p<0.005; \*\*\*: p<0.0005.

These initial results indicate that CcnE1 is essential for DEN-induced hepatocarcinogenesis, whereas ablation of CcnE2 does not affect tumor initiation or tumor progression.

Histologically, WT and CcnE2<sup>-/-</sup> liver sections of 40 week old DEN-treated animals revealed strong dysplasia and abnormal tissue architecture, whereas CcnE1<sup>-/-</sup> liver sections appeared mostly normal with infrequent small tumor lesions (Figure 3.2A), which was in good agreement with the macroscopic liver phenotype. The proliferating cell nuclear antigen (PCNA) is a key factor for onset of DNA synthesis and thus an established marker for cell proliferation. Immunostaining of randomly selected liver sections from DEN-treated WT and CcnE2<sup>-/-</sup> mice revealed

many proliferating cell PCNA positive hepatocytes hinting at excessive cell proliferation, which was much less evident in *CcnE1*<sup>-/-</sup> livers (Figure 3.2B).

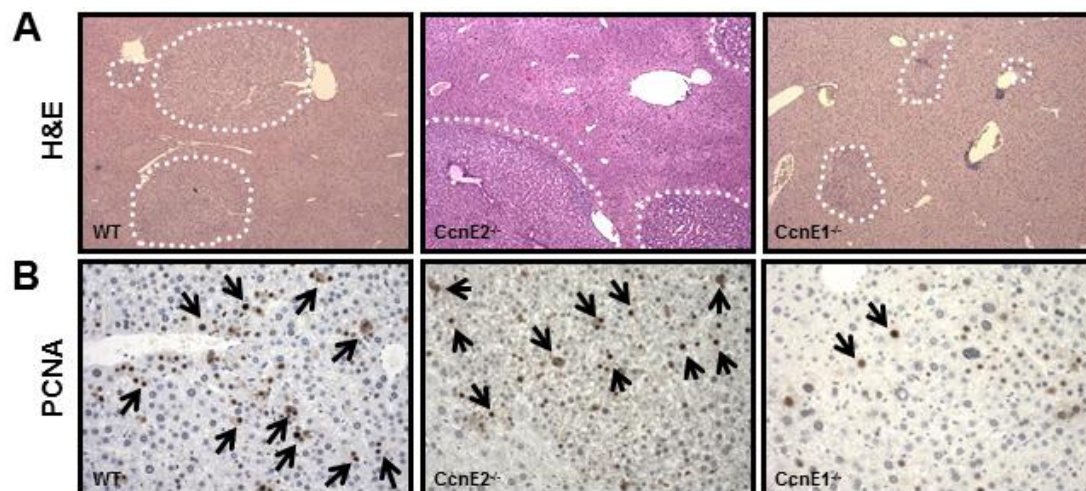


**Figure 3.2 Decreased S-phase entry of *CcnE1*<sup>-/-</sup> liver tumor cells at 40 weeks.** (A) Haematoxylin and eosin (H&E) staining of paraffin embedded tissue sections of mice treated as above. Tumor areas are highlighted with dotted line. Original magnification: 100x. (B) PCNA expression in liver samples was determined by immunohistochemistry. Positive PCNA expression is stained in brown and highlighted by arrows. Original magnification: 200x.

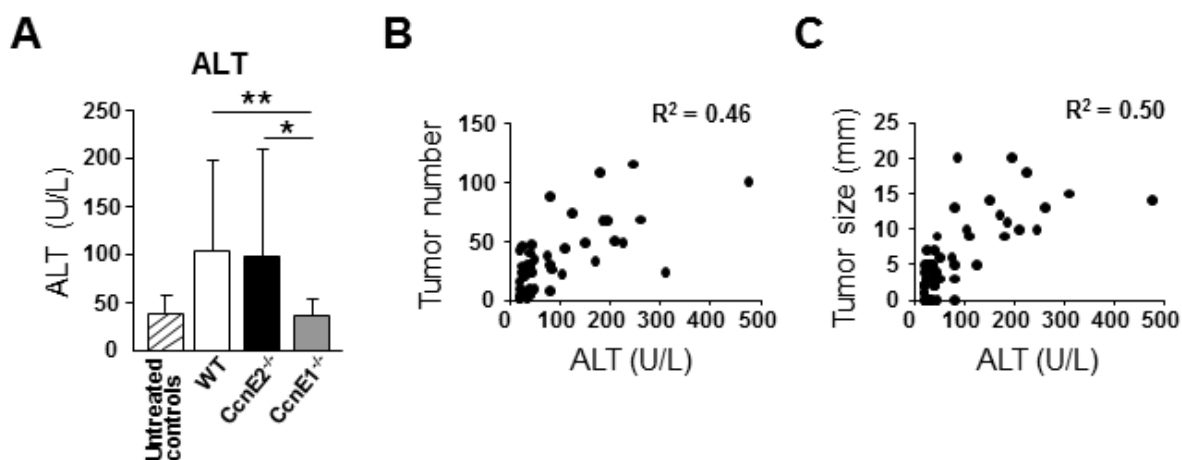


**Figure 3.3 Liver injury marker ALT correlates with tumor number and size.** (A) Serum alanine-aminotransferase (ALT) levels in DEN-treated mice at the age of 40 weeks. (B-C) Correlation analysis of tumor number or tumor size with ALT. WT, *CcnE1*<sup>-/-</sup> and *CcnE2*<sup>-/-</sup> animals 40 weeks after DEN-treatment were included in the analysis; animals were not differentiated by genotype.

Alanine-aminotransferase (ALT) is a liver enzyme used as a standard indicator for liver injury. In 40 weeks old DEN-treated WT and *CcnE2*<sup>-/-</sup> mice ALT levels were slightly increased with an average of 100 U/L although with vast oscillations (Figure 3.3A). In contrast, ALT values were significantly lower in *CcnE1*<sup>-/-</sup> animals and similar to levels of healthy untreated mice (Figure 3.3A). Interestingly, this study also

revealed that ALT levels positively correlate with tumor number and tumor size as shown in Figure 3.3B-C.

To determine a potential role of CcnE1 or CcnE2 in early tumor development, cohorts of WT, CcnE1<sup>-/-</sup> and CcnE2<sup>-/-</sup> mice were treated with DEN as before but sacrificed already at the age of 24 weeks. At this time point, small tumor nodules and liver lesions were macroscopically visible in 40% (7/15) of WT and in 47% (8/17) of

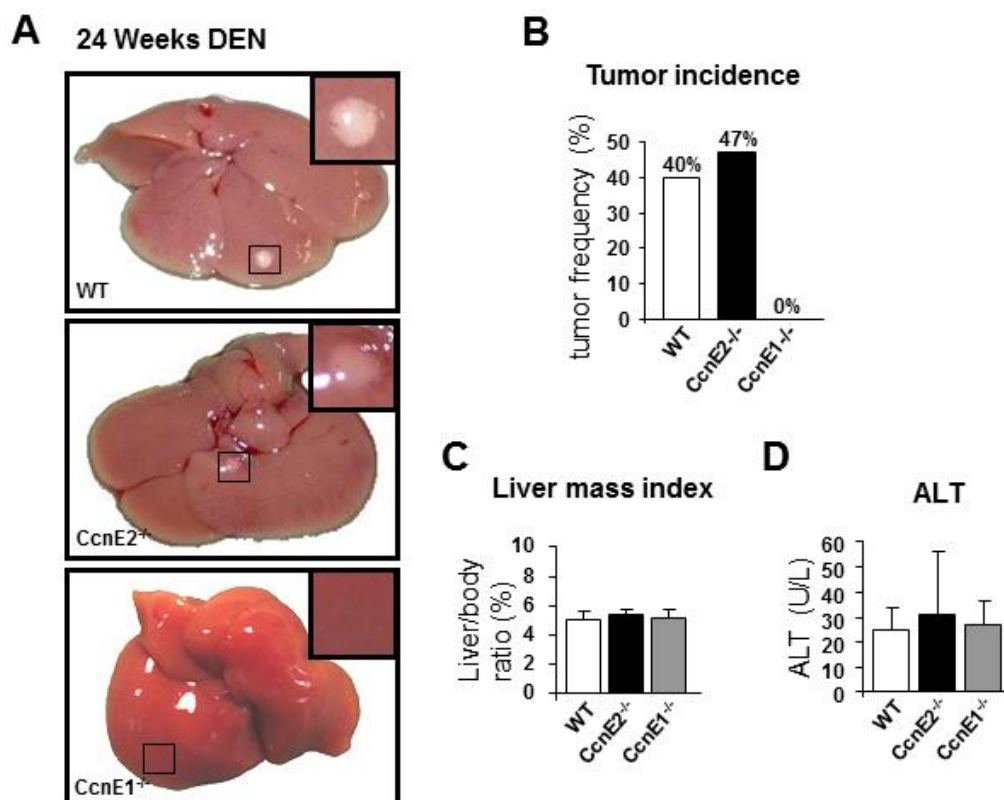


**Figure 3.4 Early inhibition of DEN-induced hepatocarcinogenesis in CcnE1<sup>-/-</sup> mice.** WT (n=15), CcnE1<sup>-/-</sup> (n=15) and CcnE2<sup>-/-</sup> (n=17) male mice were treated once with DEN (25mg/kg i.p.) at the age of 14 days. At the age of 24 weeks, animals were sacrificed and analysed for markers of hepatocellular carcinoma. (A) Macroscopic appearance of representative 24 week old livers and tumors derived from WT, CcnE2<sup>-/-</sup> and CcnE1<sup>-/-</sup> mice. (B) Tumor frequency of mice at the age of 24 weeks, the values represent the percentage of mice with macroscopic visible tumors (tumor size 0.5 – 2 mm in diameter). (C) Liver/body weight ratio in DEN-treated WT, CcnE2<sup>-/-</sup> and CcnE1<sup>-/-</sup> mice at the age of 24 weeks. (D) Serum ALT levels in DEN-treated mice at the age of 24 weeks.

CcnE2<sup>-/-</sup> mice, whereas all CcnE1-deficient animals (n=15) revealed normal liver morphology without visible tumor nodules (Figure 4A-B). However, no differences in liver mass index (Figure 3.4C) or ALT values (Figure 3.4D) were observed between the groups which rather reflects the early stage of tumor development in this experiment.

Histologically, dysplastic lesions were clearly detectable in WT and CcnE2<sup>-/-</sup> livers at this age and comprised 1.65% and 2.63% of total tissue area, respectively (Figure 3.5A). In contrast, only approximately 0.31% of liver tissue was considered dysplastic in DEN-treated CcnE1<sup>-/-</sup> mice at this age (Figure 3.5A). In line with these findings, PCNA expression was elevated in WT and CcnE2<sup>-/-</sup> livers as measured by immunostaining, which was not evident in CcnE1<sup>-/-</sup> mice (Figure 3.5B). These results demonstrate that ablation of CcnE1 is already protective in an early state of tumor development in the liver.

Overexpression of E-type cyclins is a hallmark of many human cancers including breast cancer and hepatocellular carcinoma (Caldon and Musgrove, 2010). To determine if this is also true in the DEN-model in mice, mRNA levels of CcnE1, CcnE2 and its downstream target CcnA2 were measured where applicable in DEN-induced liver tumors and compared to basal expression in untreated mice. CcnE1 mRNA expression was not changed at early stage of tumor development in the cohorts at the age of 24 weeks in comparison to untreated controls. In contrast, CcnE1 mRNA was significantly upregulated in tumor nodes of DEN-treated livers at the age of 40 weeks (Figure 3.6A), corroborating the findings in human HCC studies. This result validates the relevance of CcnE1 overexpression in DEN-induced hepatocarcinogenesis in mice designating the importance in advanced tumor development. Interestingly, CcnE2 mRNA was markedly downregulated in livers of DEN-treated CcnE1<sup>-/-</sup> mice at the age of 40 weeks (Figure 3.6B) suggesting that tumor resistance is related to overall low CcnE expression levels.

Cyclin A2 (CcnA2) is a promoter of S-phase progression. To determine if reduced tumor susceptibility in CcnE1<sup>-/-</sup> mice is associated with diminished DNA replication, CcnA2 mRNA expression was also evaluated in DEN-treated WT, CcnE1<sup>-/-</sup> and CcnE2<sup>-/-</sup> mice (Figure 3.6C). No differences in CcnA2 expression were observed between the cohorts at the age of 24 weeks, indicating that the impact of DNA synthesis is minor during early liver tumorigenesis.



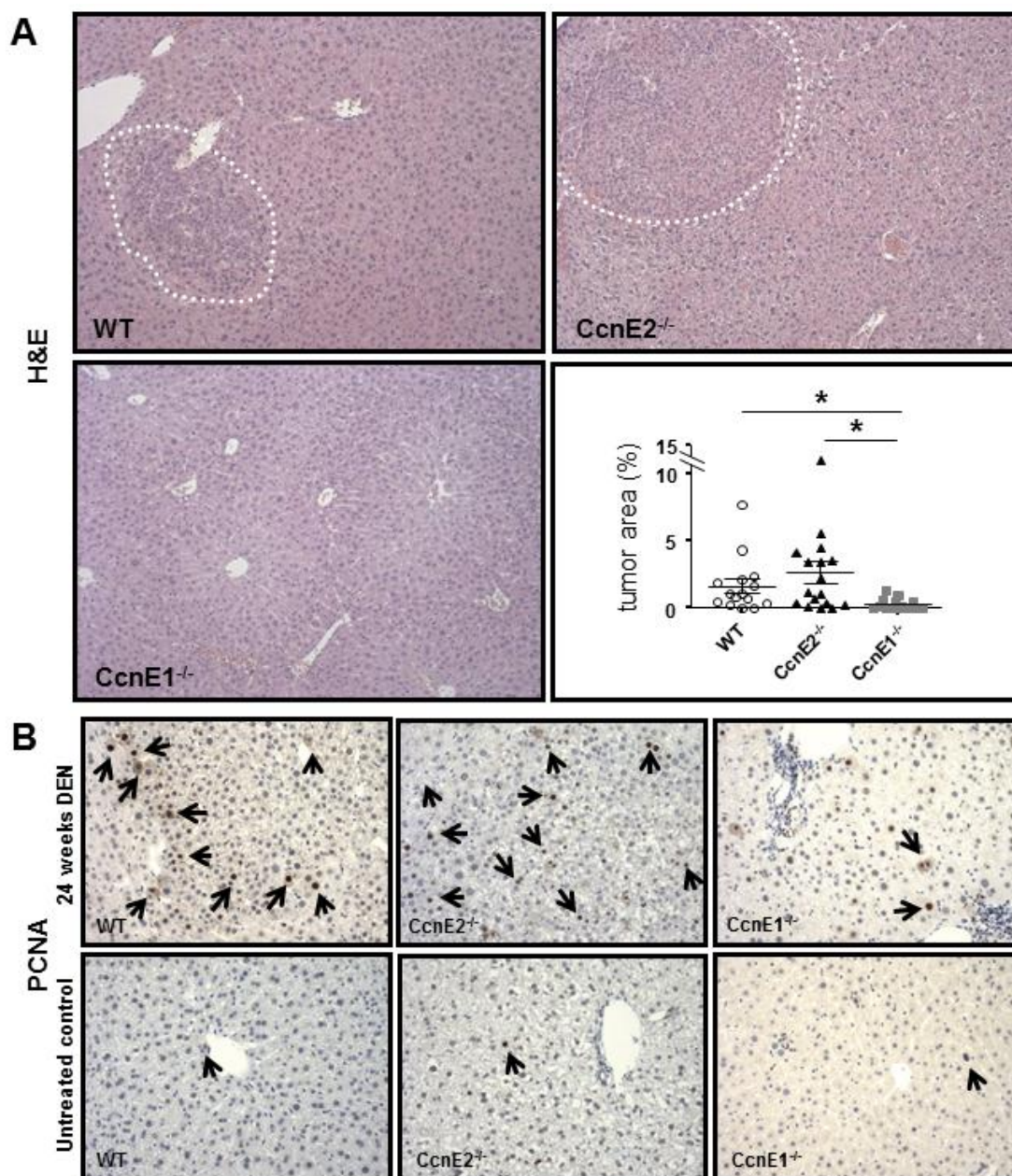


**Figure 3.5 Decreased S-phase entry of CcnE1<sup>-/-</sup> liver tumor cells at 24 weeks.** (A) H&E staining of paraffin embedded tissue sections of DEN-treated mice at the age of 24 weeks. Tumor areas are highlighted with dotted line (upper panel and lower panel left). Original magnification: 100x. Tumor area in tissue sections (lower panel right). Tumor area represents surface size occupied with tumors visible in H&E stained sections and compared to the whole section size. \*: p<0.05. (B) PCNA expression in liver samples was determined by immunohistochemistry. PCNA positive liver cells are stained in brown and are highlighted by arrows; 24 week old DEN treated animals (upper panel) are compared to untreated controls (lower panel). Original magnification: 200x.

However, at the age of 40 weeks liver samples from WT and CcnE2<sup>-/-</sup> mice revealed significantly increased CcnA2 expression. In contrast, under these conditions CcnA2 was only expressed at baseline level in CcnE1<sup>-/-</sup> livers (Figure 3.6C). Thus, CcnE1

but not CcnE2 is required for driving CcnA2 and DNA replication during tumor progression in the liver.

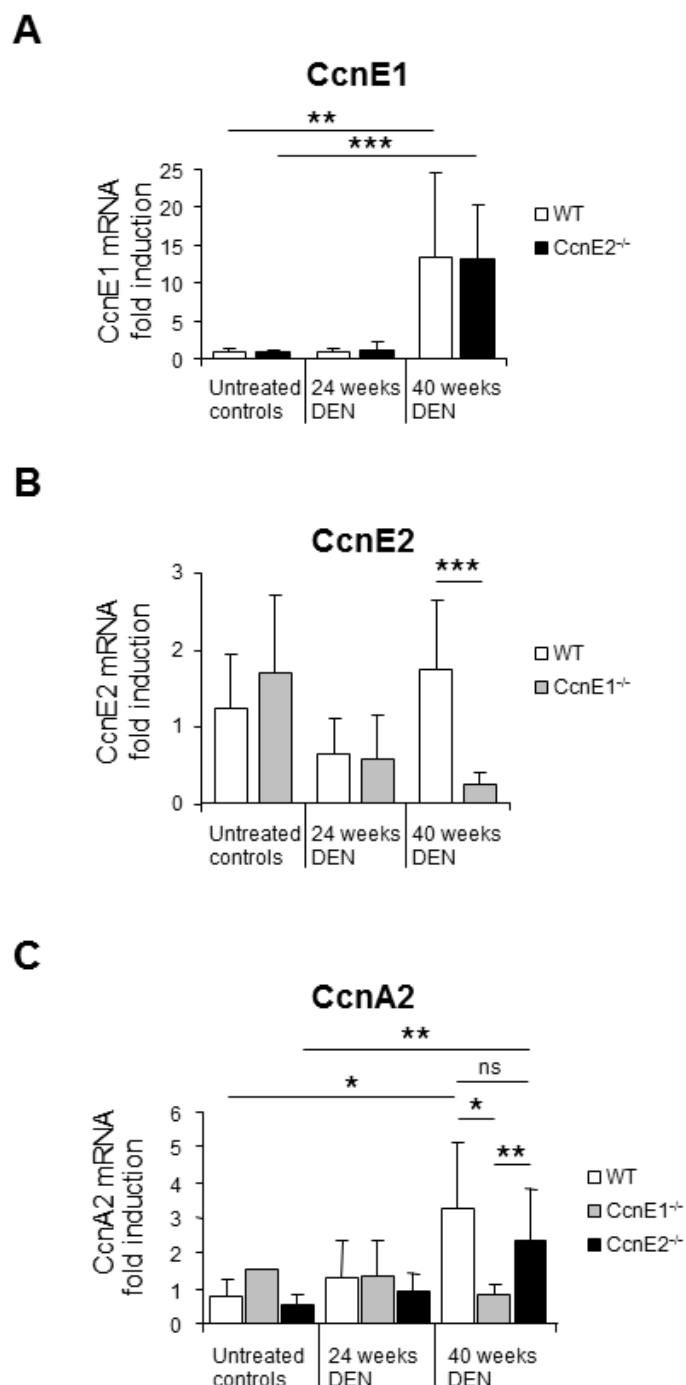


**Figure 3.6 Effects of CcnE1 on overall cyclin gene expression in DEN induced hepatocarcinogenesis.** mRNA expression was measured by real-Time PCR analysis in untreated control, 24 week and 40 week liver and liver tumor tissue for WT (white bars), CcnE1<sup>-/-</sup> (grey bars) and CcnE2<sup>-/-</sup> (black bars) mice treated as described in figures 3.1 and 3.4 (A) CcnE1 mRNA, (B) CcnE2 mRNA, (C) CcnA2 mRNA expression. Indicated gene expression levels were normalized to expression of the housekeeping gene GAPDH and calculated as fold induction in comparison to untreated controls. Each bar represents a value of minimum 4-6 animals, data are presented as the average  $\pm$  s.d. \*:  $p < 0.05$ ; \*\*:  $p < 0.005$ ; \*\*\*:  $p < 0.0005$ .

Replicative senescence is a natural barrier to clonal expansion of tumor cells which plays a vital part in limiting tumorigenesis (Mooi and Peeper, 2006; Prieur and Peeper, 2008) and is in part controlled by cell cycle inhibitors p16 and p21 (Lin et al., 1996; Palmero et al., 1997). To determine if tumor resistance in CcnE1<sup>-/-</sup> livers is



related to increased induction of senescence, senescence associated  $\beta$ -galactosidase (SA- $\beta$ -gal) activity was examined in liver sections from WT, CcnE1<sup>-/-</sup> and CcnE2<sup>-/-</sup> mice at several time points after DEN treatment. Indeed, CcnE1<sup>-/-</sup> livers showed increased SA- $\beta$ -gal activity compared to WT and CcnE2<sup>-/-</sup> counterparts 40 weeks after DEN treatment (Figure 3.7A). However, this effect was independent of p16, which was markedly upregulated during tumorigenesis in all investigated cohorts to the same extent (Figure 3.7B). Accordingly, tumor suppression in CcnE1<sup>-/-</sup> mice is associated with p16-independent replicative senescence.

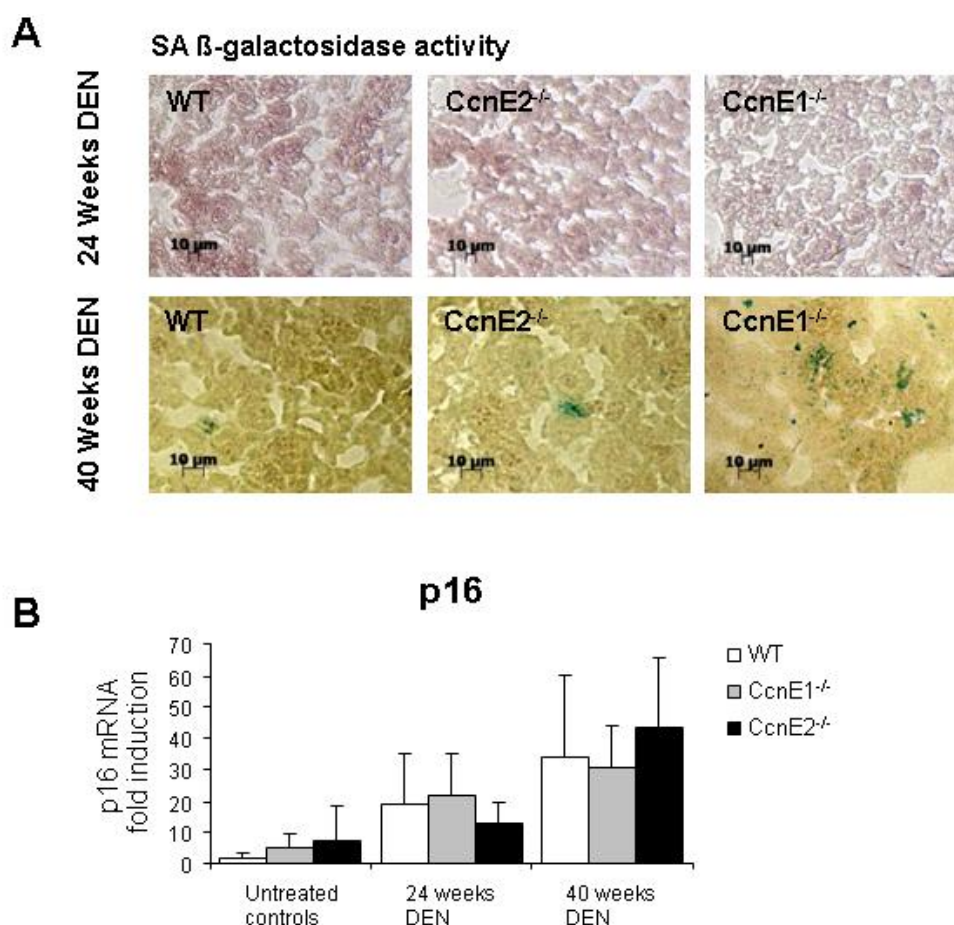


**Figure 3.7 Tumor suppression in CcnE1<sup>-/-</sup> is associated with senescence.** (A) Cryosections of DEN treated livers as described in figures 3.1 and 3.4, of the indicated genotypes at the age of 24 and 40 weeks were stained for SA- $\beta$ -galactosidase activity, positive cells are stained with blue. Scale bar = 10  $\mu$ m. (B) p16 mRNA expression in untreated control, 24 week and 40 week liver tissue for WT (white bars), CcnE1<sup>-/-</sup> (grey bars) and CcnE2<sup>-/-</sup> (black bars) animals. Expression levels were normalized to expression of the housekeeping gene GAPDH and calculated as fold induction in comparison to untreated controls. Each bar represents a value of minimum 4-6 animals, data are presented as the average  $\pm$  s.d.

## 3.2. Analysis of the immediate response after DEN-induced acute liver injury

The previous experiment clearly indicated that depletion of CcnE1 inhibits both tumor initiation and tumor progression upon DEN treatment. In order to investigate the mechanism by which CcnE1 triggers tumor initiation, the immediate response after acute DEN treatment regarding liver regeneration and cell cycle regulation were addressed in detail. Besides its mutagenic properties, DEN has the potential to induce toxic acute liver injury which is associated with centrilobular necrosis and apoptosis (Karin and Greten, 2005). The liver has a unique property to regenerate after surgical resection or toxic injury through proliferation of fully differentiated quiescent hepatocytes and biliary epithelial cells (Fabrikant, 1968; Grisham, 1962). Thus it was anticipated that following acute DEN-treatment, the injured liver would be regenerated by proliferating hepatocytes carrying malignant mutations, which potentially could be CcnE1-dependent. To test this hypothesis, 6-8 weeks old male WT, CcnE1<sup>-/-</sup> and CcnE2<sup>-/-</sup> mice were injected with a single high dose of DEN (200 mg/kg) to induce acute liver injury and analyzed for the acute response regarding liver injury, regeneration and cell cycle progression in a time frame of 0-196 hours post treatment.

### 3.2.1. Ablation of CcnE1 or CcnE2 does not result in alterations of DEN-induced liver necrosis and apoptosis

Following induction of DEN-mediated acute liver injury in CcnE1<sup>-/-</sup>, CcnE2<sup>-/-</sup> and WT mice, the kinetics and strength of tissue damage was monitored by measurement of the circulating liver enzyme ALT from blood samples showing maximal induction 48 h after treatment, which was independent of CcnE1 or CcnE2 expression, respectively (Figure 3.8A). In agreement with these findings, histological analysis of H&E stained liver sections revealed large necrotic areas mostly situated around the central veins, which were of similar size in animals of all three genotypes (Figure 3.8B upper panel).

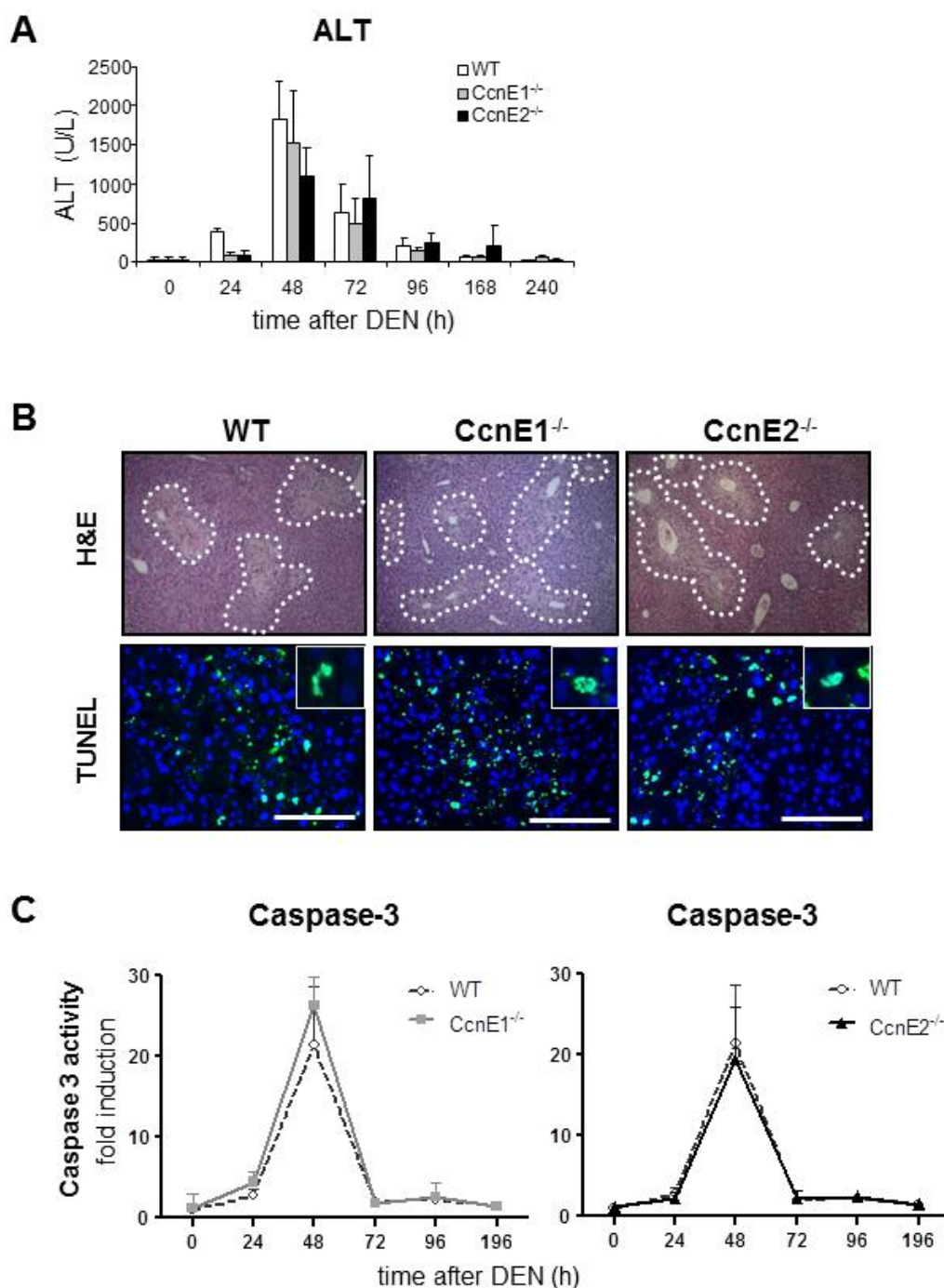


**Figure 3.8 DEN treatment induces elevated apoptosis in DEN acute liver injury model.** Male mice 6-8 weeks of age were injected with DEN (200 mg/kg i.p.) to induce acute liver injury, livers were investigated up to 240 hours after injection. (A) Serum level of alanine-aminotransferase (ALT) of mice at indicated time points after DEN injection. Each bar represents a value of minimum 3 animals, data are presented as the average  $\pm$  s.d. (B) H&E staining of paraffin embedded liver sections (top panel), apoptosis/necrosis areas are highlighted with dotted line. Original magnification: 100x. TUNEL staining on frozen liver sections (bottom panel). TUNEL positive cells are green, nuclei are visualized by DAPI: blue. Scale bar: 100  $\mu$ m. (C) Caspase-3 activity was measured by assay for specific caspase-3 substrate turnover and calculated as fold induction in comparison to untreated livers. Data are presented as comparison of CcnE1<sup>-/-</sup> (squares) to WT (circles) animals in the left graph and comparison of CcnE2<sup>-/-</sup> (triangles) to WT (circles) animals in the right graph. Each value represents a minimum of 3 animals; data are presented as the average  $\pm$  s.d.

Terminal deoxynucleotidyl transferase dUTP nick end labeling (TUNEL assay) is an established method for detecting DNA fragmentation that occurs after apoptotic signaling. Liver cryosections from DEN-treated *CcnE1*<sup>-/-</sup>, *CcnE2*<sup>-/-</sup> and WT mice revealed strongly elevated numbers of TUNEL-positive cells 48 hours after treatment (Figure 3.8B, lower panel) and the staining pattern correlated with the foci of centrolobular tissue damage (compare Figure 3.8B upper panel). However, in some cases TUNEL staining may also label necrotic cells. To clearly distinguish apoptotic cell death from necrosis, the enzymatic activity of caspase-3 was determined after DEN treatment. Caspase-3 is an executioner caspase, which acts downstream of intrinsic and extrinsic apoptotic signaling pathways. Therefore, caspase-3 activation is a highly specific indicator of apoptosis. Caspase-3 was transiently activated 48 hours after DEN treatment in *CcnE1*<sup>-/-</sup>, *CcnE2*<sup>-/-</sup> and WT mice (Figure 3.8C). Interestingly, at this time point caspase-3 activity was slightly higher in *CcnE1*<sup>-/-</sup> livers compared to WT and *CcnE2*<sup>-/-</sup> mice, although these differences were not significant. These data suggested that DEN induced the same degree of acute liver injury in *CcnE*-deficient mice and controls.

The role of pro-apoptotic signals for tumor initiation is still under discussion. Apoptosis is an important mechanism for eliminating transformed cells (Eferl et al., 2003; Maeda et al., 2005), whereas elevated apoptotic cell death may also induce compensatory proliferation and thus tumorigenesis (Liedtke et al., 2011). *CcnE1*<sup>-/-</sup> mice revealed faintly increased apoptosis after acute DEN treatment and reduced tumor incidence as long term effect hinting at a correlation between tumor resistance and apoptosis-sensitivity of *CcnE1*<sup>-/-</sup> mice. To clarify this aspect, the mRNA expression of several key players involved in apoptosis induction was investigated by quantitative real-time PCR (Figure 3.9). Given that DEN-induced DNA damage would predominantly induce intrinsic apoptosis pathways, the gene expression levels of proapoptotic Bcl-2 family members (*bax*, *bcl6*, *bim*, *bNIP3*, *noxa*, *puma* in Figure 3.9A-F) and antiapoptotic Bcl-2 family members (*bcl-2*, *bcl-xl* in Figure 3.9G-H) were analyzed. Liver tissue damage may also induce inflammation and infiltration of immune cells, which eventually could promote extrinsic apoptotic pathways.

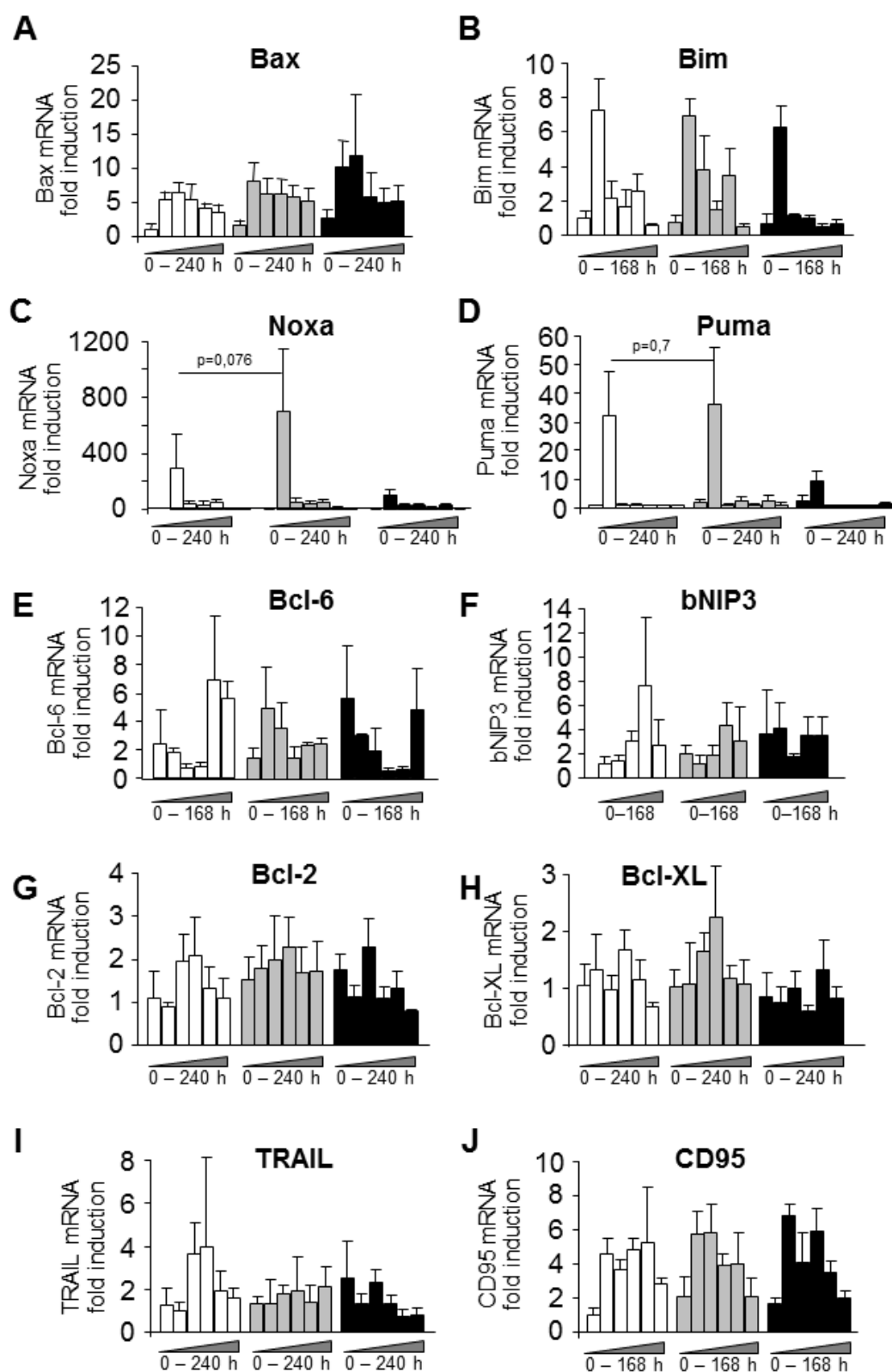


**Figure 3.9 Mediators of intrinsic and extrinsic apoptosis are elevated.** mRNA expression for indicated genes were quantified by Real-Time PCR in livers at timepoints: 0, 24, 48, 72, 96, 168 and 240 hours after DEN injection (200mg/kg i.p.) for WT (white bars), *CcnE1*<sup>-/-</sup> (grey bars) and *CcnE2*<sup>-/-</sup> (black bars) livers. Expression levels were normalized to expression of the housekeeping gene GAPDH and calculated as fold induction in comparison to untreated controls. Each bar represents a value of minimum 3 animals; data are presented as the average  $\pm$  s.d.

Therefore the expression of death receptors and their cognate ligands (*TRAIL*, *FasL*, *CD95*) were also analyzed (Figure 3.9I-J). Except for *FasL* (which will be discussed in chapter 3.2.2), the expression levels of the analyzed apoptotic genes were upregulated after DEN administration, but not significantly different between the genotypes. In conclusion from these results, *CcnE1* does not regulate the main modulators of apoptosis; consequently, inhibition of tumorigenesis as observed in *CcnE1*<sup>-/-</sup> mice cannot be explained by increased apoptosis of malignant transformed hepatocytes.

### 3.2.2. DEN induces differential immune response in *CcnE1*<sup>-/-</sup> and *CcnE2*<sup>-/-</sup> livers

Hepatic cell death has the ability to induce an immune response in the liver. Dying hepatocytes release signals that are capable of activating the resident macrophages of the liver (Kupffer cells), natural killer cells or natural killer T cells. These cells potentially secrete pro-inflammatory cytokines (e.g. TNF, IL-6, Fas) or hepatoprotective mediators (e.g. IL-10, Prostaglandins) that determine the regenerative response to drug induced liver injury (Holt and Ju, 2006).

A recent study demonstrated an essential tumor promoting role of the cytokine IL-6 in the DEN model in mice (Naugler et al., 2007). To determine, if the reduced tumor susceptibility of *CcnE1*<sup>-/-</sup> mice is associated with altered IL-6 response, the levels of IL-6 mRNA in *CcnE1*<sup>-/-</sup>, *CcnE2*<sup>-/-</sup> and WT mice were measured by quantitative Real-Time PCR at distinct time points after acute DEN treatment. WT mice showed elevated IL-6 levels beginning 48 h after DEN-treatment with maximal expression after 96 h (Figure 3.10A). Interestingly, *CcnE1*<sup>-/-</sup> mice revealed only a transient IL-6 response, which was restricted to 48 h post treatment (Figure 3.10A). Thus, ablation of *CcnE1* seems to affect the activation or proliferation of IL-6 expressing cells such as macrophages. In sharp contrast, *CcnE2*<sup>-/-</sup> mice showed an overall increased IL-6 expression compared to WT and *CcnE1*<sup>-/-</sup> mice (Figure 3.10B).



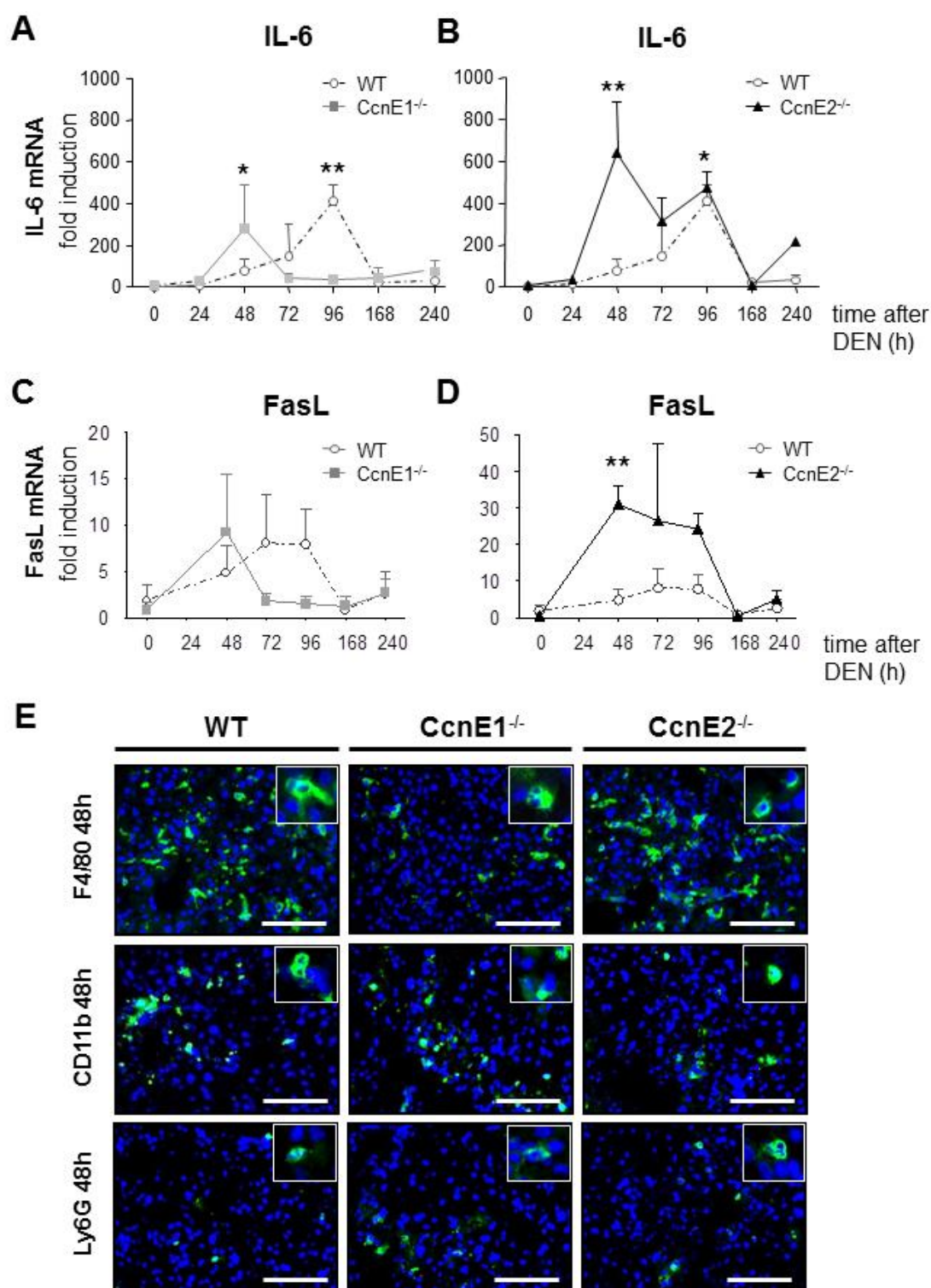


**Figure 3.10 Loss of CcnE1 is associated with attenuated immune response to DEN induced liver injury.** mRNA expression of IL-6 (A-B) and FasL (C-D) in liver tissue up to 240 hours after DEN. Expression levels were normalized to expression of the housekeeping gene GAPDH and calculated as fold induction in comparison to untreated controls. Data are presented as comparison of CcnE1<sup>-/-</sup> (squares, full line) to WT (circles, discontinued line) animals in (A, C) and comparison of CcnE2<sup>-/-</sup> (triangles, full line) to WT (circles, discontinued line) animals in (B, D). Each value represents a minimum of 3 animals, data are presented as the average  $\pm$  s.d. \*:  $p < 0.05$ ; \*\*:  $p < 0.005$  (E) Immunofluorescence analysis of liver macrophages with anti-F4/80 (upper panel) and infiltrating

immune cells with anti-CD11b (middle panel) or anti-Ly6G (bottom panel) 48 hours after induction of acute liver injury by DEN (200mg/kg i.p.). F4/80, CD11b and Ly6G positive cells are stained green, nuclei stained with DAPI are blue. Scale bar = 100  $\mu$ m.

---

As these mice also show overexpression of CcnE1 (compare Figure 3.11C) these data suggests that the CcnE1 expression levels are associated with the strength of the IL-6 response. Similar expression patterns were observed for FasL mRNA showing an overall reduced and transient induction in CcnE1<sup>-/-</sup> mice (Figure 3.10C) and substantial stronger expression in CcnE2<sup>-/-</sup> animals (Figure 3.10D). To identify the IL-6 and/or FasL expressing immune cells, DEN-treated livers were stained for F4/80, Cd11b and Ly6G (Figure 3.10E). F4/80 is a cell surface marker for murine macrophages (Leenen et al., 1994) and Cd11b is expressed on the surface of monocytes, granulocytes, macrophages and natural killer cells (Solovjov et al., 2005). Granulocytes, neutrophils and eosinophils are characterized surface expression of Ly6G (Fleming et al., 1993). Of interest, F4/80 positive liver macrophages were diminished in CcnE1<sup>-/-</sup> mice 48 h after DEN treatment in comparison to WT or CcnE2<sup>-/-</sup> mice (Figure 3.10E, upper panel). As Kupffer cells contribute to hepatocarcinogenesis e.g. by expression of IL-6 or generation of superoxide (Teufelhofer et al., 2005), these data implicates that impaired survival or activation of CcnE1-deficient Kupffer cells may contribute to inhibition of tumor initiation in the liver. In contrast to these findings, Cd11b and Ly6G positive cells were detectable in the liver starting at 48 hours post treatment without significant differences between the genotypes (Figure 3.10E, middle and lower panel respectively).

### 3.2.3. CcnE1 deficiency results in prolonged cell cycle arrest after DEN induced toxic liver injury

Following liver injury, the liver has the capacity to repair tissue damage by compensatory proliferation of surviving hepatocytes. In the DEN model, compensatory proliferation is also essential for the genetic manifestation of malignant mutations and thus tumor initiation. To investigate the role of CcnE1 and CcnE2 for compensatory proliferation after genotoxic liver damage, expression of the proliferation marker Ki67 was determined by immunofluorescence staining.



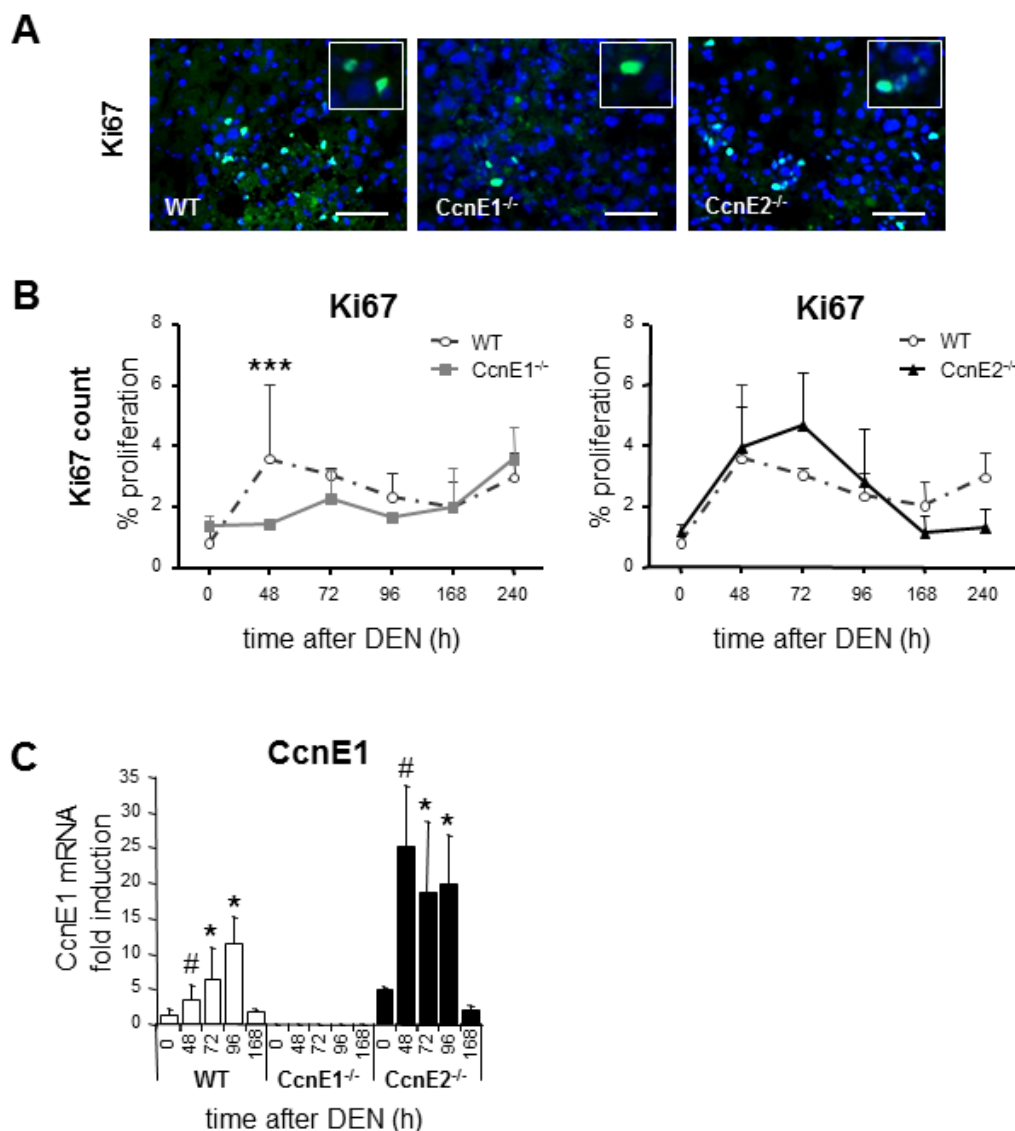


**Figure 3.11 Ablation of CcnE1 correlates with prolonged cell cycle arrest after DEN induced damage.** Cell cycle kinetics was investigated in mice treated with DEN (200mg/kg i.p.) up to 240 hours after injection. (A) Ki67 immunostaining of liver cryosections from WT, CcnE1<sup>-/-</sup> and CcnE2<sup>-/-</sup> animals 48 hours after DEN. Ki67 positive cells are stained green, nuclei are stained with DAPI (blue). Scale bar: 50  $\mu$ m. (B) Quantification of Ki67 positive cells relative to total nuclei per power field. The amount of Ki67 positive cells was determined by counting at least 4 representative high power fields per mouse. Data are presented as comparison of CcnE1<sup>-/-</sup> (squares, full line) to WT (circles, discontinued line) animals in the left graph and comparison of CcnE2<sup>-/-</sup> (triangles, full line) to WT (circles, discontinued line) animals in the right graph. Each value represents a minimum of 3 animals, data are presented as the average  $\pm$  s.d. \*\*\*:  $p < 0.0005$ . (C) CcnE1 mRNA expression quantified by real-Time PCR in livers at 0-168 hours after DEN injection for WT (white bars), CcnE1<sup>-/-</sup> (grey bars) and CcnE2<sup>-/-</sup> (black bars) livers. Expression levels were normalized to expression of the housekeeping gene GAPDH and calculated as fold induction in comparison to untreated controls. Each bar represents the mean of at least 3 animals, data are presented as the average  $\pm$  s.d. \*:  $p < 0.05$ ; #:  $p < 0.0005$ .

In WT and CcnE2<sup>-/-</sup> mice, elevated hepatocyte proliferation was first detectable 48 h post treatment (Figure 3.11A-B), In contrast, increased proliferation in CcnE1<sup>-/-</sup>

livers was first detectable after 10 days but remained at baseline levels from 48-168 h after DEN stimulation. These results indicate that CcnE1 is essential for immediate cell cycle activation after toxic liver injury. In agreement with these findings, CcnE1 levels are usually increased in irradiated cells or following treatment with chemotherapeutics (Blattner et al., 1999; Mazumder et al., 2007). To further determine the regulation of CcnE1 in liver cells after DEN-induced genotoxic injury, CcnE1 mRNA expression was measured in WT, CcnE1<sup>-/-</sup> and CcnE2<sup>-/-</sup> mice. CcnE1 was highly induced in WT livers after DEN genotoxic injury and interestingly, further upregulated in CcnE2<sup>-/-</sup> livers (Figure 3.11C). Hence, *CcnE1* is a highly responsive gene to genotoxic stress. This was also true for the G1-cyclins CcnD1, CcnE2 and CcnA2 and the downstream transcription factors E2F1 and E2F2 which were also induced by DEN although without significant differences between the genotypes (Figure 3.12).

To elucidate the mediators of cell cycle arrest in CcnE1<sup>-/-</sup> mice, the regulation of the cell cycle inhibitors p21 and p27 was intensively investigated as these Cdk inhibitors are known to negatively regulate cell cycle progression at G1 (Polyak et al., 1994a; Polyak et al., 1994b; Toyoshima and Hunter, 1994). The p21 protein inhibits cyclin-dependent kinases and proliferating-cell nuclear antigen (PCNA) that are both required for cell cycle transition. The *p21* gene is under transcriptional control of p53, indicating a role of p21 for p53-dependent cell cycle arrest. DEN induced an immediate and strong induction of p21 mRNA (approximately 40-50 fold) within 24 hours, which was similar in WT, CcnE1<sup>-/-</sup> and CcnE2<sup>-/-</sup> mice (Figure 3.13A, upper panel). However, 48-96 h after DEN treatment, increased p21 mRNA expression was evident in CcnE1<sup>-/-</sup> mice compared to WT and CcnE2<sup>-/-</sup> mice. More importantly, between 48-96 h post treatment, p21 protein levels CcnE1<sup>-/-</sup> liver were increased compared to both WT and CcnE2<sup>-/-</sup> mice (Figure 3.13A, lower panel). These data strongly suggests that the prolonged cell cycle arrest observed in CcnE1<sup>-/-</sup> mice is at least in part mediated through increased p21 gene expression and prolonged p21 protein stability.

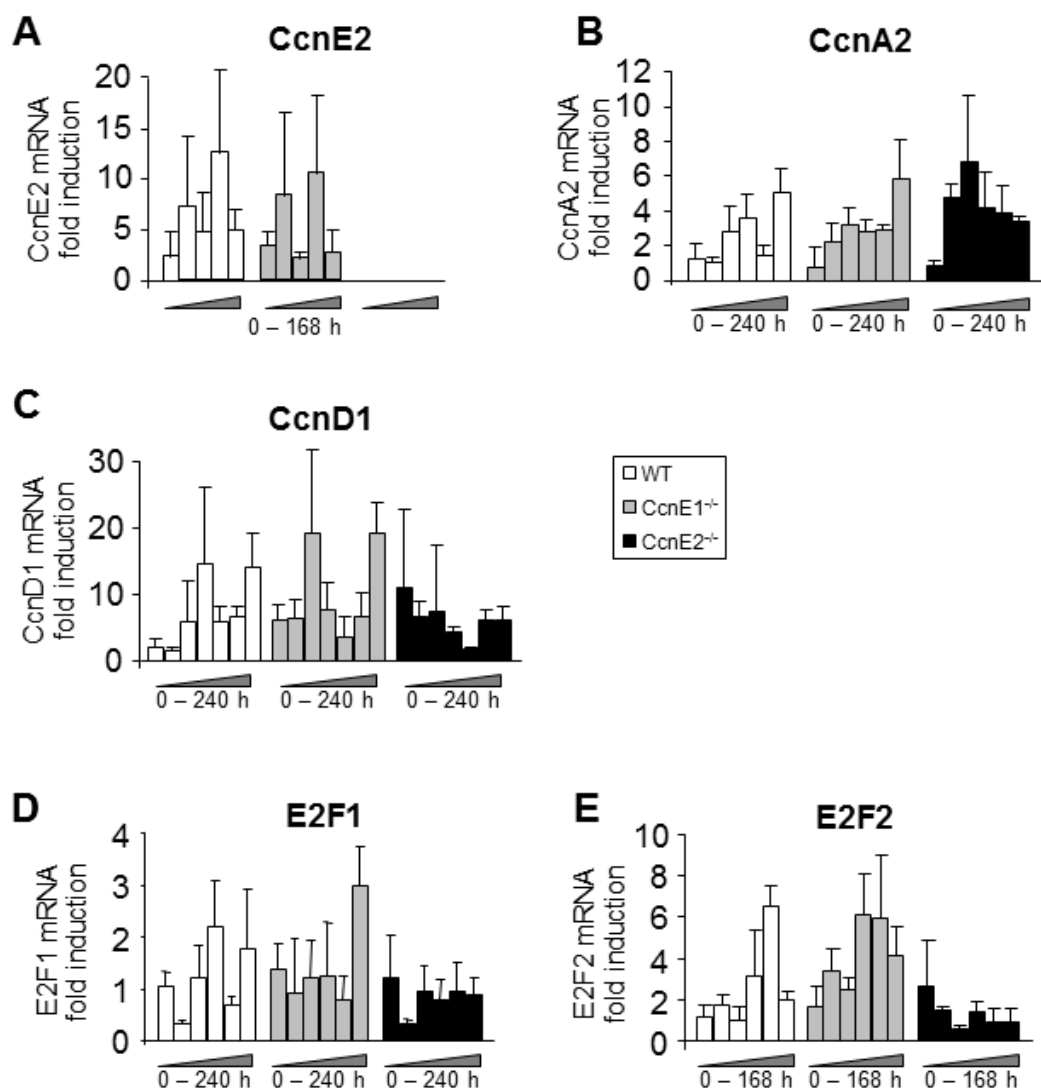


**Figure 3.12 Cell cycle regulating genes are induced after DEN application.** mRNA of cell cycle regulators (CcnE2, CcnA2, CcnD1 and transcription factors E2F1, E2F2) were quantified by Real-Time PCR in livers at 0, 24, 48, 72, 96, 168 and 240 hours after DEN injection (200mg/kg i.p.) for WT (white bars), CcnE1<sup>-/-</sup> (grey bars) and CcnE2<sup>-/-</sup> (black bars) livers. Expression levels were normalized to expression of the housekeeping gene GAPDH and calculated as fold induction in comparison to untreated controls. Each bar represents a value of minimum 3 animals, data are presented as the average  $\pm$  s.d

The p27 protein binds and thereby inactivates Cdk2-CcnE or Cdk2-CcnA complexes resulting in cell cycle arrest. Activity of p27 is regulated through transcriptional, translational and post-translational mechanisms (Lee and Kim, 2009). Following DEN treatment, p27 gene expression was not substantially induced in any of the investigated genotypes as demonstrated by quantitative Real-Time PCR (Figure 3.13B, upper panel). However, increased levels of p27 protein were observed in CcnE1<sup>-/-</sup> livers 72-96 hours after DEN genotoxic injury (Figure 3.13B lower panel)

suggesting that ablation of CcnE1 does not affect transcriptional control of p27 but increases the stability of the p27 protein. Taken together, these observations strongly suggest that p21 and p27 synergistically promote cell cycle arrest in CcnE1<sup>-/-</sup> livers after DEN-induced damage.

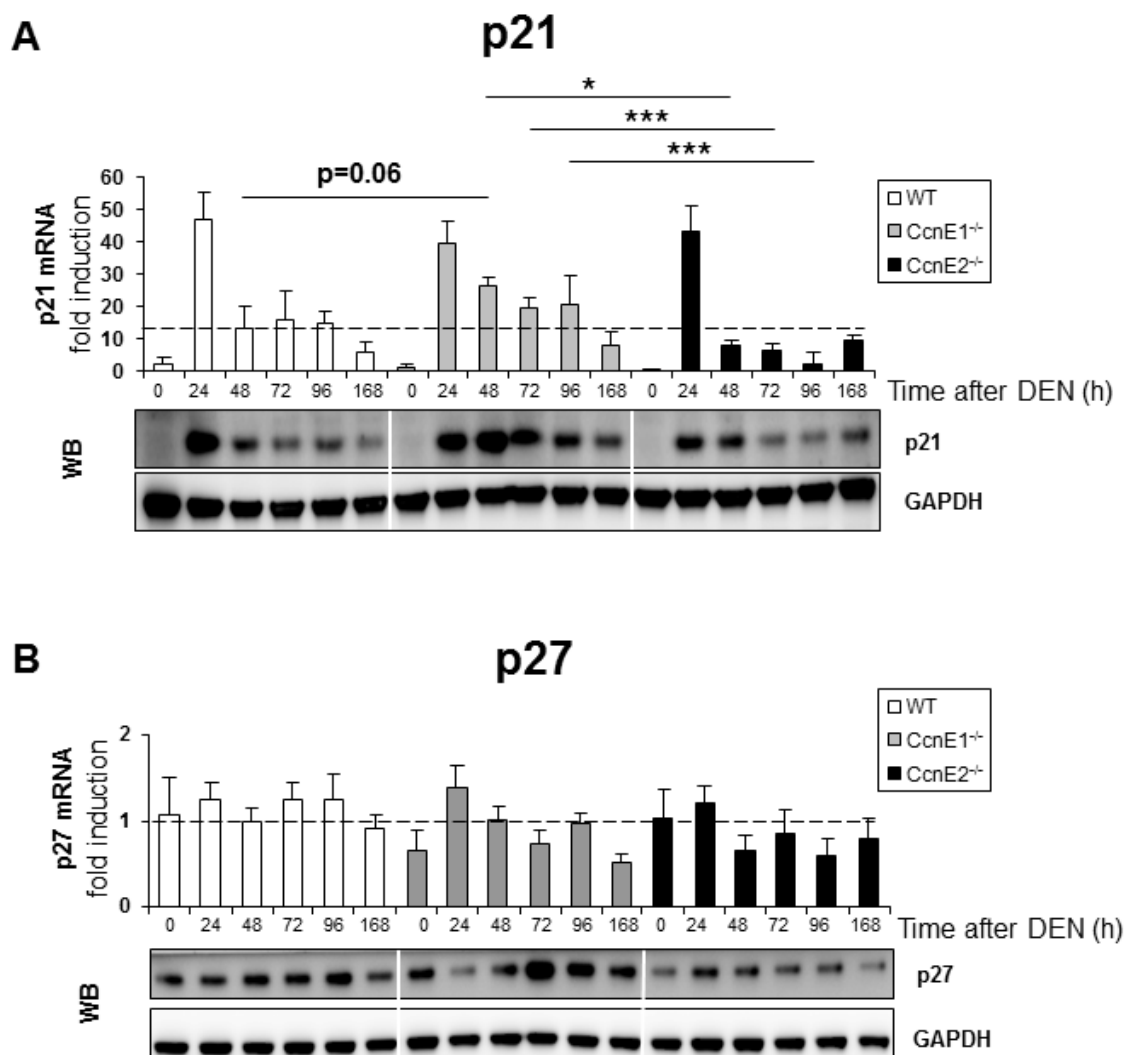


**Figure 3.13 Cell cycle inhibitors are aberrantly elevated in CcnE1-deficient animals after DEN application.** (A) p21 mRNA expression and western blot analysis of p21 protein in WT (white bars), CcnE1<sup>-/-</sup> (grey bars) and CcnE2<sup>-/-</sup> (black bars) mice. (B) p27 mRNA expression and western blot analysis of p27 protein in WT (white bars), CcnE1<sup>-/-</sup> (grey bars) and CcnE2<sup>-/-</sup> (black bars) mice. mRNA expression levels were normalized to expression of the housekeeping gene GAPDH and calculated as fold induction in comparison to untreated controls. Each bar represents a value of minimum 3 animals; data are presented as the average  $\pm$  s.d. For protein expression detected by western blot, GAPDH was used as equal loading control.

Several studies proved that p21 is not only a cyclin/Cdk inhibitor, but can also interact with diverse proteins involved in replication, proliferation, DNA damage and apoptosis (Child and Mann, 2006). To mechanistically explain the prolonged cell cycle arrest and impaired tumor initiation in CcnE1<sup>-/-</sup> mice after DEN treatment, it was speculated that p21 may form alternate protein complexes in the absence of CcnE1 triggering tumor-suppressive effects e.g. via cell cycle arrest and improved DNA repair. To test this hypothesis, complex formation of p21 in CcnE1<sup>-/-</sup> livers was investigated by a combination of immunoprecipitation experiments and a proteomics approach.

WT, CcnE1<sup>-/-</sup> and CcnE2<sup>-/-</sup> mice were treated with a high dose of DEN and sacrificed at distinct time points between 0-168 h post treatment. p21 protein complexes from livers were purified by immunoprecipitation and analyzed on a SDS PAGE by silver staining (sensitivity: 1-5 ng). Interestingly, several p21-interacting proteins with a molecular weight of approximately 40 and 260 kD were detected in cell cycle arrested CcnE1<sup>-/-</sup> livers (48-96 h after DEN treatment, Figure 3.14A, also compare Figure 3.11B). In contrast, these proteins were absent or barely visible in WT or CcnE2<sup>-/-</sup> samples (Figure 3.14A).

As these p21-interacting proteins were potential mediators of the observed tumor-suppressive effects it was next aimed to identify these factors by a proteomics approach with a kind support of Dr. Corinna Henkel (Department of Pathology, University Hospital Aachen). Immunoprecipitated p21 complexes isolated from WT and CcnE1<sup>-/-</sup> mice 48 hours after DEN treatment were analyzed by Two-dimensional difference in gel electrophoresis (2D DIGE), separating the proteins by mass and by isoelectric focusing. Genotype-specific visualization of interacting proteins revealed overall more p21 interaction partners and stronger complex formation in CcnE1<sup>-/-</sup> livers after DEN-treatment (Figure 3.14B, upper panel) compared to WT mice. In addition, a multiplicity of proteins were upregulated in CcnE1<sup>-/-</sup> liver (Figure 3.14B, lower panel) thereby confirming the increased presence of p21 in these samples as demonstrated in Figure 3.13A. Unfortunately, identification of representative proteins which selectively interacted with p21 in CcnE1<sup>-/-</sup> liver using mass spectrometry was not successful due to limited amounts of purified protein complexes. However, these data strongly suggests that ablation of CcnE1 triggers the prolonged formation of

aberrant p21 complexes potentially contributing cell cycle arrest or tumor suppression.

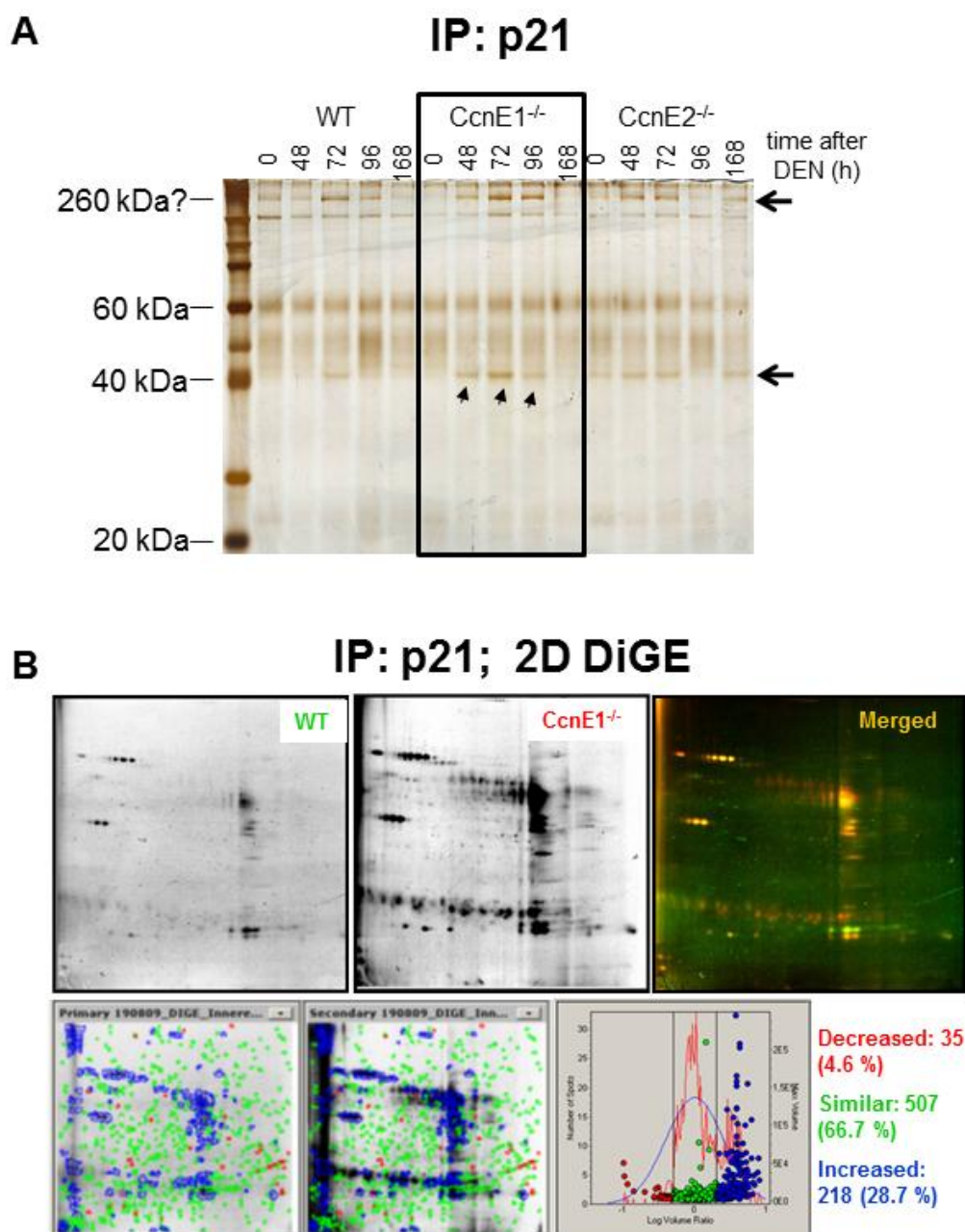


**Figure 3.14 Differential complex formation of p21 in WT and CcnE1<sup>-/-</sup> mice after DEN induced damage.** (A) Immunoprecipitated complexes with p21 were isolated from WT, CcnE1<sup>-/-</sup> and CcnE2<sup>-/-</sup> livers treated with DEN (200mg/kg) and analysed on PAGE after silver staining. (B) 2D gel electrophoresis, 2D DiGE (two-dimensional difference in gel electrophoresis) experiment comparing the p21 complexes of WT (417; cy3) and CcnE1<sup>-/-</sup> (2026; cy5) DEN-treated animals at 48 hour time point including overlay (yellow signal = overlay) indicates common protein expression in WT and CcnE1<sup>-/-</sup> sample (upper panel). Images were analysed with Decyder 5.01 (DIA Modul), up-regulated spots (blue), no difference (green) and downregulated spots (red) in CcnE1<sup>-/-</sup> compared to WT (lower panel).

### 3.2.4. Ablation of CcnE1 triggers prolonged p53-checkpoint activation after DEN-induced DNA damage

DEN is a genotoxic agent, which induces DNA damage such as DNA adducts. In addition, overexpression of CcnE1 has also been shown to induce DNA damage at least *in vitro*, which can activate a p53-dependent checkpoint (Bartkova et al., 2006; Loeb et al., 2005; Spruck et al., 1999). It was therefore speculated that ablation of CcnE1 might directly affect the strength of DNA damage after genotoxic liver injury or modulate the extent of DNA damage response (DDR) to DEN e.g. via p53-dependent pathways.

To quantify the extent of DNA damage response (DDR) to DEN in CcnE knockout mice, the levels of Ser139 phosphorylated histone variant H2A.X ( $\gamma$ H2AX) was determined which served as a marker for DNA double strand breaks. H2A.X phosphorylation was verified by immunofluorescent staining of liver cryosections and through western blot analysis in WT, CcnE1<sup>-/-</sup> and CcnE2<sup>-/-</sup> mice after DEN treatment (Figure 3.15A-B). These data hinted at a prolonged persistence of damaged DNA in DEN-treated CcnE2<sup>-/-</sup> livers (24-72 h post DEN) and overall reduced DNA damage in CcnE1<sup>-/-</sup> mice 24-48 h after treatment (Figure 3.15B).

Another mode of DNA damage is the generation of abasic (apurinic/apyrimidinic; AP) sites, which are also promoted by genotoxic agents or appear as intermediates during nucleotide excision repair (NER). Unrepaired AP sites inhibit topoisomerases, replication and transcription and can be mutagenic (Dahlmann et al., 2009). The presence of AP sites in WT, CcnE1<sup>-/-</sup> and CcnE2<sup>-/-</sup> mice at distinct time points after DEN-treatment was quantified using a commercial assay (Figure 3.15C). Although the data clearly demonstrated that DEN generated AP sites in the liver, significant differences between the groups were not evident. Thus, CcnE1 is most likely not involved in NER. However, hepatic ablation of CcnE1 may result in reduced formation or accelerated procession of DSB.

DNA damage induces phosphorylation of p53 at several residues including Ser15 (Pluquet and Hainaut, 2001). Phosphorylation at Ser15 reduces the interaction between p53 and its negative regulator Mdm2, promoting accumulation and activation of p53. Ser15 phosphorylation of p53 is mediated by ATM, ATR and DNA-PK (Meek and Anderson, 2009). Interestingly, p53 phosphorylation in CcnE1-

deficient livers was stronger and substantially prolonged upon DEN challenge in comparison to WT and *CcnE2*<sup>-/-</sup> mice, (Figure 3.15D, upper panel). These findings are consistent with the expression levels of the p53 downstream target p21 (compare Figure 3.13A) and would explain the prolonged cell cycle arrest of *CcnE1*<sup>-/-</sup> hepatocytes as a consequence of prolonged p53-dependent checkpoint activation. However, the precise mechanism of p53 modulation by *CcnE1* remains to be elucidated.

A variety of stress signals can activate c-Jun N-terminal kinases (JNK) via phosphorylation. Activated JNKs modify the activity of several proteins involved in cell growth, differentiation, survival and apoptosis (Vlahopoulos and Zoumpourlis, 2004). Of notice, p53 is also a substrate of JNK (Fuchs et al., 1998a). Accordingly, it was investigated if JNK (JNK1 and JNK2 proteins) are activated in response to DEN. Western blot analysis revealed increased phosphorylation of JNK1/2 in *CcnE1*<sup>-/-</sup> mice at critical time points after DEN application (48-72 h post DEN with maximal liver injury and cell cycle arrest) in comparison to WT and *CcnE2*<sup>-/-</sup> mice (Figure 3.15D, lower panel).

To further evaluate the role of DDR signals for preventing tumorigenesis in *CcnE1*<sup>-/-</sup> livers, the expression of selected genes potentially involved in this pathway was determined by quantitative Real-Time PCR (Figure 3.16). These gene sets involved DNA damage indicators (p53, Mdm2, Gadd45 $\alpha$  in Figure 3.16A-C), members of oxidative stress pathway (Cat, MnSOD in Figure 3.16D-E), and chromatin remodelling factors (Smarcc1/BAF155), Smarca4/BRG1 in Figure 3.16F-G). Out of these genes, only p53, Mdm2 and Gadd45 $\alpha$  mRNA levels were substantially induced after DEN application, although without significant differences between WT, *CcnE1*<sup>-/-</sup> and *CcnE2*<sup>-/-</sup> animals.



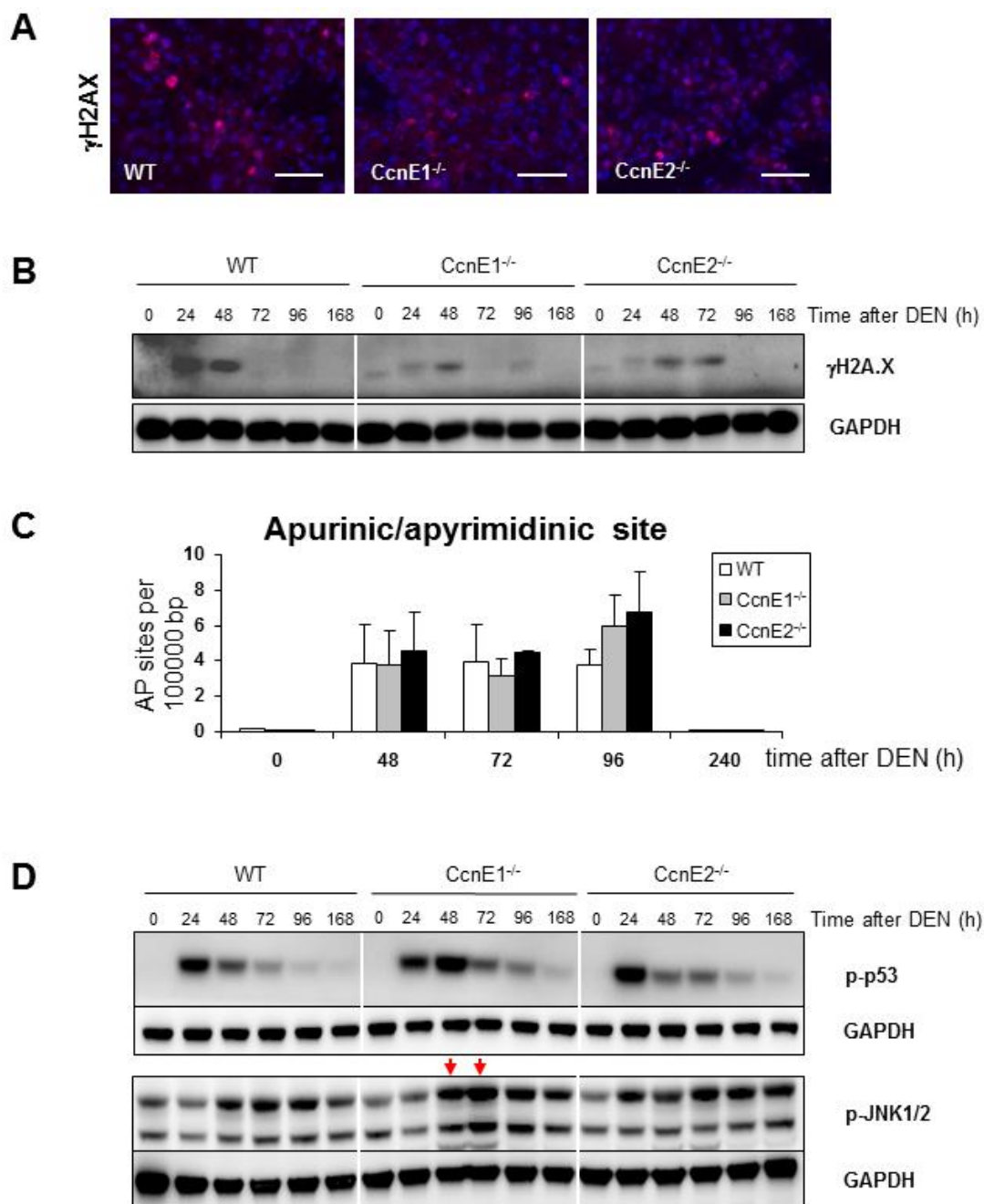


**Figure 3.15 Loss of CcnE1 allows prolonged p53 checkpoint and JNK activation.** Male mice 6-8 weeks of age were injected with DEN (200 mg/kg i.p.) to induce acute liver injury as before, livers were investigated for DNA damage response and stress markers up to 168 or 240 hours after injection. (A) Phosphorylation of H2AX on Ser139 ( $\gamma$ H2AX) was stained on liver cryosections from WT, CcnE1<sup>-/-</sup> and CcnE2<sup>-/-</sup> animals 48 hours after DEN.  $\gamma$ H2AX positive cells are stained red, nuclei are stained with DAPI: blue. Scale bar: 50  $\mu$ m. (B)  $\gamma$ H2AX was visualised by western blot analyses for WT, CcnE1<sup>-/-</sup> and CcnE2<sup>-/-</sup> liver tissues up to 168 hours after DEN application. GAPDH was used as equal loading control. (C) Abasic sites (AP sites) were measured by specific ELISA for isolated genomic DNA. Data are displayed for WT (white bars), CcnE1<sup>-/-</sup> (grey bars) and CcnE2<sup>-/-</sup> (black bars) animals at indicated time points after DEN. Each bar represents a value of 3 animals; data are presented as the average  $\pm$  s.d. (D) Western blot analysis of p53 phosphorylation status at Ser15 (upper panel) and JNK1/2 phosphorylation (lower panel) in DEN treated livers at indicated time points. GAPDH was used as equal loading control, note: p21 and pJNK1/2 were probed on the identical membrane, therefore the same GAPDH was shown in figure 3.13A and 3.15D.

In summary these data suggests that prolonged DNA damage response in CcnE1-deficient liver cells is mediated predominantly via post-translational mechanisms involving enhanced induction of JNK and prolonged activation of p53.

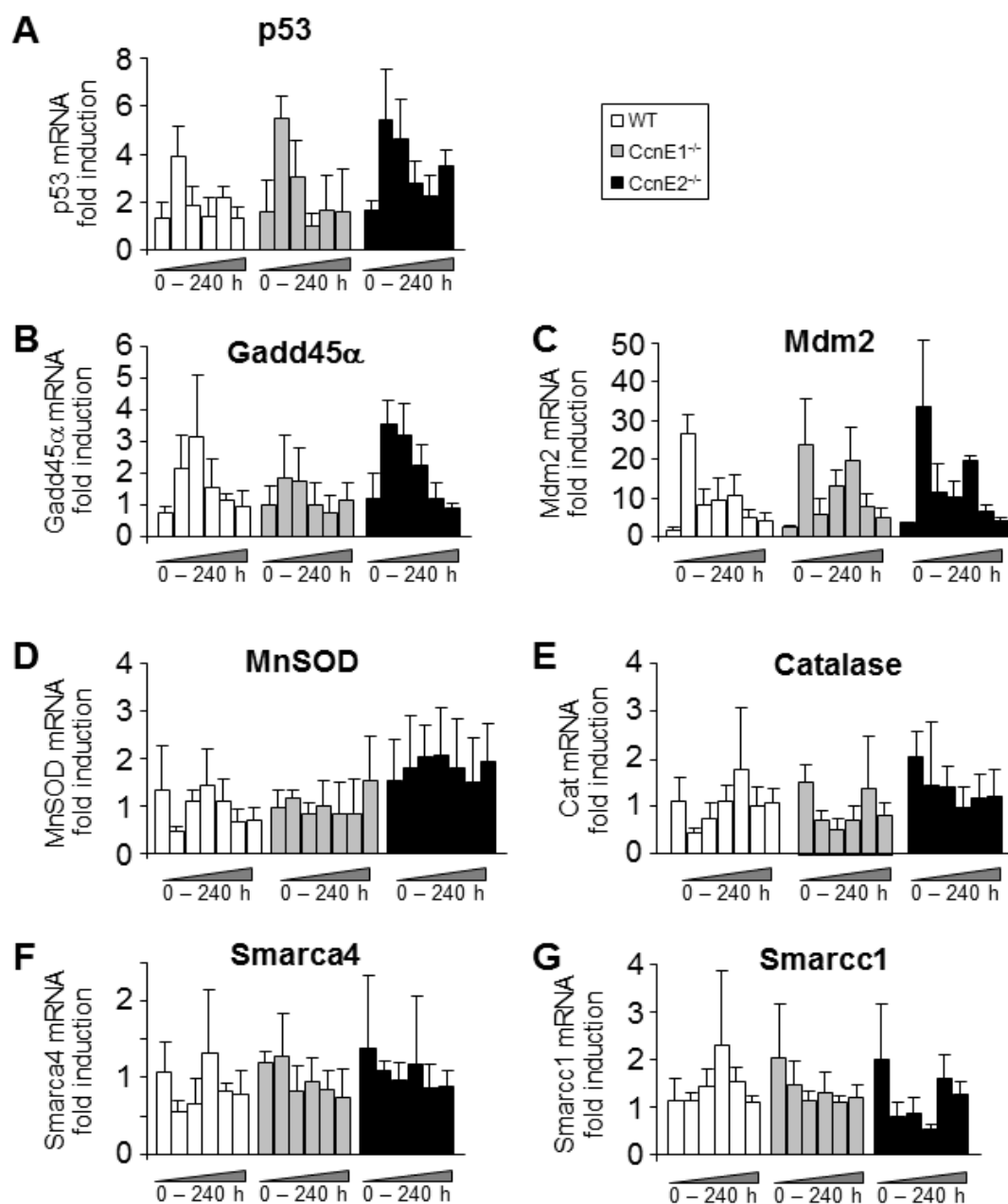
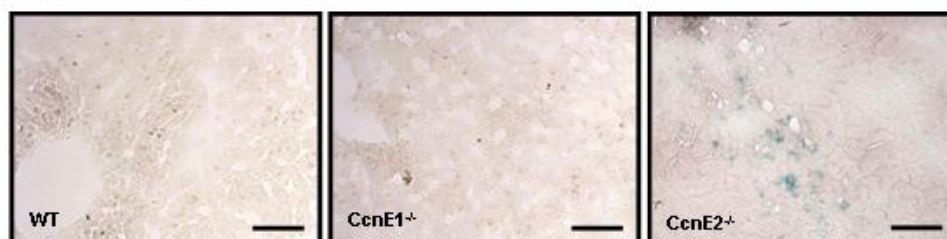


**Figure 3.16 Mediators of DNA damage response are induced after DEN application.** 6-8 weeks old male mice treated as described before, livers were investigated at 0, 24, 48, 72, 96, 168 and to 240 hours after injection for DNA damage markers: p53, GADD45 $\alpha$ , Mdm2 (A-C); members of oxidative stress pathway: MnSOD, Catalase (Cat) (D-E); and chromatin remodelling members: Smarca4 and Smarcc1 (F-G). mRNA expression for indicated genes were quantified by real-time PCR for WT (white bars), CcnE1<sup>-/-</sup> (grey bars) and CcnE2<sup>-/-</sup> (black bars) livers. Expression was normalized to the untreated control mRNA, each bar represents a value of minimum 3 animals; data are presented as the average  $\pm$  s.d.

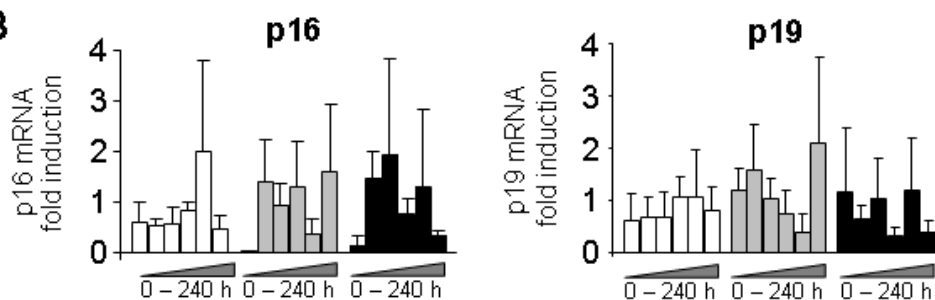
### 3.2.5. Ablation of CcnE1 does not induce cellular senescence in acute DEN-mediated liver injury

Previous results (compare Figure 3.7A) indicated that CcnE1-deficiency was associated with increased cellular senescence in aged livers. Therefore it was of interest to test if this might also apply for acute DEN-induced liver damage as CcnE1<sup>-/-</sup> mice displayed prolonged cell cycle. To address this question, SA- $\beta$ -galactosidase activity was measured by staining DEN-treated livers from WT, CcnE1<sup>-/-</sup> and CcnE2<sup>-/-</sup> mice with x-gal. Surprisingly, elevated SA- $\beta$ -galactosidase activity was only observed in CcnE2<sup>-/-</sup> cryosections, but not in samples from CcnE1<sup>-/-</sup> livers (Figure 3.17A). The underlying mechanisms could not be clarified as mRNA levels of senescence markers p16, p19 and fibronectin (Fb) were not significantly different between WT, CcnE1<sup>-/-</sup> and CcnE2<sup>-/-</sup> mice (Figure 3.17B). Thus, increased hepatic SA- $\beta$ -gal activity in CcnE2-deleted animals after DEN administration is not related to induction of established senescence markers and does not explain prolonged cell cycle arrest in CcnE1<sup>-/-</sup> mice. However, previous studies suggested that massive overexpression of CcnE1 – which was also observed in CcnE2<sup>-/-</sup> liver (compare Figure 3.10C) – may lead to senescence (Bartkova et al., 2006).

#### A SA- $\beta$ -Galactosidase



#### B



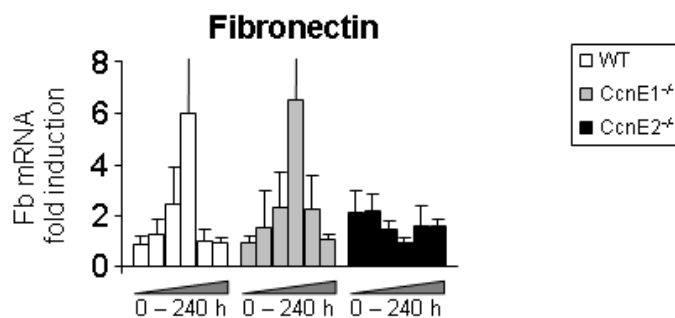


**Figure 3.17 Senescence in DEN induced acute liver injury is associated with absence of CcnE2<sup>-/-</sup>.** 6-8 weeks old male mice treated as described before, were investigated for senescence markers. (A) Representative images of WT, CcnE1<sup>-/-</sup> and CcnE2<sup>-/-</sup> cryosections of livers isolated 72 hours after DEN injection and stained for SA- $\beta$ -galactosidase activity are presented. Positive cells are stained with blue, liver tissue is counterstained with nuclear fast red. Scale bar: 50  $\mu$ m. (B) mRNA expression of p16, p19 and Fb (fibronectin) was quantified by real-time PCR for WT (white bars), CcnE1<sup>-/-</sup> (grey bars) and CcnE2<sup>-/-</sup> (black bars) animals. Expression was normalized to the untreated control mRNA, each bar represents a value of minimum 3 animals; data are presented as the average  $\pm$  s.d.

### 3.3. Implementations for the acute DEN-model in juvenile mice

The previous experiments investigated the consequences of acute DEN-mediated liver injury in adult mice using high dosage. However, the induction of HCC was performed using low dosage DEN in juvenile mice at the age of 2 weeks, raising the question if ablation of CcnE1 comprises similar effects in juvenile versus adult livers. To address this point, two week old WT and CcnE1<sup>-/-</sup> mice were injected with low dose DEN as used for HCC induction and sacrificed 48 hours after application.

As expected, untreated livers from juvenile mice (WT and CcnE1<sup>-/-</sup>) showed substantial hepatocyte proliferation as detected by immunohistochemistry with the S-phase marker PCNA (Figure 18A, upper panel) due to progressive liver development, which was a striking difference to the data obtained from adult mice. However, 48 h after DEN-treatment, juvenile CcnE1<sup>-/-</sup> livers showed a striking reduction in S-phase, which was not evident in corresponding WT mice (Figure 3.18A, lower panel and right panel). In addition, apoptosis was slightly elevated in juvenile CcnE1<sup>-/-</sup> mice as assessed by TUNEL staining and immunohistochemistry specific for cleaved caspase-3 (Figure 3.18B-C).

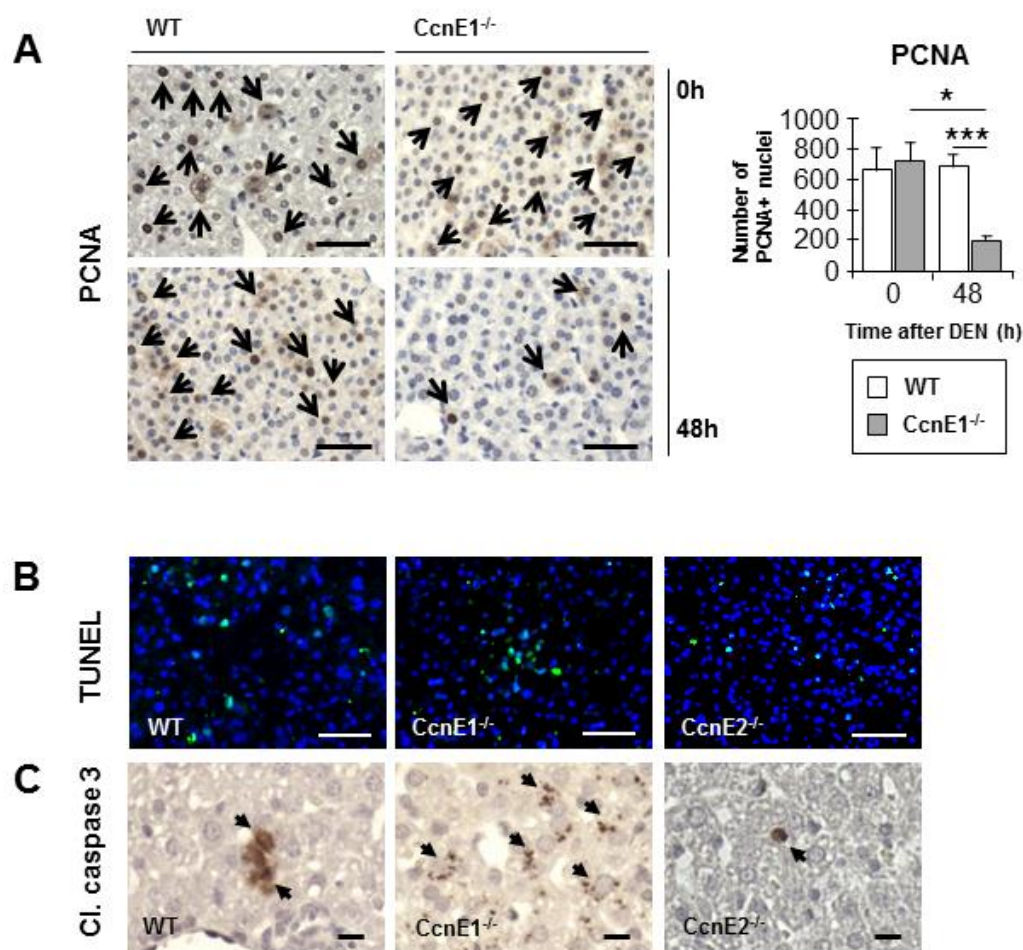


**Figure 3.18 Apoptosis and cell cycle arrest contribute to tumor suppression upon DEN treatment.** Two week old male WT, CcnE1<sup>-/-</sup> and CcnE2<sup>-/-</sup> mice were treated with low dose DEN (25mg/kg i.p.) and sacrificed 48 hours later. Livers were analyzed for markers of apoptosis and proliferation. (A) PCNA immunohistochemistry of paraffin embedded sections, WT and CcnE1<sup>-/-</sup> controls (untreated two weeks old mice) were compared to 48 hour time point after DEN application. PCNA positive cells are stained brown. Scale bar: 50 μm. The amount of PCNA positive (PCNA+) cells was determined by counting at least 3 representative high power fields per mouse. Data are presented as comparison of WT (white bars) to CcnE1<sup>-/-</sup> (grey bars) animals in the right graph. Data are presented as the average ± s.d. \*: p<0.05, \*\*\*: p<0.0005. (B) TUNEL staining of liver cryosections. TUNEL positive cells are stained in green and nuclei with DAPI (blue). Scale bar: 50 μm. (C) Cleaved caspase-3 immunohistochemistry of paraffin embedded sections. Cleaved caspase-3 positive cells are stained brown and highlighted with arrows. Scale bar: 10 μm.

Thus, the low dose DEN model in juvenile mice confirms the previous data generated from adult mice and defines CcnE1 as an essential factor for overriding cell cycle checkpoints after toxic liver injury.

### 3.4. Analysis of DEN-dependent effects on cell cycle activation and apoptosis in primary hepatocytes

To further characterize the cellular role of DEN and CcnE1 on cell cycle control and apoptosis, it was aimed to establish a suitable *in vitro* cell culture model using cultured primary hepatocytes. For this approach, primary hepatocytes were isolated from WT and CcnE1<sup>-/-</sup> mice, stimulated with DEN to initiate cell damage and additionally treated with EGF and Insulin to induce proliferation. Using fluorescence-activated cell sorting (FACS), DNA content per single cell was measured as a marker of cell cycle activity. Cell populations with DNA content <2n (subG<sub>1</sub> population) indicated DNA degradation and were considered apoptotic cells.

Interestingly, DEN stimulation alone did not affect cell death in either WT (17%) or CcnE1<sup>-/-</sup> primary hepatocytes (18%) compared to untreated controls (Figure 3.19A). Cell cycle stimulation by adding EGF and Insulin after DEN-treatment clearly increased the subG<sub>1</sub> population in CcnE1<sup>-/-</sup> primary hepatocytes to 24% in comparison to only 15% in WT cells. However, overall DNA replication was not inhibited by either DEN or ablation of CcnE1 in this cell culture model (Figure 3.19A). Prolonged exposition to EGF and Insulin after DEN stimulation (48h) also increased apoptosis in primary WT hepatocytes. These data suggests that DEN triggers apoptosis in proliferating cells which is slightly accelerated in the absence of CcnE1. Unexpectedly, reliable measurements of cell cycle activity were not feasible with this cell culture model due to the nature of primary hepatocytes to perform several rounds of endoreplication (Guidotti et al., 2003). Therefore, at the end point of the experiment (24 h DEN; 48 h EGF/Insulin, Figure 3.19A, right panel) it could not be explicitly distinguished if CcnE1<sup>-/-</sup> hepatocytes are more prone to G2/M cell cycle arrest (lack of 2n population) or defective in endoreplication (lack of >8n population) as reported recently (Nevzorova et al., 2009). Thus, the applied *in vitro* model indicated an anti-apoptotic effect of CcnE1 in the DEN model but was otherwise of limited benefit.

Changes in the DNA content of hepatocytes as shown in Figure 3.19A prompted the question if the polyploidization translated into an altered number of nuclei per cell. Counting nuclei per hepatocyte revealed a higher number of mononuclear primary hepatocytes in untreated controls compared to CcnE1<sup>-/-</sup> cells



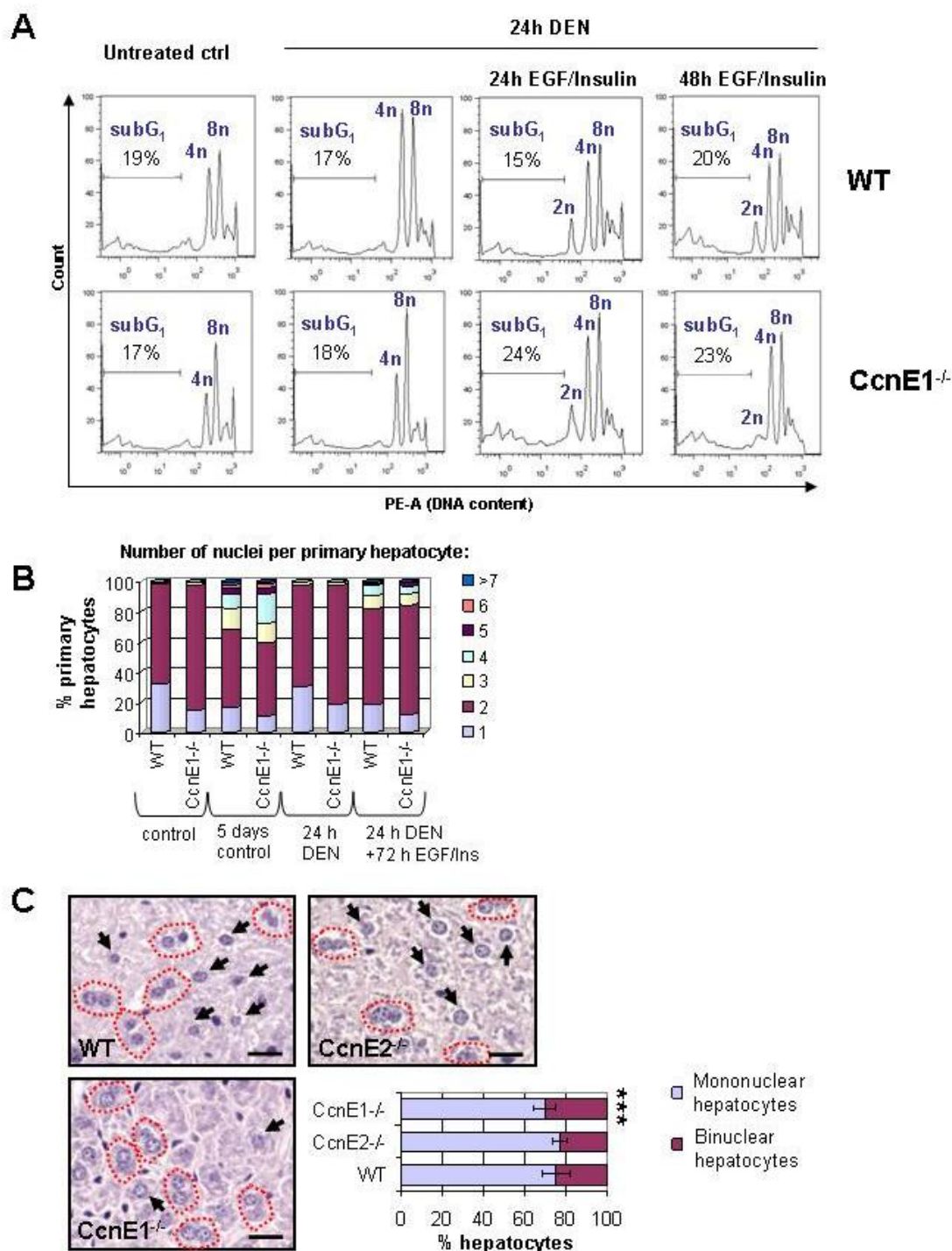


**Figure 3.19 Analysis of DEN-dependent effects on cell cycle activation and apoptosis in primary hepatocytes.** Primary hepatocytes isolated from WT and CcnE1<sup>-/-</sup> mice were cultured on collagen-coated plastic 6-well dishes and maintained in DMEM medium supplemented with 10% foetal bovine serum, penicillin and streptomycin. Primary hepatocyte culture was treated with 5 mM DEN with or without EGF (10 ng/ml) and Insulin (20 U/μl) as indicated and compared to untreated culture. (A) DNA content of cultured hepatocyte populations was determined by FACS. (B) The number of nuclei per WT and CcnE1<sup>-/-</sup> primary hepatocyte, treated as indicated, is presented as histogram. Each bar represents a value of minimum 6 images; data are presented as the average percentage. (C) Untreated livers were collected from 6-8 weeks old male mice. Images of mouse liver H&E staining were investigated for difference in number of nuclei per hepatocyte between WT, CcnE1<sup>-/-</sup> and

CcnE2<sup>-/-</sup> animals. Binucleated hepatocytes are highlighted with dotted line. Scale bar: 20  $\mu$ m. The number of binucleated and mononucleated hepatocytes in WT, CcnE1<sup>-/-</sup> and CcnE2<sup>-/-</sup> mice was presented in histogram as percentage of total hepatocyte number per high power field. \*\*\*:  $p < 0.0005$ .

---

(Figure 3.19B). Of notice, primary hepatocytes undergo spontaneous endomitosis in cell culture without any treatment as seen in untreated controls after 5 days. DEN alone did not induce any alteration, whereas treatment with EGF and insulin additionally increased a number of trinuclear and tetranuclear hepatocytes without significant differences between WT and CcnE1<sup>-/-</sup> cells. However, the observed difference in mononuclear primary hepatocytes remained constant throughout all conditions investigated, suggesting that CcnE1 is involved in control of endomitosis. This finding intrigued to determine if ablation of CcnE1 may alter the number of nuclei *in vivo*. Therefore, number of nuclei per hepatocyte was counted in H&E sections of untreated WT, CcnE1<sup>-/-</sup> and CcnE2<sup>-/-</sup> mice. Indeed, CcnE1<sup>-/-</sup> mice have a significantly reduced number of mononuclear hepatocytes (70 %) in comparison to WT (75 %) and CcnE2<sup>-/-</sup> (77 %) animals (Figure 3.19C). These results demonstrate that loss of CcnE1 affects endomitosis in favor of binucleated hepatocytes *in vitro* and *in vivo*. This could be of some relevance with respect to tumor susceptibility as binuclear hepatocytes might be less prone to malignant transformation due to the presence of redundant genetic material. However, this aspect was not further addressed in the present study.

### 3.5. The cell cycle inhibitor p27 is negatively regulated by CcnE1 during early HCC progression.

De-regulation of the cell cycle inhibitor p27 is found in various cancers including HCC (Matsuda, 2008). The previous experiments demonstrated that the p27 protein is constitutively expressed in healthy liver and further upregulated in CcnE1<sup>-/-</sup> mice upon acute challenge with DEN (compare Figure 3.13B). As CcnE1 usually targets p27 for degradation, it was hypothesized that the tumor-suppressive effect in CcnE1<sup>-/-</sup> mice might be in part due to stabilized p27 protein in basically malignant transformed tissue. To test if p27 also affects liver tumor progression under control of CcnE1, p27 western blot analyses were performed with liver



samples from WT, CcnE1<sup>-/-</sup> and CcnE2<sup>-/-</sup> mice with anticipated early tumor development (24 weeks after DEN treatment) or advanced tumor progression (40 weeks post DEN). For each condition, five randomly selected liver samples were used and the p27 protein expression was quantified by measuring signal intensity relative to GAPDH expression using ImageJ software (Rasband, 1997-2011).

As expected from earlier reports, several WT livers completely lacked p27 protein already at early tumor development (Figure 3.20A, left panel) or during advanced tumor progression (Figure 3.20B, left panel). In contrast, the majority of CcnE1<sup>-/-</sup> livers showed marked p27 protein expression, whereas CcnE2<sup>-/-</sup> liver samples revealed an intermediate effect (Figure 3.20A-B, left panel). Quantification of these data revealed that overall p27 expression in CcnE1<sup>-/-</sup> mice is significantly higher during early tumor development (Figure 3.20A, right panel), whereas the observed differences did not reach statistical significance at advanced tumor progression (Figure 3.20B, right panel). These data in combination with the previous results suggests that p27 is an important mediator of tumor suppression in CcnE1<sup>-/-</sup> mice due to increased stability.

Cdk2 - in complex with E-type or A-type cyclins - is one of the main kinases involved in p27 phosphorylation at Thr187 thereby promoting cell cycle progression. Phosphorylation of p27 at both stages of tumor progression (early versus advanced) in WT, CcnE1<sup>-/-</sup> and CcnE2<sup>-/-</sup> liver was detected by immunohistochemical staining using a Thr187-specific antibody. Of notice, p27 phosphorylation was evident within defined dysplastic tissue areas in WT, CcnE1<sup>-/-</sup> and CcnE2<sup>-/-</sup> tissue, indicating that CcnE1 is not required for p27 phosphorylation (Figure 3.20C). However, CcnE1<sup>-/-</sup> livers were characterized by an overall lower amount of p-p27 positive cells with p-p27 localized predominantly in the cytoplasm, although precise quantification of these findings were not performed due to the heterogeneity of the investigated tissue sections (i.e. highly dysplastic in WT and mostly healthy in CcnE1<sup>-/-</sup>). Thus, CcnE1-deficiency may trigger increased p27 stability through other mechanisms besides diminished phosphorylation.

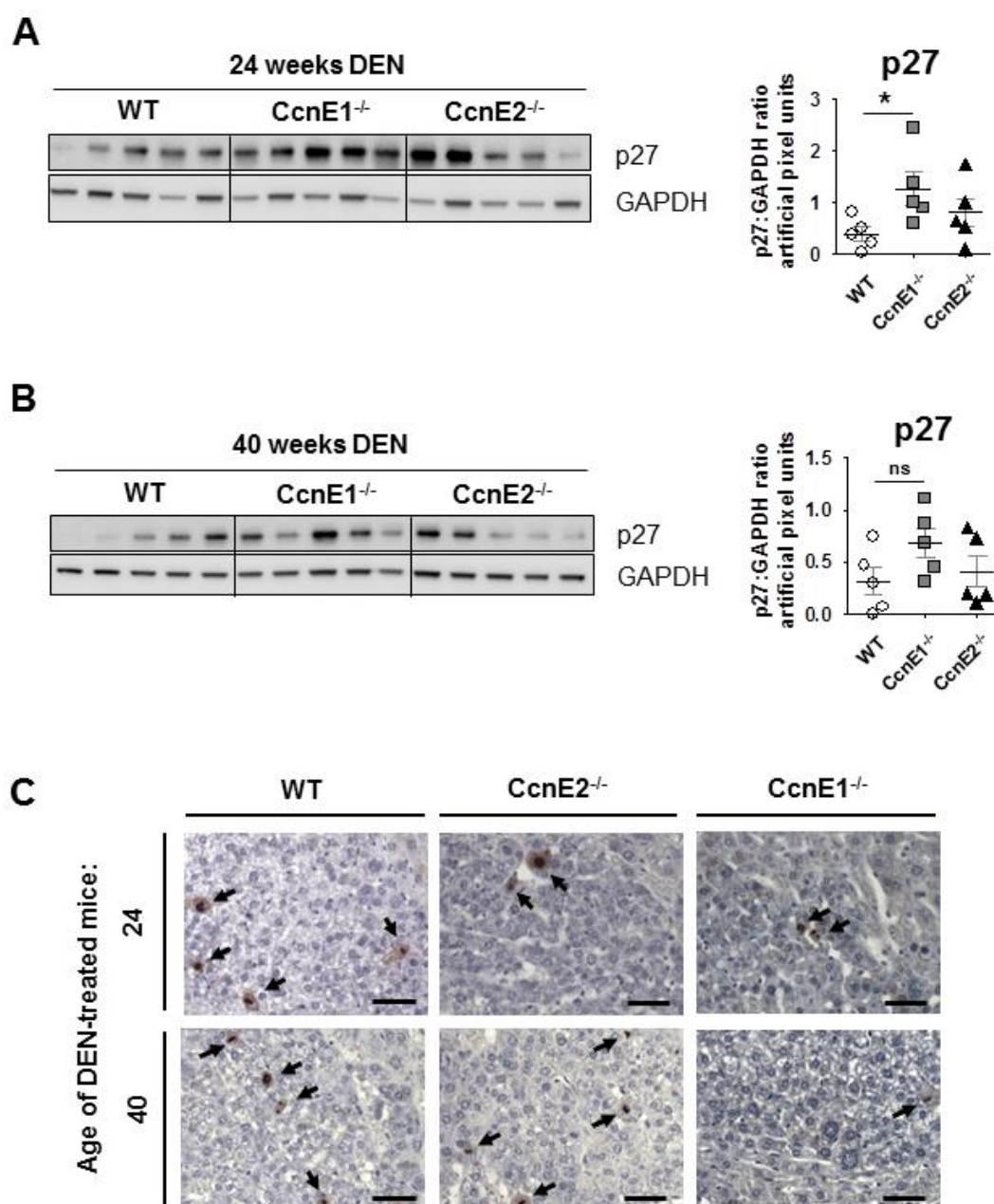


**Figure 3.20 CcnE1 is required for p27 inhibition in hepatocarcinogenesis.** (A) Left panel: p27 western blot analysis from DEN-treated WT, CcnE1<sup>-/-</sup> and CcnE2<sup>-/-</sup> livers 24 weeks after single DEN-treatment (early tumor development). GAPDH expression was determined as equal loading control. Right panel: p27 western blot signal intensity was measured by ImageJ and compared to GAPDH band intensity. The ratio was calculated for each individual mouse and indicated as artificial pixel unit. (B) Left panel: p27 western blot analysis from DEN-treated WT, CcnE1<sup>-/-</sup> and CcnE2<sup>-/-</sup> livers 40 weeks after single DEN-treatment (advanced tumor progression). Right panel: Quantification of signal intensity as in (A). (C) Phosphorylation of p27 on Thr187 in liver tumor samples was determined by immunohistochemistry of paraffin embedded sections. P-p27 positive liver cells are stained in brown and are highlighted by arrows. Scale bar: 50  $\mu$ m.

### 3.6. The oncogenic potential of CcnE1 in the liver depends on functional Cdk2 in hepatocytes

The canonical cell cycle activation in mammals involves physical interaction of CcnE1 or CcnE2 with Cdk2 thereby forming a functional kinase, which then phosphorylates and subsequently activates substrates driving the initiation of DNA synthesis (Caldon and Musgrove, 2010). However, as described before (compare chapter 3.1) genetic inactivation of Cdk2 or of a single E-Type cyclin does not affect cell proliferation during embryonic development or liver regeneration (Geng et al., 2001; Kaldis and Aleem, 2005; Nevzorova et al., 2009; Ortega et al., 2003), pointing to a non-canonical, Cdk2-independent function of CcnE and overlapping roles of CcnE1 and CcnE2. In line with this hypothesis, a recent study described a Cdk2-independent function of CcnE1 for the formation of the pre-replication complex and origin firing (Geng et al., 2007).

In order to distinguish if the tumor-promoting activity of CcnE1 in the DEN model is Cdk2-dependent or the result of a non-canonical CcnE1-function, conditional knockout mice with hepatocyte-specific deletion of Cdk2 were generated. For this approach, mice carrying loxP recombination sites in intron 1 and 3 of the Cdk2 gene ( $Cdk2^{f/f}$ , (Ortega et al., 2003) were kindly provided by Dr. M. Barbacid (CNIO, Madrid, Spain) and crossed with transgenic mice expressing the cre-recombinase under the control of the hepatocyte-specific albumin promoter (Kellendonk et al., 2000). Efficient hepatic Cdk2 inactivation in these  $Cdk2^{\Delta\text{hepa}}$  mice was confirmed by rt-PCR using specific primers for exon 1 and 4 respectively (Figure 3.21A).

Analogous to previous experiments,  $Cdk2^{\Delta\text{hepa}}$  mice and  $Cdk2^{f/f}$  animals (referred to as wild type controls) were first characterized after high-dose DEN-induced acute liver injury. Determination of ALT serum transaminase levels (Figure 3.21B) and histological analysis of H&E stained liver sections (Figure 3.21C) revealed a similar degree of strong liver injury in both groups. Liver apoptosis was determined by TUNEL staining and measurement of caspase-3 activity 0-72 h after DEN treatment (Figure 3.21D-E) revealing no significant effect of the Cdk2 inactivation on hepatocyte survival after DEN treatment. Thus, DEN induced the

same liver damage and comparable cell death response in  $Cdk2^{\Delta\text{hepa}}$  mice and controls.

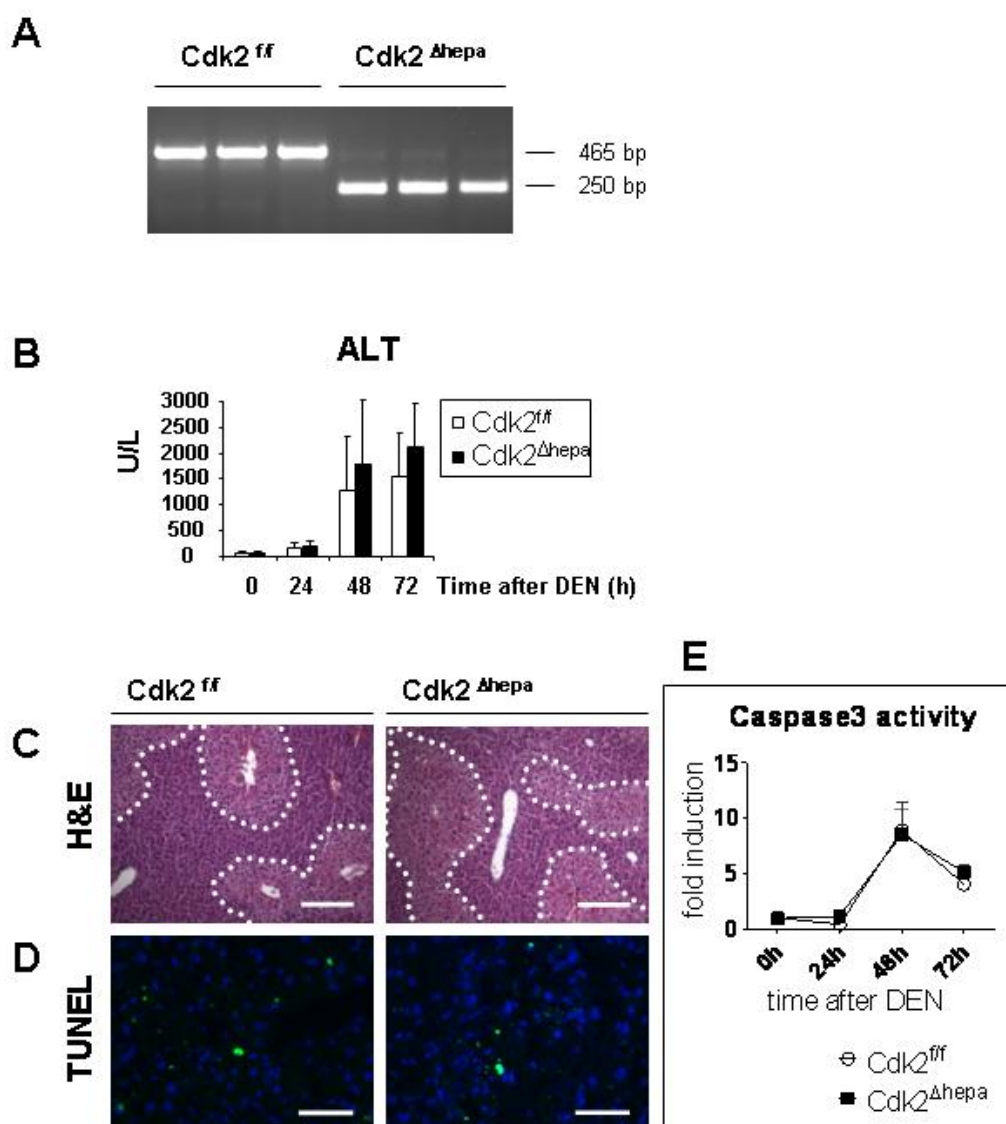


**Figure 3.21 Cdk2 specific hepatocyte loss does not alter apoptosis or proliferation in DEN-induced liver injury.** (A) Cdk2 deletion efficiency was measured by PCR with specific primers in exon1 and exon4 and with whole liver cDNA. Wildtype band ( $Cdk2^{ff}$ ) is 465 base pairs (bp) in size and product without exons 2 and 3 ( $Cdk2^{\Delta\text{hepa}}$ ) is approximately 250 bp. (B-E) 6-8 weeks old  $Cdk2^{ff}$  and  $Cdk2^{\Delta\text{hepa}}$  mice were injected with DEN (200 mg/kg i.p.) to induce acute liver injury; livers were investigated up to 96 hours after injection. (B) Serum level of alanine-aminotransferase (ALT) of mice at indicated time points after DEN injection. Each bar represents a value of minimum 3 animals, data are presented as the average  $\pm$  s.d. (C) H&E staining of paraffin embedded liver sections 48 hours after DEN. Scale bar: 100  $\mu\text{m}$ . (D) TUNEL staining on frozen liver sections 48 hours after DEN, TUNEL positive cells are green, nuclei are visualized by DAPI: blue. Scale bar: 50  $\mu\text{m}$ . (E) Caspase-3 activity was measured by assay for specific caspase-3 substrate turnover and calculated as fold induction in comparison to untreated livers for  $Cdk2^{\Delta\text{hepa}}$  (squares) and  $Cdk2^{ff}$  (circles) animals. Each value represents a minimum of 3 animals, data are presented as the average  $\pm$  s.d.

To test, if hepatocarcinogenesis in the DEN model depends on a functional CcnE1/Cdk2 complex, 2 weeks old Cdk2<sup>ff</sup> and Cdk2<sup>Δhepa</sup> mice were injected with DEN to induce HCC and analyzed 38 weeks after treatment in agreement with the previous experiments. As expected, 100 % of Cdk2<sup>ff</sup> mice (8/8) developed liver tumors with an average of 38 tumors per mouse and a mean tumor diameter of 8 mm (SD ± 4 mm, Figure 3.22A, left panel and Figure 3.22B-C). In contrast, hepatocyte-specific deletion of Cdk2 resulted in reduced tumor incidence of 90% (7/8). More interestingly, tumor frequency and tumor growth in Cdk2<sup>Δhepa</sup> mice were strongly decreased showing an average of 6 liver tumors per mouse and a mean tumor diameter of only 3mm ± 1 mm (Figure 3.22A, middle panel and Figure 3.22B-C). In agreement with strongly decreased tumor burden in DEN-treated Cdk2<sup>Δhepa</sup> mice, the liver mass index in these animals at the age of 40 weeks was normal (approximately 5 %) and comparable to healthy and untreated mice, whereas Cdk2<sup>ff</sup> mice showed significantly increased liver mass index (9% SD: ± 3%, Figure 3.22D) due to strong tumor load. Therefore, Cdk2<sup>Δhepa</sup> mice are similarly protected from DEN-mediated hepatocarcinogenesis as shown before in CcnE1<sup>-/-</sup> mice. These data suggests that HCC-development depends on both functional CcnE1 and Cdk2 in hepatocytes.

Cdk2<sup>Δhepa</sup> animals still express CcnE1 and CcnE2 and the previous data suggested that CcnE1 is a key cyclin for hepatocarcinogenesis. To further rule out that CcnE1 may perform non-canonical functions during tumor development, double mutants with a constitutive knockout of CcnE2 and conditional ablation of Cdk2 (Cdk2<sup>Δhepa</sup>CcnE2<sup>-/-</sup> mice) were generated and subjected to single low-dose DEN treatment for HCC induction. Interestingly, Cdk2<sup>Δhepa</sup>CcnE2<sup>-/-</sup> mice revealed similar protection from tumor formation and tumor growth as found in Cdk2<sup>Δhepa</sup> mice, with an average of 6 liver tumors per mouse and a mean diameter of 3mm (SD:± 1 mm, Figure 3.22A, right panel and Figure 3.22B-C).

Previous experiments demonstrated increased CcnE1 expression in DEN-induced tumors derived from WT or CcnE2<sup>-/-</sup> mice (compare Figure 3.6A). Similarly, CcnE1 mRNA expression was highly (approximately 10fold), but not significantly different induced in livers from DEN-treated Cdk2<sup>ff</sup>, Cdk2<sup>Δhepa</sup> and Cdk2<sup>Δhepa</sup>CcnE2<sup>-/-</sup> mice (Figure 3.22E). Therefore, hepatic tumor formation depends not only on CcnE1 induction but also requires availability of the canonical binding partner Cdk2. However, CcnE1 gene induction seems to be independent of Cdk2. Interestingly,

DEN-treatment did not induce CcnE2 mRNA expression in  $Cdk2^{\Delta\text{hepa}}$  mice (Figure 3.22E, medium panel).

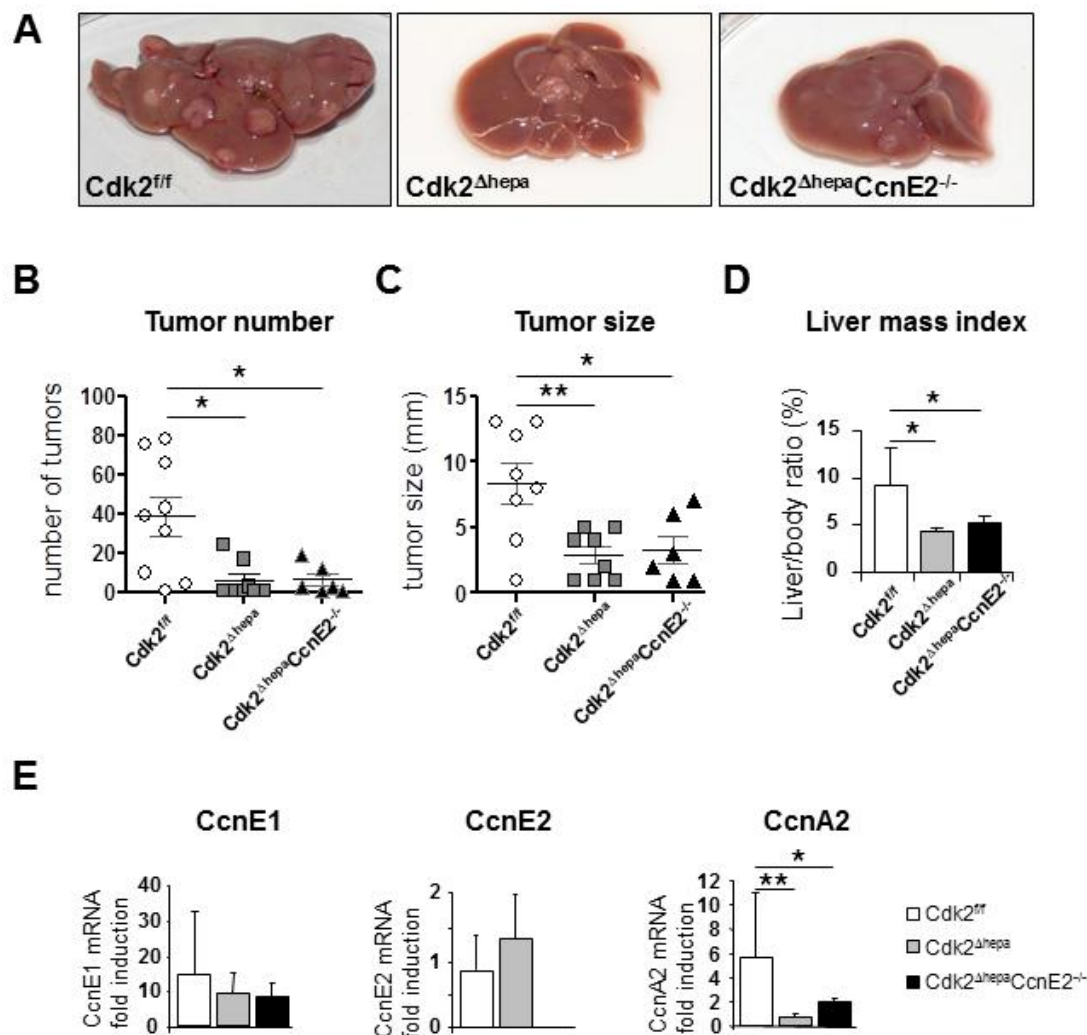


**Figure 3.22 Cdk2 is required for hepatocarcinogenesis induced by DEN.**  $Cdk2^{f/f}$  (n=8),  $Cdk2^{\Delta\text{hepa}}$  (n=8) and  $Cdk2^{\Delta\text{hepa}}CcnE2^{-/-}$  (n=6) male mice at the age of 14 days were treated once with DEN (25mg/kg i.p.). At the age of 40 weeks, animals were sacrificed and analysed for markers of hepatocellular carcinoma. (A) Macroscopic appearance of representative 40 week old livers and tumors derived from  $Cdk2^{f/f}$ ,  $Cdk2^{\Delta\text{hepa}}$  and  $Cdk2^{\Delta\text{hepa}}CcnE2^{-/-}$  animals. (B) Number of visible tumors for each individual mouse is determined. (C) For each individual mouse the size of the largest tumor is given as an indicator for tumor growth. (D) Liver/body weight ratio in DEN-treated mice at the age of 40 weeks. \*:  $p < 0.05$ . (E) mRNA expression of indicated genes was measured by real-time PCR analysis in 40 week liver tissue for  $Cdk2^{f/f}$  (white bars),  $Cdk2^{\Delta\text{hepa}}$  (grey bars) and  $Cdk2^{\Delta\text{hepa}}CcnE2^{-/-}$  (black bars) animals treated as described. Expression levels were normalized to expression of the housekeeping gene GAPDH and calculated as fold induction in comparison to untreated controls. Each bar represents a value of minimum 6 animals, data are presented as the average  $\pm$  s.d. \*:  $p < 0.05$ ; \*\*:  $p < 0.005$ .

As previously demonstrated (Figure 3.6C), CcnE1 was required for driving CcnA2 expression and DNA replication during advanced tumor progression in the liver. This gene regulation of CcnA2 is also dependent on functional Cdk2. Accordingly, CcnA2 mRNA expression was only detectable at baseline levels in aged livers from DEN-treated Cdk2<sup>Δhepa</sup> and Cdk2<sup>Δhepa</sup>CcnE2<sup>-/-</sup> mice in contrast to control mice with CcnA2 upregulation and strong tumor load (Figure 3.22E, right panel). These findings hint at an essential role of the CcnE1/Cdk2 complex for S-phase initiation and CcnA2 expression specifically during tumor progression.

In summary, CcnE1 essentially promotes liver carcinogenesis in cooperation with its canonical binding partner Cdk2, which cannot be compensated by closely related homologues such as CcnE2 or alternative Cdks.

## 4. Discussion

The main objective of this work was to examine the contribution of E-type cyclins in cancer development and progression. To address this question, the previously described CcnE1 and CcnE2 knockout mice were further characterized in DEN-induced liver cancerogenesis. Interestingly, the loss of CcnE1 leads to an impressive inhibition of chemically induced liver cancer. This approach further demonstrated that CcnE1 deficiency alters both tumor initiation and progression in mice, as depicted by a strong reduction in tumor number and tumor size. This finding suggests that CcnE1 and CcnE2 have very distinctive roles in tumorigenesis. Employing a model of acute liver injury in order to mimic early events of tumor development revealed that CcnE1 represses cell cycle arrest and attenuates the DNA damage-induced checkpoint control after genotoxic stress. Additionally, to determine whether the function of CcnE1 in tumorigenesis is a Cdk2-dependent effect,  $Cdk2^{\Delta\text{hepa}}$  and  $Cdk2^{\Delta\text{hepa}}CcnE2^{-/-}$  mice were generated and subjected to DEN treatment. CcnE1 alone in these mice was not able to severely induce and promote DEN-induced cancerogenesis. Thus, this study indicates that targeting CcnE1 in hepatocellular carcinoma to be a potential therapeutic approach.

### 4.1. Distinct roles of CcnE1 and CcnE2 in hepatocarcinogenesis

The roles of CcnE1 and CcnE2 were postulated to be redundant based on high sequence homology, and furthermore redundancies with CcnA2 have also been suggested based on findings that CcnA2-Cdk2 activity can substitute for CcnE-Cdk2 (Caldon and Musgrove, 2010; Kaldis and Aleem, 2005; Nevzorova et al., 2009). Animal knockout models have revealed that deletion of either CcnE1 or CcnE2 results in primarily normal phenotypes; however, the importance of CcnE was emphasized by the fact that  $CcnE1^{-/-}CcnE2^{-/-}$  double knockout mice are embryonic lethal (Geng et al., 2003; Parisi et al., 2003).  $CcnE1^{-/-}$  and  $CcnE2^{-/-}$  mice have only slight differences in the velocity of regenerative response, as previously investigated in a liver regeneration model (Nevzorova et al., 2009). Based on the results from



these studies, it was not expected that the loss of CcnE1 would have a striking impact on chemically induced hepatocellular carcinoma. Experiments with small interfering RNA (siRNA) targeting CcnE1 in human HCC cell lines, as well as in other cell lines, hinted toward increased sensitivity for arrest and apoptosis, although the role of CcnE2 in this setting was not analyzed (Li et al., 2003; Liang et al., 2010; Todd et al., 2009). However, recent studies targeting either CcnE1 or CcnE2 with siRNA showed comparable results in reducing the proliferative potential of cancer cell lines, again indicating to overlapping functions of CcnE1 and CcnE2 (Caldon and Musgrove, 2010; Dapas et al., 2009). In the present study, it was clearly shown that CcnE1 - but not CcnE2 - is an important oncogene in liver tumor development following carcinogen insult and its expression is likely necessary for the ability of the transformed cell to proliferate.

In addition to the effect of CcnE1 deficiency on tumor initiation and progression, its expression is apparently critical for the induction of CcnE2 and CcnA2 during tumorigenesis as CcnE1 knockout mice exposed to DEN treatment express much lower levels of CcnE2 and CcnA2 than WT animals. This correlates with results from a previous study showing a physical interaction between CcnE and the CcnA2 promoter leading to activation of transcription (Schulze et al., 1995; Zerfass-Thome et al., 1997). Moreover, it is likely that generally low cyclin expression levels considerably contribute to tumor inhibition. It is interesting to note that the low CcnE2 and CcnA2 expression levels found in CcnE1 knockout mice is likely specific for transformed cells; which is in strong contrast to the liver regeneration model where CcnA2 is highly induced and replaces CcnE1 and/or CcnE2 (Nevzorova et al., 2009). In this work it was demonstrated that transformed CcnE1-deficient cells during tumor development cease to proliferate and to some extent undergo senescence, therefore highlighting the differential and nonredundant roles of CcnE1 and CcnE2.

## 4.2. New signaling pathways involved during CcnE1-driven carcinogenesis

The model used in this study has been previously developed and established in order to expose the initial events involved in liver cell transformation following a genotoxic hit such as DEN (Maeda et al., 2005). An aim of this study was to determine if the loss of CcnE1, following acute liver injury, impacts critical elements of cellular signaling cascades that are necessary for transformation and tumor development. Surprisingly, although others have suggested that cell death is one of the decisive mechanisms deciding pro or contra tumorigenesis, no clear differences were evident in apoptosis induction in our study (Eferl et al., 2003; Maeda et al., 2005). Interesting, however, was the reduction in F4/80 positive Kupffer cells, the resident liver macrophage, in CcnE1-deficient mice after DEN treatment suggesting an important role for CcnE1 in their regulation following insult. This result further supports the finding that superoxide produced by Kupffer cells during liver damage and inflammation contributes to hepatocarcinogenesis by aggravating genotoxic and cytotoxic effects in hepatocytes (Teufelhofer et al., 2005). Taking these results together it is suggested that the temporary loss of Kupffer cells at the time of maximal tissue and cell damage presumably improves the outcome in tumorigenesis.

One mechanism by which CcnE1 might promote tumor formation is by antagonizing an arrest of transformed and/or damaged cells. Cell cycle arrest is critical in order for DNA repair to occur and the mediators regulating cell cycle progression are known as CDK inhibitors. DEN-treated CcnE1-deficient liver cells undergo arrest that is associated with elevated levels of the prominent tumor suppressors p21 and p27. In case of p27, this finding persists till later time points in tumor development, and tumors of CcnE1-deficient DEN-treated mice display aberrantly elevated levels of p27. Absence or cytoplasmic localization of p21 or p27 within solid tumor is recognized as an indicator of poor prognosis in patients (Abukhdeir and Park, 2008), and consequently, the finding that p27 is less phosphorylated (thus inactivated) in CcnE1-deficient tumors confirmed the importance of p27 in reducing tumor cell proliferation.

DNA damage checkpoint activation after genotoxic stress is the primary barrier to tumorigenesis. There are two pathways that should protect cells against excessive

CcnE activity. The first is a p53-dependent response that suppresses CcnE kinase activity through induction of the inhibitor p21, and the second is the pathway of CcnE degradation (Minella et al., 2007). p53 is a hallmark tumor suppressor which induces cell cycle arrest and/or apoptosis in response to DNA damage; its levels are commonly decreased in tumors. Phosphorylation of p53 on either Ser15 or Ser20 is an important modification that prevents Mdm2 binding and thus inhibits Mdm2-dependent degradation (Meek and Anderson, 2009). The CcnE1-deficient animals displayed stronger and prolonged p53 stabilization after DEN treatment suggesting that CcnE1 is interfering with p53-dependent checkpoint activity.

c-Jun N-terminal kinases (JNKs) are responsive to stress stimuli and play important roles in cell growth, survival and apoptosis. Analysis of the JNK pathway in CcnE1 deficient DEN-treated animals revealed an up-regulation. Substrates for JNK activity also include p53, and depending on the cellular context JNK either destabilizes p53 by binding to it or stabilizes p53 by phosphorylation thereby inhibiting ubiquitin-mediated degradation (Fuchs et al., 1998a; Fuchs et al., 1998b). Thus, the drop in JNK and p53 activity observed in the DEN-treated animals with functional CcnE1 may be the cause of dysregulated checkpoint, whereas loss of CcnE1 probably supports checkpoint activity and adequate repair. How CcnE1 exactly interferes with p53 stabilization and JNK activation still has to be identified.

During late stages of tumor progression the loss of CcnE1 is associated with enhanced senescence. For this reason senescence was also assessed in DEN-induced acute liver injury model. Unexpectedly, CcnE2 treated animals displayed high amounts of SA  $\beta$ -galactosidase activity, a well-established marker of senescence. Bartkova et al reported oncogene-induced senescence in cells with ectopic CcnE1 overexpression in response to replication stress. However, in that study, only retrovirus infected cell lines were tested. In contrast to this study, many human cancers with CcnE1 overexpression and/or amplification show elevated proliferation rather than signs of senescence. Taken together the current results as well as those from previous reports suggest that overexpression of CcnE1 in CcnE2 deficient animals during acute liver injury may be beyond "usual" levels found in tumors and thus drives cells into senescence. Furthermore, these mice also display exceptionally high levels of IL-6, which might support the described phenomenon of senescence-associated secretory phenotype (SASP), which occurs after

establishment of persistent DNA damage signaling (Rodier et al., 2009). This observation was not examined in detail in the present study but deserves further investigation.

Why does the discrepancy arise between senescence induction in the acute liver injury model as compared to mice with established tumors even when the same chemical is applied? One possible explanation is the different age conditions. Tumor induction is initiated by injecting 14-day old neonatal mice with DEN (25 mg/kg), while the animals are still developing and therefore DEN induced mutations become prominent through liver growth. The mice used in the acute liver injury model are adult (6-8 week old) and as the liver cells have reached quiescence, an 8-fold higher DEN dose was necessary to induce tissue damage and regeneration. To obtain direct insight into the immediate response of DEN relevant for tumor induction, neonatal mice were sacrificed 48 hours after injection. WT mice revealed very low levels of apoptosis, which was slightly augmented in CcnE1-deficient animals. CcnE1 deficiency resulted in obvious cell cycle arrest in comparison to WT animals as ascertained by PCNA immunostaining, whereas pH2AX staining, an indicator of DNA double strand breaks, showed comparable DEN-induced DNA damage between the genotypes as observed in the acute liver injury model. These experiments demonstrated that DEN-induced acute liver injury is an efficient tool to investigate early events in tumor development. However, the limitations in the adult mouse model are increased tissue damage and manifestation of senescence that were not present in neonatal mice. Nevertheless, in this work, new signaling pathways following DEN-induced DNA damage were identified in the DEN-induced acute liver injury model.

The results from the regeneration model with CcnE1 and CcnE2 knockout mice showed normal proliferation of liver cells due to the largely overlapping functions of these two proteins (Nevzorova et al., 2009). In contrast, the present work identifies a unique role for CcnE1 depending on the environmental milieu (toxic injury) and further emphasizes its role in cancerogenesis.

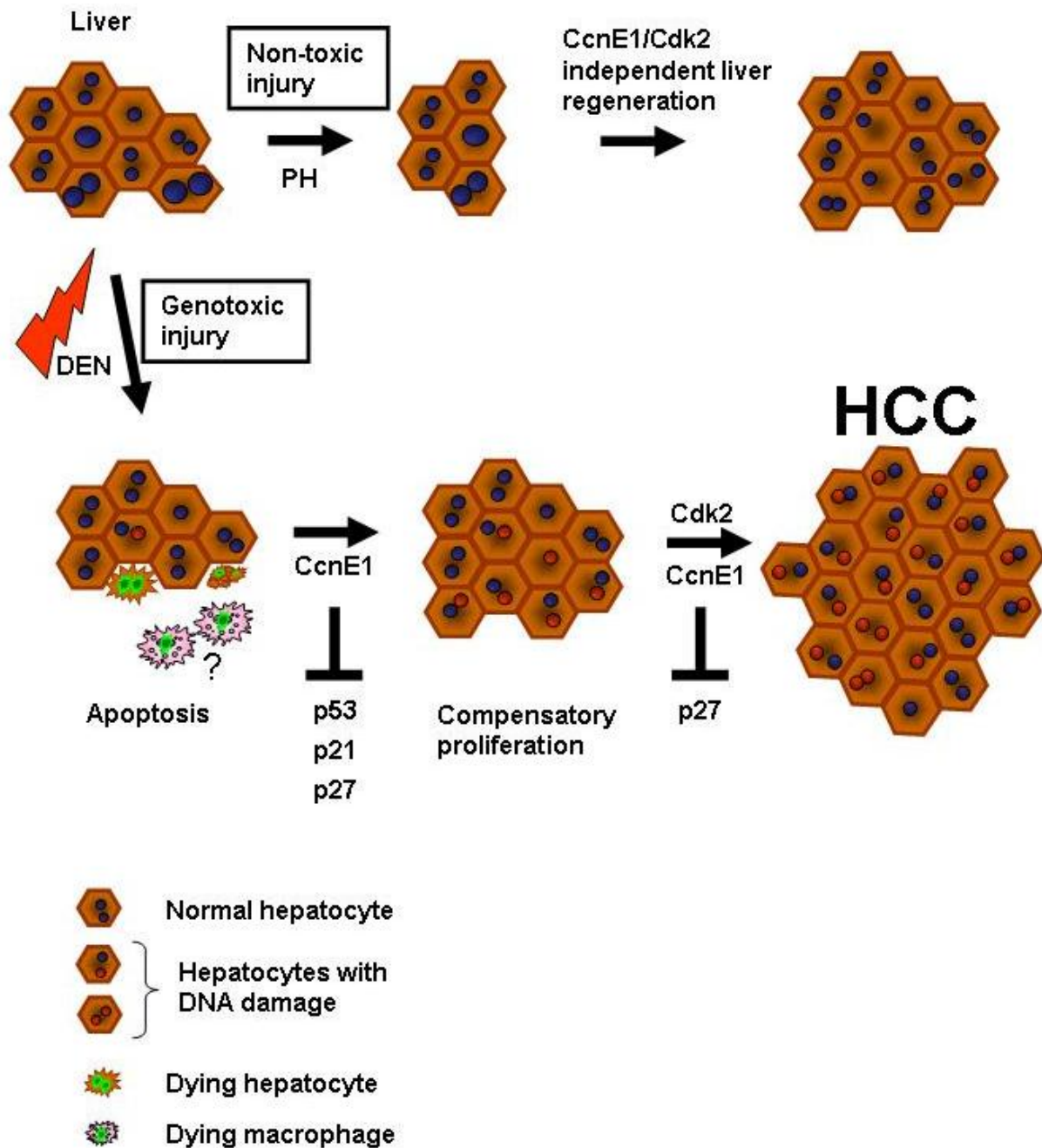


**Figure 4.1 Proposed CcnE1-Cdk2 function in non-toxic and genotoxic injury.** CcnE1-Cdk2 seems to be dispensable for proliferation following non-toxic injury such as partial hepatectomy; however, functional CcnE1-Cdk2 complex is required for tumor development after genotoxic injury e.g. DEN.

The DEN model places CcnE1 into genotoxic damage scenery and highlights its important role in tumor initiation and development. Studies with other genotoxic agents, such as carbon tetrachloride (CCl<sub>4</sub>) support this notion with the finding that CcnE1 plays an important role in CCl<sub>4</sub>-induced liver fibrosis (Nevzorova et al. unpublished data). Finally, these results support the hypothesis that CcnE1 function is different under genotoxic or non-genotoxic stress conditions (Figure 4.1).

### 4.3. Oncogene CcnE1 function is Cdk2 dependent

The present work demonstrated that CcnE1 is one of the key genes driving chemically induced hepatocarcinogenesis; however an open question remained as to whether CcnE1 can operate without its canonical interaction partner Cdk2 in tumor development. Usually CcnE1 functions as a regulatory subunit of Cdk2 which is essential for G1 to S-phase transition and DNA replication. However, CcnE1 has also been described to contain kinase-independent functions, involving the loading of minichromosome maintenance (MCM) proteins onto the replication origin (Geng et al., 2007). Very recently, two studies revealed that Cdk2-deficient mice are completely resistant to oncogene ErbB2 and LMW-CcnE mediated mammary tumors (Akli et al., 2011; Ray et al., 2011). This study has clearly shown that Cdk2 is an important component of an oncogenic complex involved in liver cancer, as exemplified by Cdk2 hepatocyte deficient animals, which display massive reduction of tumor development upon carcinogen treatment. It was also suggested that CcnE2 might control CcnE1 expression (Nevzorova et al., 2009), and in light of this theory, double knockout mice  $Cdk2^{\Delta\text{hepa}}E2^{-/-}$  were generated and treated with DEN to test whether CcnE1 alone can drive tumorigenesis. Nevertheless, these mice displayed the same resistance to DEN-induced liver tumors as single hepatocyte Cdk2-deficient animals. This observation suggests that liver cancers with CcnE1 upregulation should be considered for Cdk2 inhibitor therapy clinical trials.

Traditionally, the diagnosis of HCC was not possible before the advanced stage of disease. However in the last few years in many patients HCC was diagnosed at an early stage due to improved imaging techniques when liver function can still be preserved. Treatments usually used are surgical resection, transplantation and percutaneous ablation (Llovet et al., 2003). Molecular targeted therapy of HCC showed encouraging results in case of Sorafenib, a multikinase inhibitor (Llovet et al., 2008). CcnE1 overexpression has been demonstrated in many cancers, including HCC, and this study confirmed that inhibition of CcnE1 is promising new treatment modality for HCC. Up to date, no specific chemical inhibitors for CcnE1 have been developed, although diverse Cdk inhibitors with broad target specificity exist. Roscovitine (Seliciclib) and related compounds could be very promising for HCC treatment, showing a higher degree of selectivity.

#### 4.4. Future impacts and directions

Hepatocellular carcinoma (HCC) is the most common type of liver cancer and is among one of the leading causes of cancers worldwide associated with high mortality (Parkin, 1998). Identification of new signaling pathways and specific molecules regulating cancerogenesis is critical for development of new drug therapies. Perturbed cell cycle signaling is one of the important events leading to cancer (Villanueva and Llovet). This study showing the importance of CcnE1 and Cdk2 provides a new window for specific targeting of liver cancers. Future treatments of HCC, potentially with Cdk2-specific inhibitors such as Roscovitine, might benefit of patient stratification based on CcnE1 expression status. Existing Cdk inhibitors are not specific to only one Cdk and inhibiting Cdk2 might interfere with DNA repair. Based on this data, it would be recommendable to inhibit CcnE1 specifically, considering that ubiquitous loss of CcnE1 has no negative effect. Finally, continuing to elucidate the role of CcnE1 in cancer will hopefully lead to the development of CcnE1-specific inhibitors for cancer treatment.

## 5. Summary

E-type cyclins (CcnE) control the transition of quiescent cells into the cell cycle. Two E-type cyclins, CcnE1 and CcnE2 have been described. A variety of human cancers, including hepatocellular carcinoma (HCC), overexpress CcnE and this is frequently associated with reduced patient survival. The aim of the present study was to dissect the role of CcnE1 and CcnE2 for hepatocarcinogenesis induced by the carcinogen diethylnitrosamine (DEN) using CcnE1 and CcnE2 knockout mice. The central question was how the genetic loss of CcnE1 or CcnE2 would affect tumor initiation and/or progression.

The study revealed several unexpected findings. CcnE2<sup>-/-</sup> mice developed liver tumors of similar number and size compared to wild type (WT) animals demonstrating for the first time that CcnE2 is dispensable for development of liver cancer. Surprisingly, CcnE1-deficient animals were mostly resistant to HCC induction and showed poor tumor growth. Therefore the present data suggests that CcnE1- but not its homologue CcnE2 - is essential for initiation and progression of liver cancer.

The molecular mechanisms underlying these findings were further investigated in a model of DEN-induced acute liver injury, which reflected immediate early events of cell transformation and cellular signaling. DEN-mediated liver injury was genotoxic and triggered a DNA damage response pathway (DDR) and activation of Jun kinases (JNK) already 24 and 48 hours after treatment in all genotypes. Interestingly, CcnE1-deficient livers revealed transient hyper-activation of JNK and more importantly a stronger and prolonged expression of the tumor suppressor p53. In good agreement, CcnE1<sup>-/-</sup> livers showed also prolonged cell cycle arrest associated with increased expression of cell cycle inhibitors p21 and p27 following DEN challenge. Thus expression of CcnE1 was shown to be essential to overcome the cell cycle arrest and DDR of hepatocytes immediately after mutagenic treatment.

In another approach knockout mice with a hepatocyte-specific deletion of Cdk2 (Cdk2<sup>Δhepa</sup>) and Cdk2<sup>Δhepa</sup> CcnE2<sup>-/-</sup> double knockout mice were generated and subjected to DEN treatment. Importantly, these strains were also strongly protected from HCC formation similar to CcnE1<sup>-/-</sup> mice.

In summary, the present study demonstrated for the first time that CcnE1 is an essential oncogene in the liver and drives hepatocarcinogenesis and tumor growth in a Cdk2-dependent manner.



## 6. Zusammenfassung

E-Cycline (CcnE1 und CcnE2) kontrollieren den Übergang von ruhenden Zellen in den Zellzyklus. In vielen humanen Tumoren inklusive des hepatozellulären Karzinoms (HCC) sind E-Cycline überexprimiert, was mit einem verminderten Patientenüberleben assoziiert ist. Ziel der vorliegenden Arbeit war die funktionelle Charakterisierung von CcnE1 und CcnE2 bei der Leberkrebsentstehung in einem Modell der chemisch induzierten Hepatokarzinogenese durch Diethylnitrosamin (DEN) unter Verwendung von CcnE1- und CcnE2 knockout Mäusen. Zentrale Frage der Arbeit war, inwieweit die genetische Inaktivierung von CcnE1 oder CcnE2 die Tumorentstehung oder das Tumorwachstum beeinflusst.

Die vorliegende Arbeit zeigt mehrere unerwartete Ergebnisse: CcnE2<sup>-/-</sup> Mäuse und Wildtyp (WT) Kontrolltiere bildeten Lebertumore in gleicher Zahl und Größe. Diese Daten beweisen erstmals, dass CcnE2 für die Tumorentstehung in der Leber nicht benötigt wird. Überraschender Weise waren CcnE1<sup>-/-</sup> Mäuse weitestgehend resistent gegen die DEN-vermittelte HCC-Entstehung und Tumorwachstum. Dies zeigte, dass CcnE1 – nicht aber sein Homologes CcnE2 – für Tumorentstehung und Wachstum in der Leber essentiell ist. Zur Charakterisierung von unmittelbaren, frühen Ereignissen in der Zelltransformation und der zellulären Signaltransduktion wurde das Modell der DEN-induzierten akuten Leberschädigung verwendet. In allen drei Genotypen induzierte DEN bereits 24-48 h nach Stimulation eine DNA-Schadigungsantwort und Aktivierung von JUN-Kinasen (JNK). Interessanter Weise zeigte sich in CcnE1-defizienten Lebern eine stärkere Aktivierung von JNK sowie eine verlängerte und stärkere Expression des Tumorsuppressors p53. In Übereinstimmung mit diesem Befund zeigten diese Mäuse auch einen verlängerten Zellzyklusarrest, der mit einer erhöhten Expression der Zellzyklusinhibitoren p21 und p27 einherging. Expression von CcnE1 nach mutagener Leberschädigung führt also zu einer Überwindung des Zellzyklusarrest. In einem weiteren Ansatz wurden hepatozyten-spezifische Cdk2 knockout Mäuse (Cdk2<sup>Δhepa</sup>) und Cdk2<sup>Δhepa</sup>CcnE2<sup>-/-</sup> doppelknockout Mäuse generiert und mit DEN behandelt, und beide Mauslinien waren ähnlich wie CcnE1<sup>-/-</sup> Tiere vor Entstehung eines HCC geschützt.

Zusammenfassend beweist die vorliegende Arbeit erstmalig, dass CcnE1 in Kooperation mit seiner assoziierten Kinase Cdk2 ein essentielles Leber-Onkogen darstellt.

## 7. References

- Abbas, T., and A. Dutta, 2009. p21 in cancer: intricate networks and multiple activities. *Nat Rev Cancer*.
- Abukhdeir, A.M., and B.H. Park, 2008. P21 and p27: roles in carcinogenesis and drug resistance. *Expert Rev Mol Med* 10: e19.
- Adams, P.D., W.R. Sellers, S.K. Sharma, A.D. Wu, C.M. Nalin, and W.G. Kaelin, Jr., 1996. Identification of a cyclin-cdk2 recognition motif present in substrates and p21-like cyclin-dependent kinase inhibitors. *Mol Cell Biol* 16: 6623-33.
- Akli, S., C.S. Van Pelt, T. Bui, L. Meijer, and K. Keyomarsi, 2011. Cdk2 is required for breast cancer mediated by the low-molecular-weight isoform of cyclin E. *Cancer Res* 71: 3377-86.
- Ball, K.L., and D.P. Lane, 1996. Human and plant proliferating-cell nuclear antigen have a highly conserved binding site for the p53-inducible gene product p21WAF1. *Eur J Biochem* 237: 854-61.
- Bartek, J., J. Bartkova, and J. Lukas, 1996. The retinoblastoma protein pathway and the restriction point. *Curr Opin Cell Biol* 8: 805-14.
- Bartek, J., J. Bartkova, and J. Lukas, 1997. The retinoblastoma protein pathway in cell cycle control and cancer. *Exp Cell Res* 237: 1-6.
- Bartkova, J., N. Rezaei, M. Liontos, P. Karakaidos, D. Kletsas, N. Issaeva, L.V. Vassiliou, E. Kolettas, K. Niforou, V.C. Zoumpourlis, M. Takaoka, H. Nakagawa, F. Tort, K. Fugger, F. Johansson, M. Sehested, C.L. Andersen, L. Dyrskjot, T. Orntoft, J. Lukas, C. Kittas, T. Helleday, T.D. Halazonetis, J. Bartek, and V.G. Gorgoulis, 2006. Oncogene-induced senescence is part of the tumorigenesis barrier imposed by DNA damage checkpoints. *Nature* 444: 633-7.
- Berthet, C., E. Aleem, V. Coppola, L. Tessarollo, and P. Kaldis, 2003. Cdk2 knockout mice are viable. *Curr Biol* 13: 1775-85.
- Besson, A., S.F. Dowdy, and J.M. Roberts, 2008. CDK inhibitors: cell cycle regulators and beyond. *Dev Cell* 14: 159-69.
- Blattner, C., A. Sparks, and D. Lane, 1999. Transcription factor E2F-1 is upregulated in response to DNA damage in a manner analogous to that of p53. *Mol Cell Biol* 19: 3704-13.
- Bohlig, L., and K. Rother, 2011. One function--multiple mechanisms: the manifold activities of p53 as a transcriptional repressor. *J Biomed Biotechnol* 2011: 464916.

- Bortner, D.M., and M.P. Rosenberg, 1997. Induction of mammary gland hyperplasia and carcinomas in transgenic mice expressing human cyclin E. *Mol Cell Biol* 17: 453-9.
- Bosch, F.X., and N. Munoz, 1988. Prospects for epidemiological studies on hepatocellular cancer as a model for assessing viral and chemical interactions. *IARC Sci Publ*: 427-38.
- Bosch, F.X., J. Ribes, M. Diaz, and R. Cleries, 2004. Primary liver cancer: worldwide incidence and trends. *Gastroenterology* 127: S5-S16.
- Boucheron, J.A., F.C. Richardson, P.H. Morgan, and J.A. Swenberg, 1987. Molecular dosimetry of O4-ethyldeoxythymidine in rats continuously exposed to diethylnitrosamine. *Cancer Res* 47: 1577-81.
- Bradford, M.M., 1976. A rapid and sensitive method for the quantitation of microgram quantities of protein utilizing the principle of protein-dye binding. *Anal Biochem* 72: 248-54.
- Brady, C.A., and L.D. Attardi, 2010. p53 at a glance. *J Cell Sci* 123: 2527-32.
- Cabart, P., H.K. Chew, and S. Murphy, 2004. BRCA1 cooperates with NUFIP and P-TEFb to activate transcription by RNA polymerase II. *Oncogene* 23: 5316-29.
- Caldon, C.E., and E.A. Musgrove, 2010. Distinct and redundant functions of cyclin E1 and cyclin E2 in development and cancer. *Cell Div* 5: 2.
- Chen, J., P. Saha, S. Kornbluth, B.D. Dynlacht, and A. Dutta, 1996. Cyclin-binding motifs are essential for the function of p21CIP1. *Mol Cell Biol* 16: 4673-82.
- Cheng, M., P. Olivier, J.A. Diehl, M. Fero, M.F. Roussel, J.M. Roberts, and C.J. Sherr, 1999. The p21(Cip1) and p27(Kip1) CDK 'inhibitors' are essential activators of cyclin D-dependent kinases in murine fibroblasts. *EMBO J* 18: 1571-83.
- Chi, Y., M. Welcker, A.A. Hizli, J.J. Posakony, R. Aebersold, and B.E. Clurman, 2008. Identification of CDK2 substrates in human cell lysates. *Genome Biol* 9: R149.
- Child, E.S., and D.J. Mann, 2006. The intricacies of p21 phosphorylation: protein/protein interactions, subcellular localization and stability. *Cell Cycle* 5: 1313-9.
- Clurman, B.E., R.J. Sheaff, K. Thress, M. Groudine, and J.M. Roberts, 1996. Turnover of cyclin E by the ubiquitin-proteasome pathway is regulated by cdk2 binding and cyclin phosphorylation. *Genes Dev* 10: 1979-90.
- Dahlmann, H.A., V.G. Vaidyanathan, and S.J. Sturla, 2009. Investigating the biochemical impact of DNA damage with structure-based probes: abasic sites, photodimers, alkylation adducts, and oxidative lesions. *Biochemistry* 48: 9347-59.

- Dannenberg, J.H., A. van Rossum, L. Schuijff, and H. te Riele, 2000. Ablation of the retinoblastoma gene family deregulates G(1) control causing immortalization and increased cell turnover under growth-restricting conditions. *Genes Dev* 14: 3051-64.
- Dapas, B., R. Farra, M. Grassi, C. Giansante, N. Fiotti, L. Uxa, G. Rainaldi, A. Mercatanti, A. Colombatti, P. Spessotto, V. Lacovich, G. Guarnieri, and G. Grassi, 2009. Role of E2F1-cyclin E1-cyclin E2 circuit in human coronary smooth muscle cell proliferation and therapeutic potential of its downregulation by siRNAs. *Mol Med* 15: 297-306.
- DeGregori, J., G. Leone, K. Ohtani, A. Miron, and J.R. Nevins, 1995. E2F-1 accumulation bypasses a G1 arrest resulting from the inhibition of G1 cyclin-dependent kinase activity. *Genes Dev* 9: 2873-87.
- Delk, N.A., K.K. Hunt, and K. Keyomarsi, 2009. Altered subcellular localization of tumor-specific cyclin E isoforms affects cyclin-dependent kinase 2 complex formation and proteasomal regulation. *Cancer Res* 69: 2817-25.
- Desai, D., H.C. Wessling, R.P. Fisher, and D.O. Morgan, 1995. Effects of phosphorylation by CAK on cyclin binding by CDC2 and CDK2. *Mol Cell Biol* 15: 345-50.
- Diehl, J.A., and C.J. Sherr, 1997. A dominant-negative cyclin D1 mutant prevents nuclear import of cyclin-dependent kinase 4 (CDK4) and its phosphorylation by CDK-activating kinase. *Mol Cell Biol* 17: 7362-74.
- Ducommun, B., P. Brambilla, M.A. Felix, B.R. Franza, Jr., E. Karsenti, and G. Draetta, 1991. cdc2 phosphorylation is required for its interaction with cyclin. *EMBO J* 10: 3311-9.
- Dulic, V., E. Lees, and S.I. Reed, 1992. Association of human cyclin E with a periodic G1-S phase protein kinase. *Science* 257: 1958-61.
- Edgar, B.A., D.A. Lehman, and P.H. O'Farrell, 1994a. Transcriptional regulation of string (*cdc25*): a link between developmental programming and the cell cycle. *Development* 120: 3131-43.
- Edgar, B.A., F. Sprenger, R.J. Duronio, P. Leopold, and P.H. O'Farrell, 1994b. Distinct molecular mechanisms regulate cell cycle timing at successive stages of *Drosophila* embryogenesis. *Genes Dev* 8: 440-52.
- Eferl, R., R. Ricci, L. Kenner, R. Zenz, J.P. David, M. Rath, and E.F. Wagner, 2003. Liver tumor development. c-Jun antagonizes the proapoptotic activity of p53. *Cell* 112: 181-92.
- Ekholm, S.V., P. Zickert, S.I. Reed, and A. Zetterberg, 2001. Accumulation of cyclin E is not a prerequisite for passage through the restriction point. *Mol Cell Biol* 21: 3256-65.

- Elledge, S.J., and M.R. Spottswood, 1991. A new human p34 protein kinase, CDK2, identified by complementation of a *cdc28* mutation in *Saccharomyces cerevisiae*, is a homolog of *Xenopus* Eg1. *EMBO J* 10: 2653-9.
- Ezhevsky, S.A., A. Ho, M. Becker-Hapak, P.K. Davis, and S.F. Dowdy, 2001. Differential regulation of retinoblastoma tumor suppressor protein by G(1) cyclin-dependent kinase complexes in vivo. *Mol Cell Biol* 21: 4773-84.
- Fabrikant, J.I., 1968. The kinetics of cellular proliferation in regenerating liver. *J Cell Biol* 36: 551-65.
- Fisher, R.P., and D.O. Morgan, 1994. A novel cyclin associates with MO15/CDK7 to form the CDK-activating kinase. *Cell* 78: 713-24.
- Fisher, R.P., P. Jin, H.M. Chamberlin, and D.O. Morgan, 1995. Alternative mechanisms of CAK assembly require an assembly factor or an activating kinase. *Cell* 83: 47-57.
- Fleming, W.H., E.J. Alpern, N. Uchida, K. Ikuta, G.J. Spangrude, and I.L. Weissman, 1993. Functional heterogeneity is associated with the cell cycle status of murine hematopoietic stem cells. *J Cell Biol* 122: 897-902.
- Fotedar, R., P. Fitzgerald, T. Rousselle, D. Cannella, M. Doree, H. Messier, and A. Fotedar, 1996. p21 contains independent binding sites for cyclin and cdk2: both sites are required to inhibit cdk2 kinase activity. *Oncogene* 12: 2155-64.
- Fu, T.J., J. Peng, G. Lee, D.H. Price, and O. Flores, 1999. Cyclin K functions as a CDK9 regulatory subunit and participates in RNA polymerase II transcription. *J Biol Chem* 274: 34527-30.
- Fuchs, S.Y., V. Adler, M.R. Pincus, and Z. Ronai, 1998a. MEKK1/JNK signaling stabilizes and activates p53. *Proc Natl Acad Sci U S A* 95: 10541-6.
- Fuchs, S.Y., V. Adler, T. Buschmann, Z. Yin, X. Wu, S.N. Jones, and Z. Ronai, 1998b. JNK targets p53 ubiquitination and degradation in nonstressed cells. *Genes Dev* 12: 2658-63.
- Geng, Y., E.N. Eaton, M. Picon, J.M. Roberts, A.S. Lundberg, A. Gifford, C. Sardet, and R.A. Weinberg, 1996. Regulation of cyclin E transcription by E2Fs and retinoblastoma protein. *Oncogene* 12: 1173-80.
- Geng, Y., Q. Yu, E. Sicinska, M. Das, J.E. Schneider, S. Bhattacharya, W.M. Rideout, R.T. Bronson, H. Gardner, and P. Sicinski, 2003. Cyclin E ablation in the mouse. *Cell* 114: 431-43.
- Geng, Y., Y.M. Lee, M. Welcker, J. Swanger, A. Zagodzoon, J.D. Winer, J.M. Roberts, P. Kaldis, B.E. Clurman, and P. Sicinski, 2007. Kinase-independent function of cyclin E. *Mol Cell* 25: 127-39.

- Geng, Y., Q. Yu, W. Whoriskey, F. Dick, K.Y. Tsai, H.L. Ford, D.K. Biswas, A.B. Pardee, B. Amati, T. Jacks, A. Richardson, N. Dyson, and P. Sicinski, 2001. Expression of cyclins E1 and E2 during mouse development and in neoplasia. *Proc Natl Acad Sci U S A* 98: 13138-43.
- Grasso, P., 1973. The range of carcinogenic substances in human foods and the problems of testing for them. *Proc R Soc Med* 66: 26-7.
- Gray, R., R. Peto, P. Brantom, and P. Grasso, 1991. Chronic nitrosamine ingestion in 1040 rodents: the effect of the choice of nitrosamine, the species studied, and the age of starting exposure. *Cancer Res* 51: 6470-91.
- Grisham, J.W., 1962. A morphologic study of deoxyribonucleic acid synthesis and cell proliferation in regenerating rat liver; autoradiography with thymidine-H3. *Cancer Res* 22: 842-9.
- Gudas, J.M., M. Payton, S. Thukral, E. Chen, M. Bass, M.O. Robinson, and S. Coats, 1999. Cyclin E2, a novel G1 cyclin that binds Cdk2 and is aberrantly expressed in human cancers. *Mol Cell Biol* 19: 612-22.
- Guidotti, J.E., O. Bregerie, A. Robert, P. Debey, C. Brechot, and C. Desdouets, 2003. Liver cell polyploidization: a pivotal role for binuclear hepatocytes. *J Biol Chem* 278: 19095-101.
- Harbour, J.W., R.X. Luo, A. Dei Santi, A.A. Postigo, and D.C. Dean, 1999. Cdk phosphorylation triggers sequential intramolecular interactions that progressively block Rb functions as cells move through G1. *Cell* 98: 859-69.
- Harper, J.W., and S.J. Elledge, 1996. Cdk inhibitors in development and cancer. *Curr Opin Genet Dev* 6: 56-64.
- Harper, J.W., S.J. Elledge, K. Keyomarsi, B. Dynlacht, L.H. Tsai, P. Zhang, S. Dobrowolski, C. Bai, L. Connell-Crowley, E. Swindell, and et al., 1995. Inhibition of cyclin-dependent kinases by p21. *Mol Biol Cell* 6: 387-400.
- Hartwell, P.S.a.J.L., 1967. Survey of compounds which have been tested for carcinogenic activity. U.S. Public Health Serv. Publ. 1.
- Heindryckx, F., I. Colle, and H. Van Vlierberghe, 2009. Experimental mouse models for hepatocellular carcinoma research. *Int J Exp Pathol* 90: 367-86.
- Higashi, H., I. Suzuki-Takahashi, Y. Taya, K. Segawa, S. Nishimura, and M. Kitagawa, 1995. Differences in substrate specificity between Cdk2-cyclin A and Cdk2-cyclin E in vitro. *Biochem Biophys Res Commun* 216: 520-5.
- Hoffmann, D., J.D. Adams, J.J. Piade, and S.S. Hecht, 1980. Chemical studies on tobacco smoke LXVIII. Analysis of volatile and tobacco-specific nitrosamines in tobacco products. *IARC Sci Publ*: 507-16.

- Holt, M.P., and C. Ju, 2006. Mechanisms of drug-induced liver injury. *AAPS J* 8: E48-54.
- Hui, L., K. Zatloukal, H. Scheuch, E. Stepniak, and E.F. Wagner, 2008. Proliferation of human HCC cells and chemically induced mouse liver cancers requires JNK1-dependent p21 downregulation. *J Clin Invest* 118: 3943-53.
- Hwang, H.C., and B.E. Clurman, 2005. Cyclin E in normal and neoplastic cell cycles. *Oncogene* 24: 2776-86.
- Jackson, P.K., S. Chevalier, M. Philippe, and M.W. Kirschner, 1995. Early events in DNA replication require cyclin E and are blocked by p21CIP1. *J Cell Biol* 130: 755-69.
- Jemal, A., R. Siegel, E. Ward, Y. Hao, J. Xu, and M.J. Thun, 2009. Cancer statistics, 2009. *CA Cancer J Clin* 59: 225-49.
- Jirawatnotai, S., Y. Hu, W. Michowski, J.E. Elias, L. Becks, F. Bienvenu, A. Zagozdzon, T. Goswami, Y.E. Wang, A.B. Clark, T.A. Kunkel, T. van Harn, B. Xia, M. Correll, J. Quackenbush, D.M. Livingston, S.P. Gygi, and P. Sicinski, 2011. A function for cyclin D1 in DNA repair uncovered by protein interactome analyses in human cancers. *Nature* 474: 230-4.
- Jung, Y.J., K.H. Lee, D.W. Choi, C.J. Han, S.H. Jeong, K.C. Kim, J.W. Oh, T.K. Park, and C.M. Kim, 2001. Reciprocal expressions of cyclin E and cyclin D1 in hepatocellular carcinoma. *Cancer Lett* 168: 57-63.
- Kaldis, P., and E. Aleem, 2005. Cell cycle sibling rivalry: Cdc2 vs. Cdk2. *Cell Cycle* 4: 1491-4.
- Karin, M., and F.R. Greten, 2005. NF-kappaB: linking inflammation and immunity to cancer development and progression. *Nat Rev Immunol* 5: 749-59.
- Kellendonk, C., C. Opherk, K. Anlag, G. Schutz, and F. Tronche, 2000. Hepatocyte-specific expression of Cre recombinase. *Genesis* 26: 151-3.
- Kelly, B.L., K.G. Wolfe, and J.M. Roberts, 1998. Identification of a substrate-targeting domain in cyclin E necessary for phosphorylation of the retinoblastoma protein. *Proc Natl Acad Sci U S A* 95: 2535-40.
- Kobayashi, H., E. Stewart, R. Poon, J.P. Adamczewski, J. Gannon, and T. Hunt, 1992. Identification of the domains in cyclin A required for binding to, and activation of, p34cdc2 and p32cdk2 protein kinase subunits. *Mol Biol Cell* 3: 1279-94.
- Koepp, D.M., L.K. Schaefer, X. Ye, K. Keyomarsi, C. Chu, J.W. Harper, and S.J. Elledge, 2001. Phosphorylation-dependent ubiquitination of cyclin E by the SCFFbw7 ubiquitin ligase. *Science* 294: 173-7.

- Koff, A., F. Cross, A. Fisher, J. Schumacher, K. Leguellec, M. Philippe, and J.M. Roberts, 1991. Human cyclin E, a new cyclin that interacts with two members of the CDC2 gene family. *Cell* 66: 1217-28.
- Koff, A., A. Giordano, D. Desai, K. Yamashita, J.W. Harper, S. Elledge, T. Nishimoto, D.O. Morgan, B.R. Franza, and J.M. Roberts, 1992. Formation and activation of a cyclin E-cdk2 complex during the G1 phase of the human cell cycle. *Science* 257: 1689-94.
- Kossatz, U., N. Dietrich, L. Zender, J. Buer, M.P. Manns, and N.P. Malek, 2004. Skp2-dependent degradation of p27kip1 is essential for cell cycle progression. *Genes Dev* 18: 2602-7.
- LaBaer, J., M.D. Garrett, L.F. Stevenson, J.M. Slingerland, C. Sandhu, H.S. Chou, A. Fattaey, and E. Harlow, 1997. New functional activities for the p21 family of CDK inhibitors. *Genes Dev* 11: 847-62.
- Laemmli, U.K., 1970. Cleavage of structural proteins during the assembly of the head of bacteriophage T4. *Nature* 227: 680-5.
- Laufer, N., A.R. Beck, S. Cariou, L. Richman, K. Hofmann, W. Reith, J.M. Slingerland, and B. Amati, 1998. Cyclin E2: a novel CDK2 partner in the late G1 and S phases of the mammalian cell cycle. *Oncogene* 17: 2637-43.
- Le Cam, L., J. Polanowska, E. Fabbrizio, M. Olivier, A. Philips, E. Ng Eaton, M. Classon, Y. Geng, and C. Sardet, 1999. Timing of cyclin E gene expression depends on the regulated association of a bipartite repressor element with a novel E2F complex. *EMBO J* 18: 1878-90.
- Leclerc, V., and P. Leopold, 1996. The cyclin C/Cdk8 kinase. *Prog Cell Cycle Res* 2: 197-204.
- Leclerc, V., J.P. Tassan, P.H. O'Farrell, E.A. Nigg, and P. Leopold, 1996. *Drosophila* Cdk8, a kinase partner of cyclin C that interacts with the large subunit of RNA polymerase II. *Mol Biol Cell* 7: 505-13.
- Lee, J., and S.S. Kim, 2009. The function of p27 KIP1 during tumor development. *Exp Mol Med* 41: 765-71.
- Lee, J.S., I.S. Chu, A. Mikaelyan, D.F. Calvisi, J. Heo, J.K. Reddy, and S.S. Thorgeirsson, 2004. Application of comparative functional genomics to identify best-fit mouse models to study human cancer. *Nat Genet* 36: 1306-11.
- Leenen, P.J., M.F. de Bruijn, J.S. Voerman, P.A. Campbell, and W. van Ewijk, 1994. Markers of mouse macrophage development detected by monoclonal antibodies. *J Immunol Methods* 174: 5-19.
- Lees, E.M., and E. Harlow, 1993. Sequences within the conserved cyclin box of human cyclin A are sufficient for binding to and activation of cdc2 kinase. *Mol Cell Biol* 13: 1194-201.



- Lew, D.J., V. Dulic, and S.I. Reed, 1991. Isolation of three novel human cyclins by rescue of G1 cyclin (Cln) function in yeast. *Cell* 66: 1197-206.
- Li, K., S.Y. Lin, F.C. Brunicardi, and P. Seu, 2003. Use of RNA interference to target cyclin E-overexpressing hepatocellular carcinoma. *Cancer Res* 63: 3593-7.
- Li, Z., X. Jiao, C. Wang, L.A. Shirley, H. Elsaleh, O. Dahl, M. Wang, E. Soutoglou, E.S. Knudsen, and R.G. Pestell, 2010. Alternative cyclin D1 splice forms differentially regulate the DNA damage response. *Cancer Res* 70: 8802-11.
- Liang, Y., H. Gao, S.Y. Lin, J.A. Goss, F.C. Brunicardi, and K. Li, 2010. siRNA-based targeting of cyclin E overexpression inhibits breast cancer cell growth and suppresses tumor development in breast cancer mouse model. *PLoS One* 5: e12860.
- Liedtke, C., J.M. Bangen, J. Freimuth, N. Beraza, D. Lambertz, F.J. Cubero, M. Hatting, K.R. Karlmark, K.L. Streetz, G.A. Krombach, F. Tacke, N. Gassler, D. Riethmacher, and C. Trautwein, Loss of caspase-8 protects mice against inflammation-related hepatocarcinogenesis but induces non-apoptotic liver injury. *Gastroenterology* 141: 2176-87.
- Lin, J., C. Reichner, X. Wu, and A.J. Levine, 1996. Analysis of wild-type and mutant p21WAF-1 gene activities. *Mol Cell Biol* 16: 1786-93.
- Llovet, J.M., A. Burroughs, and J. Bruix, 2003. Hepatocellular carcinoma. *Lancet* 362: 1907-17.
- Llovet, J.M., S. Ricci, V. Mazzaferro, P. Hilgard, E. Gane, J.F. Blanc, A.C. de Oliveira, A. Santoro, J.L. Raoul, A. Forner, M. Schwartz, C. Porta, S. Zeuzem, L. Bolondi, T.F. Greten, P.R. Galle, J.F. Seitz, I. Borbath, D. Haussinger, T. Giannaris, M. Shan, M. Moscovici, D. Voliotis, and J. Bruix, 2008. Sorafenib in advanced hepatocellular carcinoma. *N Engl J Med* 359: 378-90.
- Loeb, K.R., H. Kostner, E. Firpo, T. Norwood, D.T. K, B.E. Clurman, and J.M. Roberts, 2005. A mouse model for cyclin E-dependent genetic instability and tumorigenesis. *Cancer Cell* 8: 35-47.
- Lundberg, A.S., and R.A. Weinberg, 1998. Functional inactivation of the retinoblastoma protein requires sequential modification by at least two distinct cyclin-cdk complexes. *Mol Cell Biol* 18: 753-61.
- Ma, Y., S. Fiering, C. Black, X. Liu, Z. Yuan, V.A. Memoli, D.J. Robbins, H.A. Bentley, G.J. Tsongalis, E. Demidenko, S.J. Freemantle, and E. Dmitrovsky, 2007. Transgenic cyclin E triggers dysplasia and multiple pulmonary adenocarcinomas. *Proc Natl Acad Sci U S A* 104: 4089-94.
- Maeda, S., H. Kamata, J.L. Luo, H. Leffert, and M. Karin, 2005. IKKbeta couples hepatocyte death to cytokine-driven compensatory proliferation that promotes chemical hepatocarcinogenesis. *Cell* 121: 977-90.

- Malumbres, M., and M. Barbacid, 2005. Mammalian cyclin-dependent kinases. *Trends Biochem Sci* 30: 630-41.
- Matsuda, Y., 2008. Molecular mechanism underlying the functional loss of cyclin-dependent kinase inhibitors p16 and p27 in hepatocellular carcinoma. *World J Gastroenterol* 14: 1734-40.
- Mazumder, S., D. Plesca, and A. Almasan, 2007. A jekyll and hyde role of cyclin E in the genotoxic stress response: switching from cell cycle control to apoptosis regulation. *Cell Cycle* 6: 1437-42.
- McClain, R.M., D. Keller, D. Casciano, P. Fu, J. MacDonald, J. Popp, and J. Sagartz, 2001. Neonatal mouse model: review of methods and results. *Toxicol Pathol* 29 Suppl: 128-37.
- Meek, D.W., 2009. Tumour suppression by p53: a role for the DNA damage response? *Nat Rev Cancer* 9: 714-23.
- Meek, D.W., and C.W. Anderson, 2009. Posttranslational modification of p53: cooperative integrators of function. *Cold Spring Harb Perspect Biol* 1: a000950.
- Michejda, C.J., and S.R. Koepke, 1982. O-alkylation of N-nitrosamines. Transalkylation of N-nitrosamines and formation of electrophilic intermediates. *IARC Sci Publ*: 451-7.
- Minella, A.C., J.E. Grim, M. Welcker, and B.E. Clurman, 2007. p53 and SCFFbw7 cooperatively restrain cyclin E-associated genome instability. *Oncogene* 26: 6948-53.
- Mooi, W.J., and D.S. Peeper, 2006. Oncogene-induced cell senescence--halting on the road to cancer. *N Engl J Med* 355: 1037-46.
- Moore, M.A., K. Nakagawa, K. Satoh, T. Ishikawa, and K. Sato, 1987. Single GST-P positive liver cells--putative initiated hepatocytes. *Carcinogenesis* 8: 483-6.
- Morgan, D.O., 1996. The dynamics of cyclin dependent kinase structure. *Curr Opin Cell Biol* 8: 767-72.
- Morgan, D.O., 1997. Cyclin-dependent kinases: engines, clocks, and microprocessors. *Annu Rev Cell Dev Biol* 13: 261-91.
- Nakayama, K., 1998. Cip/Kip cyclin-dependent kinase inhibitors: brakes of the cell cycle engine during development. *Bioessays* 20: 1020-9.
- Nasmyth, K., 1996. At the heart of the budding yeast cell cycle. *Trends Genet* 12: 405-12.

- Naugler, W.E., T. Sakurai, S. Kim, S. Maeda, K. Kim, A.M. Elsharkawy, and M. Karin, 2007. Gender disparity in liver cancer due to sex differences in MyD88-dependent IL-6 production. *Science* 317: 121-4.
- Nevzorova, Y.A., D. Tschaharganeh, N. Gassler, Y. Geng, R. Weiskirchen, P. Sicinski, C. Trautwein, and C. Liedtke, 2009. Aberrant cell cycle progression and endoreplication in regenerating livers of mice that lack a single E-type cyclin. *Gastroenterology* 137: 691-703, 703 e1-6.
- Nigg, E.A., 1995. Cyclin-dependent protein kinases: key regulators of the eukaryotic cell cycle. *Bioessays* 17: 471-80.
- Nigg, E.A., 1996. Cyclin-dependent kinase 7: at the cross-roads of transcription, DNA repair and cell cycle control? *Curr Opin Cell Biol* 8: 312-7.
- Norbury, C., and P. Nurse, 1992. Animal cell cycles and their control. *Annu Rev Biochem* 61: 441-70.
- Ohtani, K., J. DeGregori, and J.R. Nevins, 1995. Regulation of the cyclin E gene by transcription factor E2F1. *Proc Natl Acad Sci U S A* 92: 12146-50.
- Ohtsubo, M., A.M. Theodoras, J. Schumacher, J.M. Roberts, and M. Pagano, 1995. Human cyclin E, a nuclear protein essential for the G1-to-S phase transition. *Mol Cell Biol* 15: 2612-24.
- Ortega, S., M. Malumbres, and M. Barbacid, 2002. Cyclin D-dependent kinases, INK4 inhibitors and cancer. *Biochim Biophys Acta* 1602: 73-87.
- Ortega, S., I. Prieto, J. Odajima, A. Martin, P. Dubus, R. Sotillo, J.L. Barbero, M. Malumbres, and M. Barbacid, 2003. Cyclin-dependent kinase 2 is essential for meiosis but not for mitotic cell division in mice. *Nat Genet* 35: 25-31.
- Palmero, I., B. McConnell, D. Parry, S. Brookes, E. Hara, S. Bates, P. Jat, and G. Peters, 1997. Accumulation of p16INK4a in mouse fibroblasts as a function of replicative senescence and not of retinoblastoma gene status. *Oncogene* 15: 495-503.
- Parisi, T., A.R. Beck, N. Rougier, T. McNeil, L. Lucian, Z. Werb, and B. Amati, 2003. Cyclins E1 and E2 are required for endoreplication in placental trophoblast giant cells. *EMBO J* 22: 4794-803.
- Parkin, D.M., 1998. The global burden of cancer. *Semin Cancer Biol* 8: 219-35.
- Peng, J., Y. Zhu, J.T. Milton, and D.H. Price, 1998. Identification of multiple cyclin subunits of human P-TEFb. *Genes Dev* 12: 755-62.
- Peters, J.M., R.W. King, C. Hoog, and M.W. Kirschner, 1996. Identification of BIME as a subunit of the anaphase-promoting complex. *Science* 274: 1199-201.

- Peto, R., R. Gray, P. Brantom, and P. Grasso, 1984. Nitrosamine carcinogenesis in 5120 rodents: chronic administration of sixteen different concentrations of NDEA, NDMA, NPYR and NPIP in the water of 4440 inbred rats, with parallel studies on NDEA alone of the effect of age of starting (3, 6 or 20 weeks) and of species (rats, mice or hamsters). *IARC Sci Publ*: 627-65.
- Pfaffl, M.W., 2001. A new mathematical model for relative quantification in real-time RT-PCR. *Nucleic Acids Res* 29: e45.
- Pietsch, E.C., S.M. Sykes, S.B. McMahon, and M.E. Murphy, 2008. The p53 family and programmed cell death. *Oncogene* 27: 6507-21.
- Planas-Silva, M.D., and R.A. Weinberg, 1997. The restriction point and control of cell proliferation. *Curr Opin Cell Biol* 9: 768-72.
- Pluquet, O., and P. Hainaut, 2001. Genotoxic and non-genotoxic pathways of p53 induction. *Cancer Lett* 174: 1-15.
- Polyak, K., M.H. Lee, H. Erdjument-Bromage, A. Koff, J.M. Roberts, P. Tempst, and J. Massague, 1994a. Cloning of p27Kip1, a cyclin-dependent kinase inhibitor and a potential mediator of extracellular antimitogenic signals. *Cell* 78: 59-66.
- Polyak, K., J.Y. Kato, M.J. Solomon, C.J. Sherr, J. Massague, J.M. Roberts, and A. Koff, 1994b. p27Kip1, a cyclin-Cdk inhibitor, links transforming growth factor-beta and contact inhibition to cell cycle arrest. *Genes Dev* 8: 9-22.
- Prieur, A., and D.S. Peeper, 2008. Cellular senescence in vivo: a barrier to tumorigenesis. *Curr Opin Cell Biol* 20: 150-5.
- Rasband, W.S., 1997-2011. ImageJ, U. S. National Institutes of Health, Bethesda, Maryland, USA
- Ray, D., Y. Terao, K. Christov, P. Kaldis, and H. Kiyokawa, 2011. Cdk2-null mice are resistant to ErbB-2-induced mammary tumorigenesis. *Neoplasia* 13: 439-44.
- Rechsteiner, M., and S.W. Rogers, 1996. PEST sequences and regulation by proteolysis. *Trends Biochem Sci* 21: 267-71.
- Rempel, R.E., S.B. Sleight, and J.L. Maller, 1995. Maternal *Xenopus* Cdk2-cyclin E complexes function during meiotic and early embryonic cell cycles that lack a G1 phase. *J Biol Chem* 270: 6843-55.
- Resnitzky, D., and S.I. Reed, 1995. Different roles for cyclins D1 and E in regulation of the G1-to-S transition. *Mol Cell Biol* 15: 3463-9.
- Resnitzky, D., M. Gossen, H. Bujard, and S.I. Reed, 1994. Acceleration of the G1/S phase transition by expression of cyclins D1 and E with an inducible system. *Mol Cell Biol* 14: 1669-79.

- Rickert, P., W. Seghezzi, F. Shanahan, H. Cho, and E. Lees, 1996. Cyclin C/CDK8 is a novel CTD kinase associated with RNA polymerase II. *Oncogene* 12: 2631-40.
- Rodier, F., J.P. Coppe, C.K. Patil, W.A. Hoeijmakers, D.P. Munoz, S.R. Raza, A. Freund, E. Campeau, A.R. Davalos, and J. Campisi, 2009. Persistent DNA damage signalling triggers senescence-associated inflammatory cytokine secretion. *Nat Cell Biol* 11: 973-9.
- Rogers, S.W., and M.C. Rechsteiner, 1986. Microinjection studies on selective protein degradation: relationships between stability, structure, and location. *Biomed Biochim Acta* 45: 1611-8.
- Roussel, M.F., 1999. The INK4 family of cell cycle inhibitors in cancer. *Oncogene* 18: 5311-7.
- Ruehl-Fehlert, C., B. Kittel, G. Morawietz, P. Deslex, C. Keenan, C.R. Mahrt, T. Nolte, M. Robinson, B.P. Stuart, and U. Deschl, 2003. Revised guides for organ sampling and trimming in rats and mice--part 1. *Exp Toxicol Pathol* 55: 91-106.
- Saffhill, R., 1985. In vitro miscoding of alkylthymines with DNA and RNA polymerases. *Chem Biol Interact* 53: 121-30.
- Saffhill, R., and J.A. Hall, 1985. The incorporation of O6-methyldeoxyguanosine monophosphate and O4-methyldeoxythymidine monophosphate into polynucleotide templates leads to errors during subsequent in vitro DNA synthesis. *Chem Biol Interact* 56: 363-70.
- Sage, J., G.J. Mulligan, L.D. Attardi, A. Miller, S. Chen, B. Williams, E. Theodorou, and T. Jacks, 2000. Targeted disruption of the three Rb-related genes leads to loss of G(1) control and immortalization. *Genes Dev* 14: 3037-50.
- Santamaria, D., C. Barriere, A. Cerqueira, S. Hunt, C. Tardy, K. Newton, J.F. Caceres, P. Dubus, M. Malumbres, and M. Barbacid, 2007. Cdk1 is sufficient to drive the mammalian cell cycle. *Nature* 448: 811-5.
- Satyanarayana, A., M.B. Hilton, and P. Kaldis, 2008. p21 Inhibits Cdk1 in the absence of Cdk2 to maintain the G1/S phase DNA damage checkpoint. *Mol Biol Cell* 19: 65-77.
- Scherer, E., M. Hoffmann, P. Emmelot, and M. Friedrich-Freksa, 1972. Quantitative study on foci of altered liver cells induced in the rat by a single dose of diethylnitrosamine and partial hepatectomy. *J Natl Cancer Inst* 49: 93-106.
- Schulze, A., K. Zerfass, D. Spitkovsky, S. Middendorp, J. Berges, K. Helin, P. Jansen-Durr, and B. Henglein, 1995. Cell cycle regulation of the cyclin A gene promoter is mediated by a variant E2F site. *Proc Natl Acad Sci U S A* 92: 11264-8.

- Sen, N.P., S. Seaman, and M. McPherson, 1980. Further studies on the occurrence of volatile and non-volatile nitrosamines in foods. *IARC Sci Publ*: 457-65.
- Sherr, C.J., 1996. Cancer cell cycles. *Science* 274: 1672-7.
- Sherr, C.J., 2000. Cell cycle control and cancer. *Harvey Lect* 96: 73-92.
- Sherr, C.J., and F. McCormick, 2002. The RB and p53 pathways in cancer. *Cancer Cell* 2: 103-12.
- Shiyanov, P., S. Bagchi, G. Adami, J. Kokontis, N. Hay, M. Arroyo, A. Morozov, and P. Raychaudhuri, 1996. p21 Disrupts the interaction between cdk2 and the E2F-p130 complex. *Mol Cell Biol* 16: 737-44.
- Singer, B., 1985. In vivo formation and persistence of modified nucleosides resulting from alkylating agents. *Environ Health Perspect* 62: 41-8.
- Singer, G.M., and A.W. Andrews, 1983. Mutagenicity and chemistry of N-nitroso-N-(p-substituted-benzyl)methylamines. *J Med Chem* 26: 309-12.
- Singer, J.D., M. Gurian-West, B. Clurman, and J.M. Roberts, 1999. Cullin-3 targets cyclin E for ubiquitination and controls S phase in mammalian cells. *Genes Dev* 13: 2375-87.
- Solovjov, D.A., E. Pluskota, and E.F. Plow, 2005. Distinct roles for the alpha and beta subunits in the functions of integrin alphaMbeta2. *J Biol Chem* 280: 1336-45.
- Soos, T.J., H. Kiyokawa, J.S. Yan, M.S. Rubin, A. Giordano, A. DeBlasio, S. Bottega, B. Wong, J. Mendelsohn, and A. Koff, 1996. Formation of p27-CDK complexes during the human mitotic cell cycle. *Cell Growth Differ* 7: 135-46.
- Spruck, C.H., K.A. Won, and S.I. Reed, 1999. Deregulated cyclin E induces chromosome instability. *Nature* 401: 297-300.
- Starley, B.Q., C.J. Calcagno, and S.A. Harrison, 2010. Nonalcoholic fatty liver disease and hepatocellular carcinoma: a weighty connection. *Hepatology* 51: 1820-32.
- Stern, B., and P. Nurse, 1996. A quantitative model for the cdc2 control of S phase and mitosis in fission yeast. *Trends Genet* 12: 345-50.
- Svejstrup, J.Q., P. Vichi, and J.M. Egly, 1996. The multiple roles of transcription/repair factor TFIIH. *Trends Biochem Sci* 21: 346-50.
- Swenberg, J.A., D.G. Hoel, and P.N. Magee, 1991. Mechanistic and statistical insight into the large carcinogenesis bioassays on N-nitrosodiethylamine and N-nitrosodimethylamine. *Cancer Res* 51: 6409-14.

- Tassan, J.P., M. Jaquenoud, A.M. Fry, S. Frutiger, G.J. Hughes, and E.A. Nigg, 1995. In vitro assembly of a functional human CDK7-cyclin H complex requires MAT1, a novel 36 kDa RING finger protein. *EMBO J* 14: 5608-17.
- Teufelhofer, O., W. Parzefall, E. Kainzbauer, F. Ferk, C. Freiler, S. Knasmuller, L. Elbling, R. Thurman, and R. Schulte-Hermann, 2005. Superoxide generation from Kupffer cells contributes to hepatocarcinogenesis: studies on NADPH oxidase knockout mice. *Carcinogenesis* 26: 319-29.
- Thorgeirsson, U.P., D.W. Dalgard, J. Reeves, and R.H. Adamson, 1994. Tumor incidence in a chemical carcinogenesis study of nonhuman primates. *Regul Toxicol Pharmacol* 19: 130-51.
- Todd, M.C., S.C. Spruill, and K.L. Meerbrey, 2009. Small interference RNA-mediated suppression of overexpressed cyclin E protein restores G1/S regulation in NIH-OVCAR-3 ovarian cancer cells. *Int J Oncol* 35: 375-80.
- Toyoshima, H., and T. Hunter, 1994. p27, a novel inhibitor of G1 cyclin-Cdk protein kinase activity, is related to p21. *Cell* 78: 67-74.
- Tsai, L.H., E. Harlow, and M. Meyerson, 1991. Isolation of the human cdk2 gene that encodes the cyclin A- and adenovirus E1A-associated p33 kinase. *Nature* 353: 174-7.
- Verna, L., J. Whysner, and G.M. Williams, 1996. N-nitrosodiethylamine mechanistic data and risk assessment: bioactivation, DNA-adduct formation, mutagenicity, and tumor initiation. *Pharmacol Ther* 71: 57-81.
- Vervoorts, J., and B. Luscher, 2008. Post-translational regulation of the tumor suppressor p27(KIP1). *Cell Mol Life Sci* 65: 3255-64.
- Vesselinovitch, S.D., 1980. Infant mouse as a sensitive bioassay system for carcinogenicity of N-nitroso compounds. *IARC Sci Publ*: 645-55.
- Villanueva, A., and J.M. Llovet, Targeted therapies for hepatocellular carcinoma. *Gastroenterology* 140: 1410-26.
- Vlahopoulos, S., and V.C. Zoumpourlis, 2004. JNK: a key modulator of intracellular signaling. *Biochemistry (Mosc)* 69: 844-54.
- Weinberg, R.A., 1996. E2F and cell proliferation: a world turned upside down. *Cell* 85: 457-9.
- Wingate, H., A. Puskas, M. Duong, T. Bui, D. Richardson, Y. Liu, S.L. Tucker, C. Van Pelt, L. Meijer, K. Hunt, and K. Keyomarsi, 2009. Low molecular weight cyclin E is specific in breast cancer and is associated with mechanisms of tumor progression. *Cell Cycle* 8: 1062-8.

- Won, K.A., and S.I. Reed, 1996. Activation of cyclin E/CDK2 is coupled to site-specific autophosphorylation and ubiquitin-dependent degradation of cyclin E. *EMBO J* 15: 4182-93.
- Zariwala, M., J. Liu, and Y. Xiong, 1998. Cyclin E2, a novel human G1 cyclin and activating partner of CDK2 and CDK3, is induced by viral oncoproteins. *Oncogene* 17: 2787-98.
- Zerfass-Thome, K., A. Schulze, W. Zwerschke, B. Vogt, K. Helin, J. Bartek, B. Henglein, and P. Jansen-Durr, 1997. p27KIP1 blocks cyclin E-dependent transactivation of cyclin A gene expression. *Mol Cell Biol* 17: 407-15.
- Zhang, H., G.J. Hannon, and D. Beach, 1994. p21-containing cyclin kinases exist in both active and inactive states. *Genes Dev* 8: 1750-8.
- Zhu, L., G. Enders, J.A. Lees, R.L. Beijersbergen, R. Bernards, and E. Harlow, 1995. The pRB-related protein p107 contains two growth suppression domains: independent interactions with E2F and cyclin/cdk complexes. *EMBO J* 14: 1904-13.



## 8. Appendix

### 8.1 Abbreviations

A	Ampere
aa	Amino acid
ALT	Alanine-aminotransferase
AP	Apurinic/apirimidinic
APC/C	Anaphase promoting complex / cyclosome
APS	Ammoniumperoxodisulfat
ARP	Aldehyde reactive probe
AST	Aspartate-aminotransferase
ATP	Adenosintrisphosphat
ATM	Ataxia-telangiectasia mutated protein kinase
ATR	ATM + Rad3-related protein kinase
bp	Base pair
BSA	Bovine Serum Albumin
Bq	Becquerel
CAK	Cdk-activating kinase
Cat	Catalase
CcnA	Cyclin A
CcnD	Cyclin D
CcnE	Cyclin E
Cdk	Cyclin dependent kinase
cDNA	Complementary DNA
°C	Degree Celsius
Cip	Cdk interacting protein
CKI	Cyclin dependent kinase inhibitor
CLS	Centrosome localization signal
CTD	C-terminal domain
2D	two dimension
2D-DiGE	2D in-Gel electrophoresis
Da	Dalton
DAB	3,3'-diamino benzidine
DAPI	4,6-diamino-2-phenylindole
DDR	DNA damage response
DEN	diethylnitrosamine
DMEM	Dulbecco's modified Eagle's medium
DNA	Desoxyribonucleic acid

dNTP	Desoxyribonukleotidtrispohspate
DTT	Dithiothreitol
EDTA	Ethylendiamintetraacetic acid
ECL	Enhanced chemiluminescence
EGF	Epidermal growth factor
FACS	Fluorescence activated cell sorting
Fb	Fibronectin
Fbw7	F-box and WD repeat domain-containing 7
FCS	Fetal calf serum
FITC	Fluoresceinisothocyanat
g	gram
<i>g</i>	gravity
G6P	Glucose-6-phosphatase
Gadd45	Growth arrest and DNA damage 45
GAPDH	Glyceraldehyde 3-phosphate dehydrogenase
h	hour
H&E	Hematoxylin and eosin
HCC	Hepatocellular carcinoma
HRP	Horseradish peroxidase
IF	Immunofluorescence
IHC	Immunohistochemistry
IL	interleukine
JNK	c-Jun N-terminal kinase
k	kilo
kb	kilo base
Kip	kinase inhibitory protein
L	liter
LMW	Low molecular weight
μ-	micro (10 <sup>-6</sup> )
m-	mili (10 <sup>-3</sup> )
m	Meter
M	Molar
MCM	Minichromosome maintenance
Mdm2	Murine double minute 2
min	Minute
MnSOD	Manganese superoxide dismutase
MOPS	Morpholinopropansulfon
mRNA	Messenger RNA
NAFLD	Nonalcoholic fatty liver disease
NASH	Nonalcoholic steatohepatitis

NLS	Nuclear localization signal
NSLC	non-small-cell lung carcinoma
O <sup>6</sup> -EtdG	O <sup>6</sup> -ethyldeoxyguanosine
O <sup>4</sup> -EtdT	O <sup>4</sup> -ethyldeoxythymidine
OD	Optical density
PBS	Phosphate buffered saline
PBST	PBS-Tween
PCNA	Proliferating cell nuclear antigen
PCR	Polymerase chain reaction
PEST	prolin (P), Glutamic acid (E), Serine (S), Threonine (T)
PFA	Paraformaldehyde
PH	Partial hepatectomy
PI	Propidium iodide
ppb	Parts per bilion
Rb	Retinoblastoma
RNA	Ribonucleic acid
rpm	Rotations per Minute
RPMI	Roswell Park Memorial Institute
RT	Room temperature
s	second
SA-β-gal	Senescence associated β-galactosidase
SCF	Skp1-cullin-F-box-Komplex
s.d.	Standard deviation
SDS	Sodium dodecyl sulphate
Ser	Serine
siRNA	Small interference RNA
Skp	S-phase kinase associated protein
Tab.	Table
TAE	Tris Acetate EDTA Buffer
TAK/P-TEFb	CyclinT1/P-TEFb
P-TEFb	Positive transcription elongation factor b
TBE	Tris Borate EDTA Buffer
TBS	Tris buffered saline
TE	Tris-EDTA-Buffer
TEMED	N',N',N',N'-Tetramethyldiamine
TFIIH	Transcription factor II H
TGF-beta	Transforming growth factor beta
Thr	Threonine
Tris	2-Amino-2(hydroxymethyl)-1,3-propandiol
TUNEL	Terminal deoxynucleotidyl transferase dUTP nick end labeling

Tween 20	Polyoxyethylensorbitanmonolaureat
UV	ultraviolet
V	Volt
v/v	Volume per Volume
VXCXE	Valine (V), unspecified (X), Cysteine (C), X, Glutamic acid (E)
WT	Wild type
w/v	Weight per Volume
X-Gal	5-Bromo-4-Chloro-3-indolyl $\beta$ -D-Galactopyranoside

## 9. Eidesstattliche Erklärung

Hiermit erkläre ich, Nives Moro, dass ich die Dissertation mit dem Titel:

### **Inactivation of cyclin E1 inhibits chemically induced hepatocarcinogenesis in mice**

selbständig verfasst habe.

Bei der Anfertigung wurden folgende Hilfen Dritter in Anspruch genommen:

1. In der Abteilung Gastroenterologie und Stoffwechselkrankheiten der medizinischen Klinik III im Universitätsklinikum Aachen habe ich die Versuche mit den im Kapitel „Material und Methoden“ aufgeführten Hilfen und Hilfsmitteln durchgeführt.
2. Die Anfertigung erfolgte unter der Leitung von PD Dr. rer. nat. Christian Liedtke, Abteilung Gastroenterologie und Stoffwechselkrankheiten der Medizinischen Klinik III im Universitätsklinikum Aachen. Die fachliche Betreuung wurde von Univ. Prof. Dr. rer. nat. Michael Huber, Abteilung Lehr- und Forschungsgebiet für Biochemie und Molekulare Immunologie im Universitätsklinikum Aachen übernommen.
3. Die immunhistochemische Färbungen und die Auswertung HE gefärbter Gewebeschnitte wurden von Herrn Univ. Prof. Dr. med. Nikolaus Gaßler, M.A., Institut der Pathologie im Universitätsklinikum Aachen durchgeführt.
4. Die zweidimensionale Gelelektrophorese und die Auswertung gefärbter Gele wurden von Frau Dr. rer. nat. Corinna Henkel, Institut der Pathologie im Universitätsklinikum Aachen durchgeführt.

Ich habe keine entgeltliche Hilfe von Vermittlungs- bzw. Beratungsdiensten in Anspruch genommen. Niemand hat von mir unmittelbar oder mittelbar entgeltliche Leistung für Arbeiten erhalten, die im Zusammenhang mit dem Inhalt der vorgelegten Dissertation stehen. Die Synthesen der verwendeten Primer und Antikörper wurden von den jeweils erwähnten Firmen durchgeführt.

Ich habe die Dissertation an folgenden Instituten angefertigt:

Abteilung Gastroenterologie und Stoffwechselkrankheiten der Medizinischen Klinik  
III im Universitätsklinikum Aachen

Die Dissertation wurde bisher nicht für eine Prüfung oder Promotion oder für einen  
ähnlichen Zweck zur Beurteilung eingereicht.

Ich versichere, dass ich die vorstehenden Angaben nach bestem Wissen  
vollständig und der Wahrheit entsprechend gemacht habe.

---

Aachen, 06.09.2011

## 10. Acknowledgements

First of all, I want to thank **PD Dr. rer. nat. Christian Liedtke** for his patient guidance, scientific and technical advice and helpful discussions throughout this project, in addition to making it possible to visit international congresses and for the excellent corrections of this thesis. I am very grateful for your friendly and generous help from the beginning of my stay in Germany.

I would like to thank **Prof. Dr. med. Christian Trautwein** for making it possible to carry out the project in his department. I am grateful for his supervision, guidance and advice during the project and throughout my studies.

I thank **Prof. Dr. rer. nat. Michael Huber** for the engagement, interesting discussions and ideas at our meetings and for accepting to review my PhD work.

To my doctoral committee, **Prof. Dr. rer. nat. Lothar Elling** and **Prof. Dr. rer. nat. Johannes Bohrmann** thanks for giving me a nice and uncomplicated thesis defense.

Many thanks to my lab for all the patience, help, great support and friendship and special thanks go to my fellow PhD student **Roland Sonntag** for all the work and time he invested to my project.

Extra thanks go to **Dr. Sara Dutton Sackett, PhD** who was sharing lab, computer and protocols with me. Thank you for your friendship, inspiration, encouragement, constructive discussions and critical reading of my thesis, you are a real treasure !

Thanks to **Dr. rer. nat. Jörg-Martin Bangen** for help in diverse lab crises and as well as for your friendship.

I am grateful to **Daniela Lamberts**, **Sonja Strauch** and **Ute Haas** for everyday help and advice in and out of the lab.

I would like to thank **Prof. Dr. med. Nikolaus Gaßler** and **Ursula Schneider** for cooperation, tissue staining and explanation of liver histology.

I want to also thank all animal caretakers, especially **Birgit Müller** and **Dunja Sieger** for the support and care of my animal lines which contributed greatly to this work.

I am grateful to **Sibille Sauer-Lehnen** and **Carmen G. Tag** from the Q3 platform for all their help with hepatocyte isolations as well as helpful advice.

Thanks to **all current and former members of Tumor-START** for discussions, advice and help. Special thanks to **Prof. Dr. rer. nat. Bernhard Lüscher** for inviting me to Aachen.

A big thanks to **all current and former colleagues at the Klinikum**, for the friendly atmosphere, support, coffee brakes and going out, which made working so much more fun.

My greatest appreciation goes to **my parents** and **my brother** for their unconditional support and belief in me.

Finally, I want to express my deep gratitude to **Dr. rer. nat. Arne Giebeler and his parents** for all your understanding, support and encouragement during these five years. Arne, thanks for making me feel at home in Aachen !



# 11. Lebenslauf

## **Persönliche Daten**

Name: Moro  
Vorname: Nives  
Geburtstag: 17. Oktober 1980  
Geburtsort: Zagreb, Kroatien  
Staatsangehörigkeit: Kroatisch

## **Schulbildung**

1987 – 1995 Grundschule in Velika Gorica, Kroatien  
1995 – 1999 Gymnasium in Velika Gorica, Kroatien  
1999 Abitur

## **Studium**

1999 – 2006 Universität Zagreb, Fakultät für Mathematik und  
Naturwissenschaften, Molekular Biologie  
2005 Molekularbiologische Untersuchungen für Diplomarbeit:  
Characterization of novel alcohol dehydrogenases from  
*Candida magnoliae* and *Azoarcus sp.* in BASF,  
Ludwigshafen, bei Dr. Michael Breuer  
2006 Diplomprüfung; Abschluss: Diplom-Ingenieurin

## **Wissenschaftliche**

### **Tätigkeit**

2006 - 2011 Forschungslabor der Medizinischen Klinik III  
(Klinikdirektor: Prof. Dr. med. Christian Trautwein) in der  
Arbeitsgruppe von PD Dr. rer. nat. Christian Liedtke am  
Universitätsklinikum Aachen der RWTH in Aachen  
2011 Mündliche Promotionsprüfung; Abschluss: Dr. rer. nat.